AFCEC-CX-TY-TR-2022-0010

Fuel Spill Fire Testing of an Ignitable Liquid Drainage Floor Assembly (ILDFA) for Chemical-Free Fire Control/Suppression

Steven Wells, Nathaniel Horn, Malena Maraviglia, Heather Luckarift
Battelle Memorial Institute
505 King Avenue
Columbus, OH, 43201

Glenn Johnson
ARCTOS Technology Solutions LLC
1270 North Fairfield Road
Dayton, OH 45432

Bridgett Ashley
Air Force Civil Engineer Center AFCEC/CXAE
139 Barnes Drive
Tyndall AFB, FL 32403

Contract: GS00Q14OADU402

April 14, 2022

AIR FORCE CIVIL ENGINEER CENTER
READINESS DIRECTORATE

■ Requirements & Acquisition Division ■ United States Air Force ■ Tyndall Air Force Base, FL 32403-5323

NOTICE AND SIGNATURE PAGE

Using Government drawings, specifications, or other data included in this document for any purpose other than Government procurement does not in any way obligate the U.S. Government. The fact that the Government formulated or supplied the drawings, specifications, or other data does not license the holder or any other person or corporation; or convey any rights or permission to manufacture, use, or sell any patented invention that may relate to them.

This report was cleared for public release by the AFIMSC Public Affairs Office at Joint Base San Antonio-Lackland Air Force Base, Texas and available to the general public, including foreign nationals. Copies may be obtained from the Defense Technical Information Center (DTIC) (http://www.dtic.mil).

AFCEC-CX-TY-TR-2022-0010 HAS BEEN REVIEWED AND IS APPROVED FOR PUBLICATION IN ACCORDANCE WITH ASSIGNED DISTRIBUTION STATEMENT.

//SIGNED//	//SIGNED//
Dr. Ashley Bridgett	Mr. Reza Salavani
Contracting Officer Representative	Technical Advisor

This report is published in the interest of scientific and technical information exchange, and its publication does not constitute the Government's approval or disapproval of its ideas or findings.

REPORT DOCUMENTATION PAGE

Form Approved
OMB No. 0704-0188

PLEASE DO NOT RETURN YOUR FORM TO THE ABOVE ADDRESS.

1. REPORT DATE *(DD-MM-YYYY)*	2. REPORT TYPE	3. DATES COVERED *(From - To)*
14-04-2022	Technical Report	

4. TITLE AND SUBTITLE

Fuel Spill Fire Testing of an Ignitable Liquid Drainage Floor Assembly (ILDFA) for Chemical-Free Fire Control/Suppression

5a. CONTRACT NUMBER

GS00Q14OADU402

5b. GRANT NUMBER

5c. PROGRAM ELEMENT NUMBER

6. AUTHOR(S)

Steven Wells, Nathaniel Horn,Malena Maraviglia, Heather Luckarift, Glenn Johnson, Bridgett Ashley

5d. PROJECT NUMBER

5e. TASK NUMBER

5f. WORK UNIT NUMBER

7. PERFORMING ORGANIZATION NAME(S) AND ADDRESS(ES)

Battelle Memorial Institute
505 King Avenue
Columbus, OH, 43201

ARCTOS Technology Solutions
1270 North Fairfield Road
Dayton, OH 45432

Air Force Civil Engineer Center AFCEC/CXAE
139 Barnes Drive
Tyndall AFB, FL 32403

8. PERFORMING ORGANIZATION REPORT NUMBER

9. SPONSORING/MONITORING AGENCY NAME(S) AND ADDRESS(ES)

Air Force Civil Engineer Center
Readiness Directorate
Requirements and Acquisition Division
139 Barnes Drive, Suite 1
Tyndall Air Force Base, FL 32403-5323

10. SPONSOR/MONITOR'S ACRONYM(S)

AFCEC/CXA

11. SPONSOR/MONITOR'S REPORT NUMBER(S)

AFCEC-CX-TY-TR-2022-0010

12. DISTRIBUTION/AVAILABILITY STATEMENT

DISTRIBUTION STATEMENT A. Approved for public release; distribution unlimited. AFCEC-20220020, 12 April 2022

13. SUPPLEMENTARY NOTES

14. ABSTRACT

Fire suppression systems in modern USAF aircraft hangars typically include the use of aqueous film-forming foams (AFFF) containing poly- and perfluoroalkyl substances (PFAS) and high expansion (Hi-Ex) foaming agents. Several inadvertent activations of both the legacy AFFF, and newer Hi-Ex based suppression systems have resulted in significant damage to aircraft systems due to submersion of the aircraft in foam. The Air Force is pursuing fire protection strategies for aircraft hangars that minimize use of chemical additives but meet mission requirements and mitigate asset losses from fuel spill fires. One potential solution is flooring that provides rapid drainage of fuel spills with water flushing active removal of the flammable liquids from the aircraft hangar.
A commercial Ignitable Liquid Drainage Floor Assembly (ILDFA) was installed at Tyndall Air Force Base (AFB) for evaluating its effectiveness. A range of fuel spill fires, with and without the ILDFA, were conducted to measure the potential damage that would occur to aircraft and equipment in the vicinity of a spill fire. Fire test quantitative analysis and documentation were supported by video imagery, temperature measurements, and heat absorption calculations to provide critical and interpretable information on fire

15. SUBJECT TERMS

Fuel spill, Fire testing, Ignitable Liquid Drainage Floor Assembly, ILDFA, Fire control, Fire suppression, Chemical-Free Fire Control, Liquid fuel fire, fire protection, aircraft hangar,

16. SECURITY CLASSIFICATION OF:			17. LIMITATION OF ABSTRACT	18. NUMBER OF PAGES	19a. NAME OF RESPONSIBLE PERSON
a. REPORT	b. ABSTRACT	c. THIS PAGE			Bridgett Ashley
U	U	U	SAR	75	19b. TELEPHONE NUMBER *(Include area code)* 850-283-6004

Contents

LIST OF FIGURES

Page

LIST OF TABLES

1. EXECUTIVE SUMMARY

This report summarizes objectives, progress, and outcome of technical work performed under prime contract GS00Q14OADU402, in support of the Air Force Civil Engineering Center (AFCEC) Airbase Technologies Branch (AFCEC/CXAE) and AFCEC/COSM.

Fire suppression systems in modern USAF aircraft hangars typically include the use of aqueous film-forming foams (AFFF) containing poly- and perfluoroalkyl substances (PFAS) and high expansion (Hi-Ex) foaming agents. Several inadvertent activations of both the legacy AFFF, and newer Hi-Ex based suppression systems at USAF and Air National Guard (ANG) facilities, however, have resulted in significant damage to aircraft systems due to submersion of the aircraft in foam. The Air Force is pursuing fire protection strategies for aircraft hangars that minimize use of chemical additives but meet mission requirements and mitigate asset losses. Systems that rely on water only, advanced delivery or suppression methods, or non-aqueous solutions are options to address the challenging requirements.

Damage from fuel spill fires may be decreased by installing flooring that provides rapid drainage and active removal of the flammable liquid from the originating source using flowing water. The approach is intended to eliminate fuel from the fire triangle (i.e., oxygen, heat, and fuel). A commercial Ignitable Liquid Drainage Floor Assembly (ILDFA) manufactured by Safespill Systems, LLC (Houston TX) has been demonstrated for Department of Defense (DoD) and industrial safety applications. Following a recent demonstration of the system at a firefighter training site, the civil engineers for the United States Air Force (USAF) initiated projects in order to assess whether the ILDFA system may be appropriate for new hangar designs and retrofit installation into existing structures. The technology is proposed for use in aircraft service and storage hangars, as well as outdoor fueling, maintenance, and staging aprons.

This report documents testing of an ILDFA for chemical-free fire suppression of fuel spill fires. The demonstration and evaluation of the technology led by AFCEC/CXAE is described herein on a test system installed at Tyndall Air Force Base (AFB). Fuel spill fires were conducted to simulate the potential damage that would occur to aircraft and equipment in the vicinity of an open fuel spill fire. Fire tests, quantitative analysis, and documentation were supported by video imagery (visual and thermal), temperature measurements, and heat absorption calculations that provided critical and interpretable information on fire spread, extent of engulfed area, and potential material damage. The findings were compared to available data on thermal delamination of modern aircraft composites and previous fuel spill fire tests.

The commercial ILDFA effectively reduced the spread, temperature, and heat absorption profile for various fuel spill fire sizes compared to unmitigated fuel spill fires on concrete. The system significantly reduced the thermal profile of fuel fires– limiting potential damage to aircraft, equipment, and risk to personnel in the vicinity of a fire. The primary suppression mechanism of the ILDFA is elimination of the fuel by funneling the fuel through drainage channels to a collection trench and tank. The fuel would otherwise remain pooled on the spill surface, maintaining the fire. By limiting the amount of fuel available to burn, the heat flux (thermal energy/area) is obviously reduced, moreover the active flushing flowing water provides additional heat sink to reduce temperature and further suppress fire. The test results showed fire suppression to the extent that potential heat flux on aircraft was below the delamination threshold

for a representative composite material. The heat flux reduction was significant even without the water flushing system activated, suggesting that system design sufficiently reduced the volume of liquid fuel even by simple gravity flow alone.

After completion of testing, an ILDFA was installed at the Edwards AFB as an operational test. Appendix B reviews the information gathered from a survey of users of the ILDFA at Edwards AFB. Survey questions were designed to understand the level of difficulty to assemble, maintain and perform standard tasks on the IDLFA system.

2. INTRODUCTION AND BACKGROUND

Fire suppression systems in modern USAF aircraft hangars typically include the use of aqueous film-forming foams (AFFF) or other high expansion foaming agents (Hi-Ex). AFFF contains various poly- and perfluoroalkyl substances (PFAS) and legacy systems may include traces of the now highly scrutinized synthetic chemicals perfluorooctanoic acid (PFOA) and perfluorooctane sulfonate (PFOS) (often collectively referred to as C8 PFAS due to the C8 carbon chain length) from previous formulations. Although exceptionally effective, environmental and human health exposure concerns require development of alternative fire mitigation systems. The USAF began implementation of Hi-Ex foam systems in 1999. Hi-Ex foams use other synthetic detergents to blanket fuels and limit the release of flammable vapors. The systems comprise an overhead series of foam generators and water sprinklers (specified in the Unified Facilities Criteria (UFC) 4-211-01) (1). Several inadvertent activations of both the AFFF, and the Hi-Ex based suppression systems at USAF and ANG facilities caused significant damage to aircraft systems due to submersion of the aircraft in foam. The Air Force is pursuing fire protection strategies for aircraft hangars that minimize use of chemical additives, meet mission requirements, and mitigate asset losses. Systems that rely on water only, advanced delivery or suppression methods, or non-aqueous products are options to address the challenges from volatile liquid fuel fires.

The fire suppression systems currently approved for installation in USAF maintenance aircraft hangars are designed for a worst-case fire threat scenario in which hundreds of gallons of fuel, spill, pool, and ignite near an aircraft. One of the past studies of this large fuel spill scenario is reported in EST-TR-86-13 (2). The tests mimicked a so called “drop-wing” fire scenario with a jet fuel spill (165 gal of JP-4) and ignition within a five second timeframe. Fuel fires were suppressed using a Halon 1211 system set up in a hardened aircraft shelter. The tests compiled temperature data at selected points in the facility and recorded fire suppression times. Similar fuel fire tests using foam and water suppression systems for USAF hangars have also been reported (3), in which JP-8 fuel was spilled and ignited on concrete surfaces in order to measure the ability of water-based systems to suppress flame spread and fire growth. In these tests, calorimeters were positioned around the perimeter of a 28 × 30 ft. concrete pad to measure and record the potential heat exposure to aircraft during suppressed and unsuppressed liquid fuel fires. The damage thresholds for representative aircraft structural materials and heat flux calculations to determine delamination times for composite materials have been previously reported in “Firefighting and Emergency Response Study of Advanced Composites Aircraft; Objective 1: Composite Material Damage in Minor Aircraft Fires”, AFRL-RX-TY-TR-2011-0046 (4).

Fuel spill fires, and the damages associated with them, could be mitigated by systems that actively remove flammable liquid from the spill source. The objective of this work was to evaluate fuel spill fire suppression by a commercial off-the-shelf (COTS) floor drainage system. The technology concept is generically referred to as an Ignitable Liquid Drainage Flooring Assembly (ILDFA). Safespill Systems, LLC (Houston TX) developed an ILDFA that actively flushes water through channeled flooring and propose implementing the system for Department of Defense (DoD) and industrial safety applications. Safespill also promotes their work for mitigation of alcohol fires and flowing (3D) kerosene fires. The manufacturer completed recent demonstrations (5) of the platform at the Fort Bend County firefighter training site (Texas) and shared test results that examined whether the flooring manages a simulated "drop-wing" fuel spill fire. The test documentation was compelling enough to encourage further independent tests, and USAF engineers developed test regimen to rigorously evaluate the ILDFA. The Safespill "drop wing" test was a derivative of prior USAF tests (2) but lacked instrumentation to collect quantitative data during the demonstration fire testing. If the USAF and DoD choses to implement the ILDFA product it is critical that there are independent tests, collection, and interpretation of relevant data in order to evaluate performance and its potential utility for AF Fire Protection.

After completion of testing, an ILDFA was installed at Edwards AFB as an operational test. Appendix B reviews the information gathered from a survey of users of the ILDFA at Edwards AFB. Survey questions were designed to understand the level of difficulty to assemble, maintain and perform standard tasks on the IDLFA system. Written responses were assigned to a category or positive, neutral, or negative while ease-of-use questions had a five point scale ranging from very easy to very difficult.

The ILDFA may have additional DoD application for the mitigation of hazardous waste spills. Storage, handling, and shipping areas have risks of container damage, decay, or other mishap that would release hazardous spills. An ILDFA could collect and transfer the spilled material to safe containment vessel minimizing risk and clean-up costs.

3. METHODS AND PROCEDURES

Tests were designed to measure the heat impact from different volume fuel spills on a concrete floor (Objective 1 (baseline control)), and then compared to heat impact from different volume fuel spills on an ILDFA (Objective 2). The ILDFA includes an active water flushing system that assists with rapidly removing fuel from the spill area. Another series of fuel spill fires was done with the ILDFA flushing system inactivated (passive), which evaluated suppression effect from simple gravity-driven flow of the liquid fuel through the channels (Objective 3).

3.1. Facility and Test Infrastructure

All tests were done at the Test Range II fire test facilities at AFCEC/CXAE, Tyndall AFB. The fires were done inside the site's Quonset-style structure (30 ft. peak ceiling height, interior floor dimensions 74 × 80 ft.). The facility has concrete walls and ceilings; a 20 ft. apron near the front entry has a steel ceiling and steel wall, there are two metal doors that were open during fire

testing (each ca. 10 × 17 ft. (w × h)). The facility was used for all tests, with fuel spills confined by the 30 × 30 ft. steel pan. Fuel spills were designed to mimic the spill fires previously reported (2) and similar manufacturer demonstrations so that test data and system performance could be justifiably compared.

3.1.1. Concrete Flooring

A concrete floor was installed inside the facility for the baseline fire tests. A pan was constructed by welding steel panels (7 gauge) to form a 30 × 30 ft. floor. The perimeter of the pan was 6×3½× ⅜ in. angle iron continuously welded to the floor panels to frame the concrete and contain fuel. Concrete was poured into the pan to an average depth of 3½ in. The concrete was a high temperature resistant formulation, 5,000 psi compressive strength, and included 1.5 lbs. of fiber reinforcement per yard. The fiber was substituted for steel reinforcement with intent to reduce spalling of the concrete from the expected extreme temperatures.

3.1.2. ILDFA System Installation

The ILDFA (Figure 1) was purchased from Safespill Systems, LLC, Houston, TX, and installed above the concrete flooring as described below.

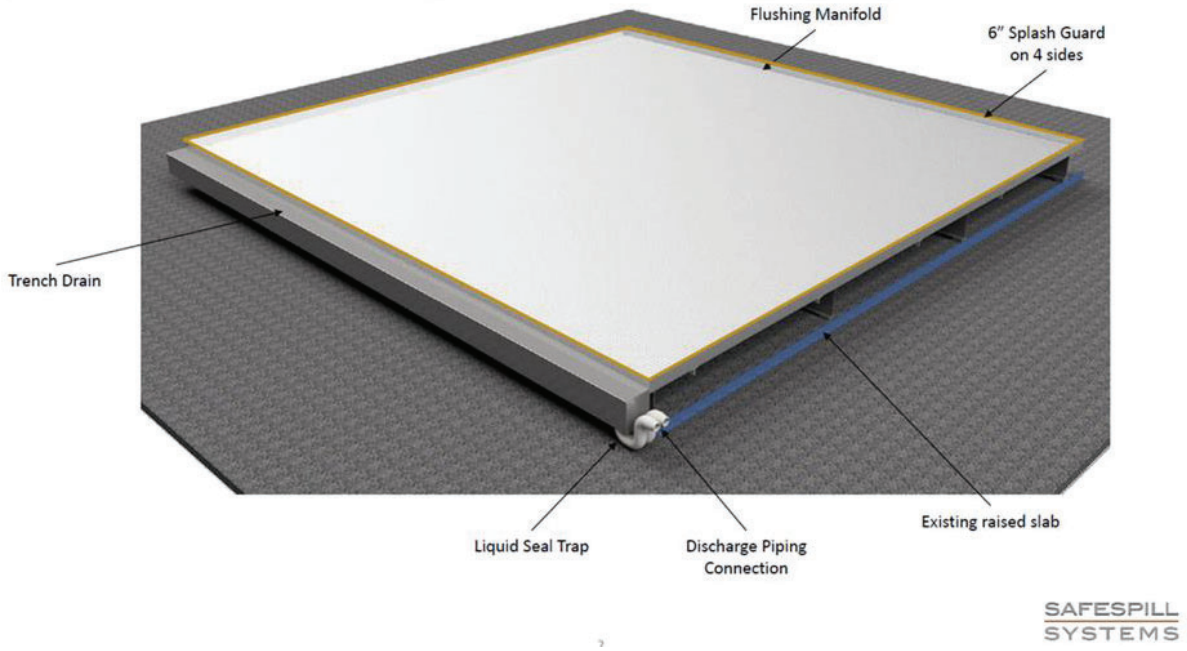

Figure 1. Artist Rendering of Safespill ILDFA Drainage Deck

The system was delivered in sections that were 29.3 ft. long by six and eight feet wide, the panels were mechanically fastened together using stainless steel machine screws. The ILDFA covered a 29.3 x 30 ft. floor area and comprised 180 individual 2 in. wide channels. Each channel included 60 ½ in. diameter drainage holes on the upper floor surface as shown in Figure 2. Hardware cloth beneath the drain holes are intended to reduce foreign objects entering the drain channel. The entire system was installed on I-beams for a nominal height of 26 in. above the concrete floor. The floor was installed with a 0.5 percent slope (ca. 1¾" over length of platform) to provide the grade for spills to flow toward the trench drain (Figure 1). A control panel coordinates operation of all system components. The ILDFA manifold injects water into the individual drain channels to actively flush fuel spills toward the trench drain. An optical fluid

sensor installed in the trench drain activates the flushing system when a fuel spill is detected. The activation starts the water flushing manifold (water flow 45 gpm at 120 psi) and the trench drain discharge diaphragm pumps remove fuel and water from the drain.

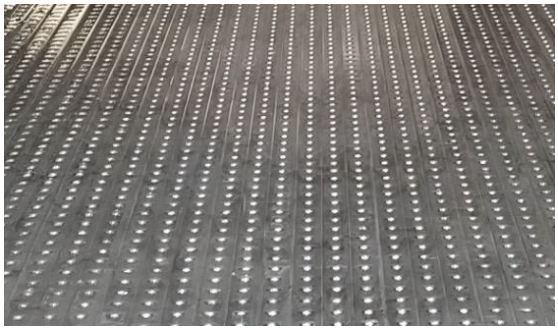

Figure 2. ILDFA Walking Surface with Machined Holes for Liquid Drainage

3.1.3. Aircraft Mockup

A test structure was constructed from steel in order to withstand numerous liquid fuel fire tests and estimate the heat transfer from the fuel spill fire to the lower surfaces of an aircraft. The mockup represented a specific portion of a fighter fuselage, a portion of a wing, and the area where the wing and fuselage join. An illustration of the mockup relative to the size of a representative fighter aircraft is shown in Figure 3.

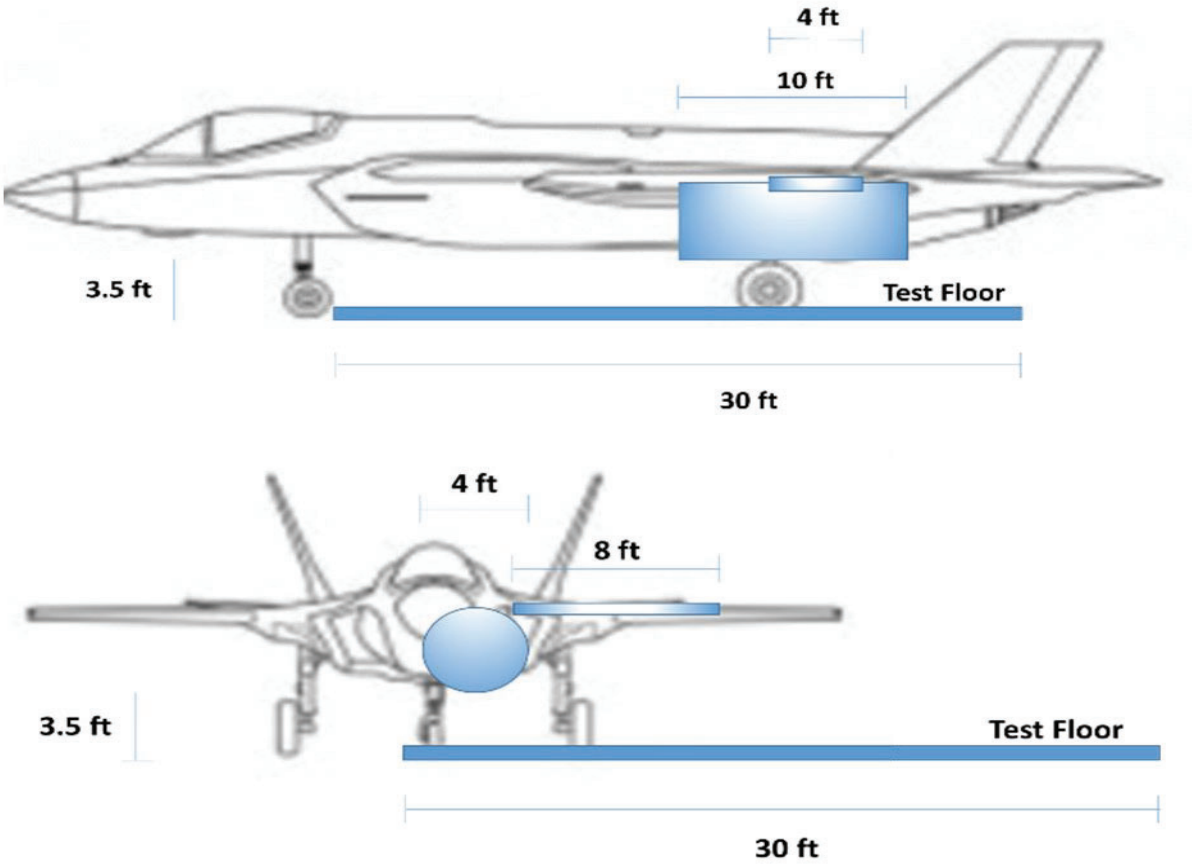

Figure 3. Fuselage (Upper Image) and Wing (Lower Image) Mockup

Note: Schematic shows relative scale to a fighter aircraft and the test flooring

The fuselage mockup is a 4 × 10 ft. (internal diameter × length) steel tube (¼ in. thick), held 3½ ft. above the floor by steel support framing. The wing mockup is fabricated from a 4 x 8 ft. steel sheet (¼ in. thick) that is attached to the fuselage mockup and is held 7 ft. above the floor by steel framing (Figure 4). Heat flux sensors were mounted flush to the surface of the mockup (Figure 3) facing toward the floor to best measure heat impact to the aircraft surface.

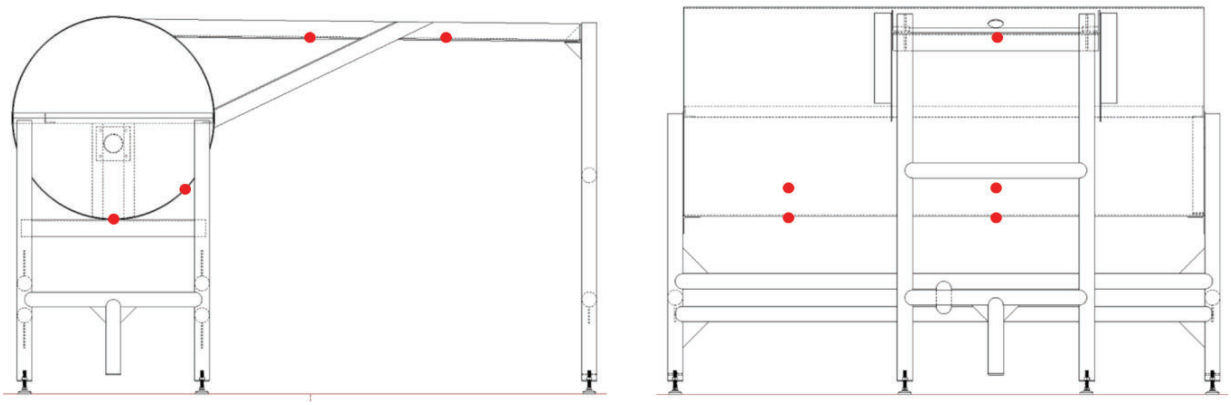

Figure 4. Front and Side Views of the Mockup Fuselage and Wing Showing Heat Flux Sensor Placement (Depicted by Red Dots)

3.1.4. Instrumentation and Measurements

Digital videography was used to document the fire tests. A minimum of three high-definition (HD) video cameras were used to record each live fire test. Still images were made from the videos in order to highlight selected points for records. A thermal imaging camera was also used for analysis of fires and the ILDFA system. Additional cameras transmitted live video feed to the control room during tests. Heat flux sensors and thermocouples were installed to monitor heat impact to mock aircraft surfaces, areas adjacent to the fuel spill, and air temperatures in the facility during fire tests. Variables during testing included fuel spill volume, spill surface, and flow rate. Measurements recorded included heat flux on the aircraft mockup and adjacent to the fuel spill area (Table 1 and Figure 5) and air temperature of the surrounding area and center of the ILDFA platform (Table 2 and Figure 5). Instrumentation measurements and ignition were controlled using National Instruments c-Daq hardware and LabView software.

3.1.4.1. Video Analysis

Fire tests were captured using standard video and infrared (IR) cameras to view the spread of the fire, fire duration, and estimate fire intensity based on thermal energy profiles. The fire duration times were determined by using IR video data and comparisons to captured videos of the fire. The starting time of the fire (t-0), was the instant when the ignited fuel made the first contact with the floor. The burning fuel contact point was used to synchronize video footage. The intensity of the fire was monitored by inspection of the IR video. The peak intensity was selected at a point when the greatest area of image was at thermal imaging limit (i.e., >300 °F ("white-hot")). The IR images were then inspected and times points noted when peak temperature zones decreased in area. The standard live video footage was also evaluated but sometimes obscured by

smoke. At 99% suppression, there were typically a few “candling” flames, but otherwise fires had self-extinguished.

3.1.4.2. Heat Flux Measurements

Heat flux was measured to determine the incident heat impact to the aircraft wing, fuselage, and other equipment adjacent to a fuel spill fire. Sensors were located on the underside of the mockup fuselage and wing surfaces, on all four sides of the concrete and ILDFA floor system, 10 ft. above the center of the fuel containment area. An additional sensor was placed in position representing an adjacent aircraft wingtip location in a portion of the tests. Schmidt-Bolter type, water-cooled heat flux gauges from Medtherm Corporation model # 64-25SB-18, calibrated from 0 to 250 kW/m^2, were used to measure total heat flux at the wing and fuselage surfaces. Perimeter heat flux was measured with Medtherm Schmidt-Bolter type, water-cooled heat flux gauges models 64-25SB-20, 64-25T-25R(s)-21735, and 96-2530T-30RP(ZnSe)-120-21746. Two additional non-water-cooled high-temperature heat flux sensors with a measurement range of ± 1,000 kW/m^2 (FluxTeq LLC (Blacksburg, VA) model # HTHFS-01) were used at three locations above the center of the fuel spill area (10 ft. elevation), on the wing, and at a point representing an adjacent aircraft fuselage. Figure 5 shows the location of the heat flux sensors relative to the fuselage and wing mockup and relative size and position of the mockups superimposed on a typical fighter aircraft.

Total heat flux incident to the underside of the aircraft wing mockup was collected at two locations. The sensors were installed equidistant from each other, the fuselage, and from the outboard edge of mockup wing structure. The sensor orientations were perpendicular to the floor. Data for total heat flux incident to the fuselage of the aircraft wing mockup were collected at four locations. Two sensors were placed on the underside of the mockup fuselage and perpendicular to the floor (F1 and F3 in Table 1) and two sensors were placed on the side of the mockup fuselage facing the floor at a 45° angle (F2 and F4). Heat flux around the perimeter of the ILDFA containment fuel spill area was measured with four heat flux gauges installed 16 ft. from the center of the ILDFA containment area, one at the mid-point of each side, two feet above the containment pan floor, and facing the pan center (Table 1). These sensors were positioned to collect data similar to previous sensor locations for JP-8 fuel spills fires on concrete surfaces (3). Two additional sensors were installed 10 ft above the center of the test floor, perpendicular to the floor, and at a location representing an adjacent aircraft fuselage, 33 ft away from and facing the mockup fuselage.

Table 1. Heat Flux Sensor Location and Notation

Sensor Name	Location	Notation in Data
WH (West Heat Flux)	West	W or West
EH (East Heat Flux)	East	E or East
NH (North Heat Flux)	North	N or North
SH (South Heat Flux)	South	S or South
Fuselage point 1	F1	F1
Fuselage point 2	F2	F2
Fuselage point 3	F3	F3
Fuselage point 4	F4	F4
Wing Outboard	WO	Wing Outboard
Wing Inboard	WI	Wing Inboard
Center Heat Flux	10 ft. Above Center of Pan	Center
Adjacent Fuselage	33 ft. East of Mockup	Adjacent Fuselage

3.1.4.3. Temperature measurements

The locations of the installed thermocouples (TC) (denoted as TC in Figure 5) are summarized in Table 2. The TC positions effectively replicated prior tests (2) and allowed the comparison between trials. Thermocouples were installed on steel structure framework at four different locations (Figure 4), adjacent to the fuel spill origin on the North edge of the pan, above the center of the flooring, and on the center edge of two sides of the spill area. For tests on bare concrete, thermocouples were installed at 5, 10, 19, and 26 ft. above the floor. The uppermost thermocouple height was limited in one instance by the curvature of the facility ceiling and set at approximately 23 ft. With the ILDFA floor installed, the thermocouples at 5 and 10 ft. above the concrete floor were repositioned to remain 5 and 10 ft. above the ILDFA floor. The upper thermocouples were not repositioned and accordingly were ca 17 and 24 ft. (or 21 ft.) above the ILDFA surface.

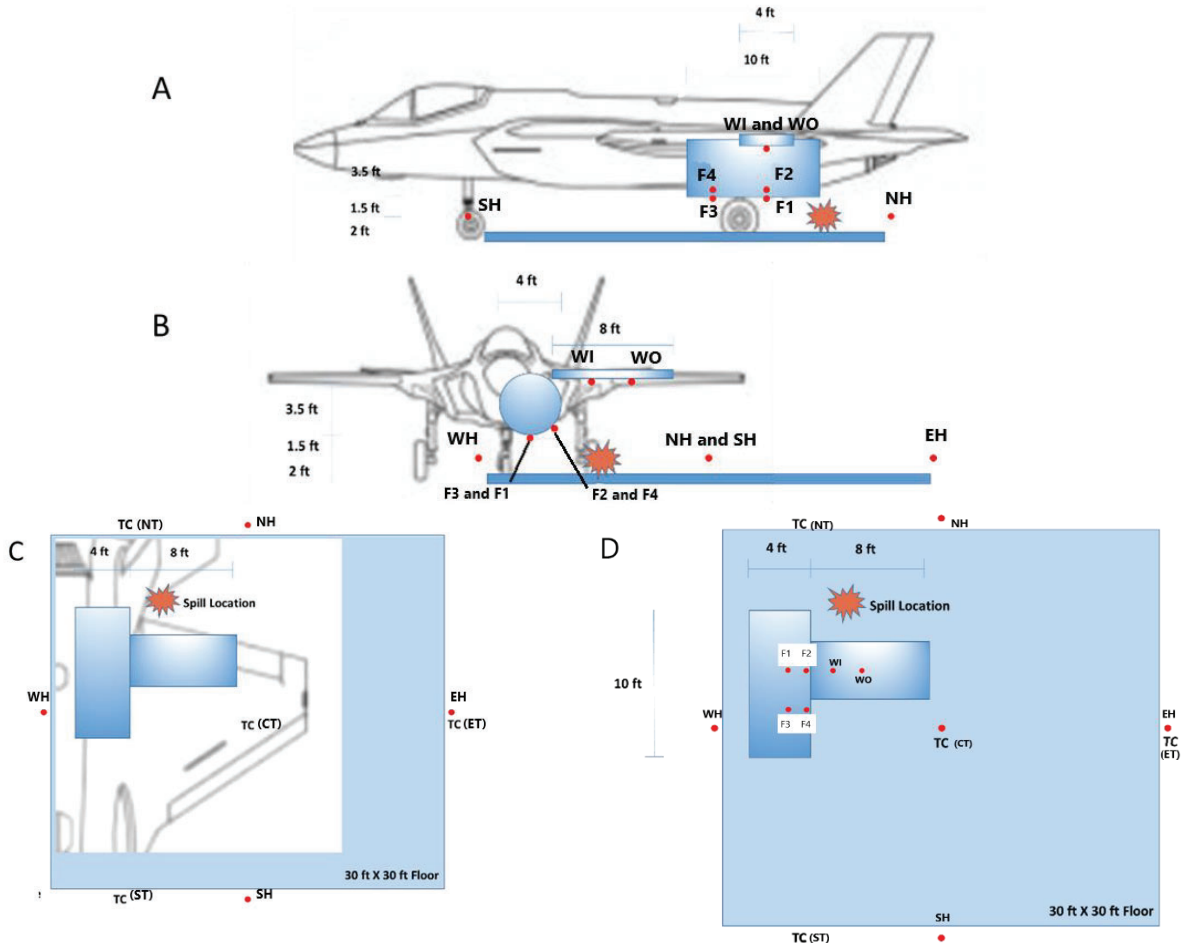

Figure 5. Fuselage and Wing Mockup, Heat Flux (red dots) Thermocouple (TC), and Fuel Spill Locations

Note: Shown are side (A), front (B), top (C), and bottom (D) views respectively. Thermocouple (TC) tree locations are noted.

Table 2. Thermocouple Tree Location and Notation

Sensor Name	Location	Notation in Data
ET (East thermocouple)	East	E or East
ST (South thermocouple)	South	S or South
NT (North thermocouple)	North	N or North
CT (central thermocouple)	Center	C or Center

3.1.5. Fuel Spills

Synthetic JP-4 fuel was blended for each test (kerosene and gasoline (2:1 (vol:vol)) and dispensed into a 200 gal steel hopper (Figure 6). Figure 7 shows the final test area setup with fuselage and wing mockup, spill hopper on the concrete floor, three of the four thermocouple trees, and three of the four perimeter heat flux sensors. The same locations and orientations were used for ILDFA testing.

Figure 6. Fuel Spill Hopper

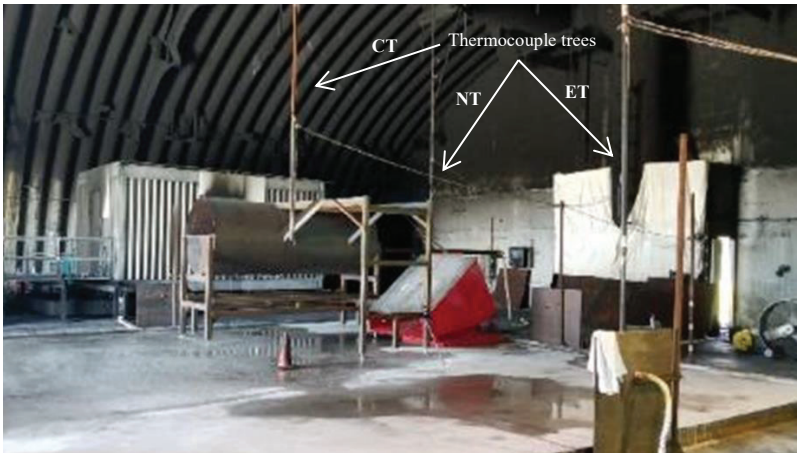

Figure 7. Test Stand Configuration Setup for Concrete Floor Trials.
(South thermocouple tree is outside of frame)

Five fuel spill quantities were tested in triplicate for each of the 3 test objectives (Table 3). The initial fuel spill sizes planned were 15, 30, 55, 110, and 165 gal. These volumes provided progressively larger fuel spills and the largest volume matched the quantity in prior testing (2). Initial spill trials were conducted substituting water for fuel in the hopper. The spill trials were conducted on both the concrete floor and the ILDFA flooring to estimate the spread of the fuel before testing (Figure 7). For concrete floor spills, however, the 55 gal fuel spill was determined to be the maximum fire intensity acceptable to prevent damage to the facility and test structures. As a result, the fuel spill volumes on concrete were modified to 15, 22.5, 30, 42.5, and 55 gal. Table 3 shows the overall test matrix for fire tests.

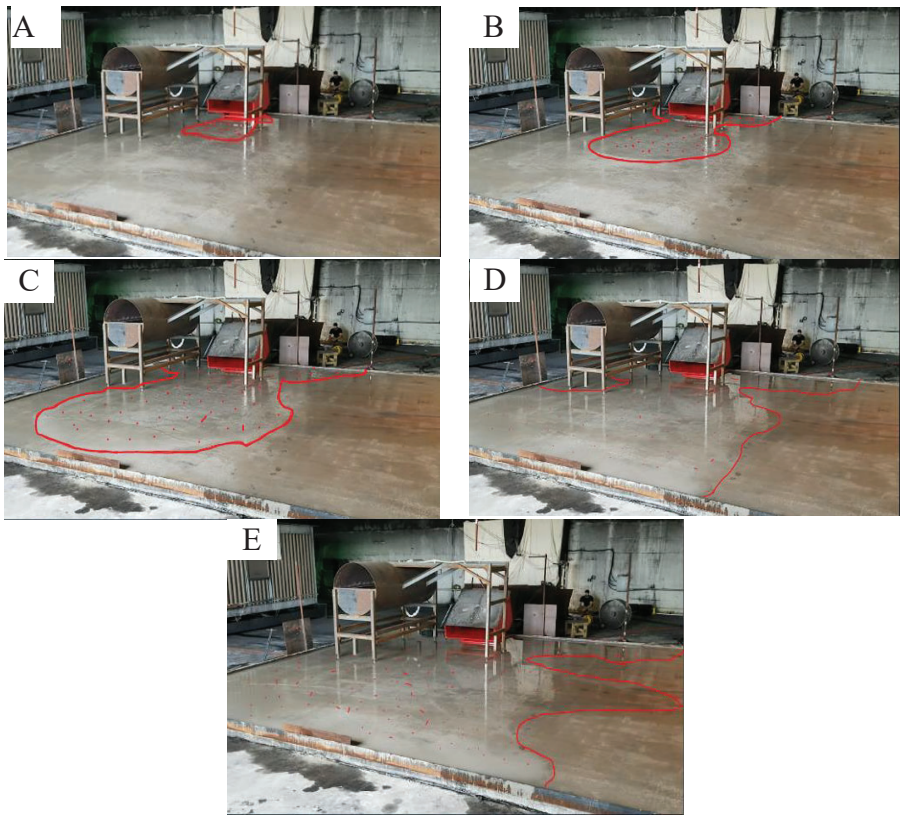

Figure 8. Water Spill Trials to Estimate Fuel Spread from Dump Hopper. Thin Red Lines Depict Edges of Spilled Liquid on the Concrete

Table 3. Test Matrix for Fuel Spill Fire Tests

Fuel Volume (gal)	Concrete	ILDFA	ILDFA (passive)	Hopper rotated
15	X[a] (3[b])	X (3)	X (3)	
22.5	X (3)			
30	X (3)	X (3)	X (3)	
42.5	X (3)			
55	X (3)	X (3)	X (3)	X (1)
110		X (3)	X (3)	
165		X (3)	X (3)	

Key: a-tests done, b-number of valid replicates

Fuel was ignited and 15 s pre-burn allowed before being spilled onto the floor (Figure 9). The hopper was released by a spring mechanism and then tipped using an electric winch to consistently "spill" (pour) the fuel in each test. The same hopper tipping rate was used for all spills and resulted in a higher average flow rate as fuel volumes increased. (Table 4). On average, the fuel completely drained from the hopper in fewer than 15 s.

Table 4. Hopper Spill Flow Rate

Fuel Volume (gal)	Flow Rate (gpm)
15	150
30	257
55	330
110	508
165	582

Flow rates estimated using total time to drain hopper after tipping (water tests)

Figure 9. Fuel "Pre-burn" Before Fuel Spill on Concrete

The momentum of the spill resulted in a consistent fuel flow in one direction from the rear of the mockup wing toward the nose of the fuselage in all tests. In each test, a small quantity of the spill flowed under and around the spill hopper.

3.1.5.1. Fuel Ignition System

A remote ignition system was used to ignite the synthetic JP-4. A small coil of nichrome wire was used to ignite a small bundle of wood wool (excelsior material). The system is powered by 120 VAC that is switched using the data acquisition system and a solid-state relay. The voltage was reduced to approximately 15 volts of alternating current (VAC) with an auto transformer and used to heat the nichrome wire. A small coil of nichrome wire was heated to the ignition temperature of wood shaving excelsior material. The coil and excelsior were prepositioned inside the hopper prior to transferring fuel into the hopper. Prior to testing, excelsior was stored to limit absorption of moisture that would affect ignition. A propane torch was used by firefighter personnel as a back-up ignition process if remote system failed. If torch ignition was used, approximately five seconds were added to the pre-burn interval.

4. RESULTS

4.1. Unmitigated Liquid Fuel Fires on Concrete

The liquid fuel fires on concrete progressed rapidly and the fire and smoke quickly obscured the standard digital videos. As a result, the fire progression was more effectively monitored by using infrared imaging. To facilitate side-by-side comparisons for the range of fuel volumes tested, the same infrared dynamic temperature range was applied during all fire tests. The snapshots in Figure 10 show intensity progression of the fire on the concrete floor from a 30 gal fuel spill and is typical of all concrete spill fire tests. The size (diameter) of the burning fuel does not change significantly from the initial fuel spread (15 s, Figure 10A) to later peak time points, the volume of hot gases/smoke are, however, clearly greater as the fuel continues to burn (ca. 90 s, Figure 10B). The IR image at the 180 s mark (Figure 10C) shows signature appearance of active flames in lower left quadrant.

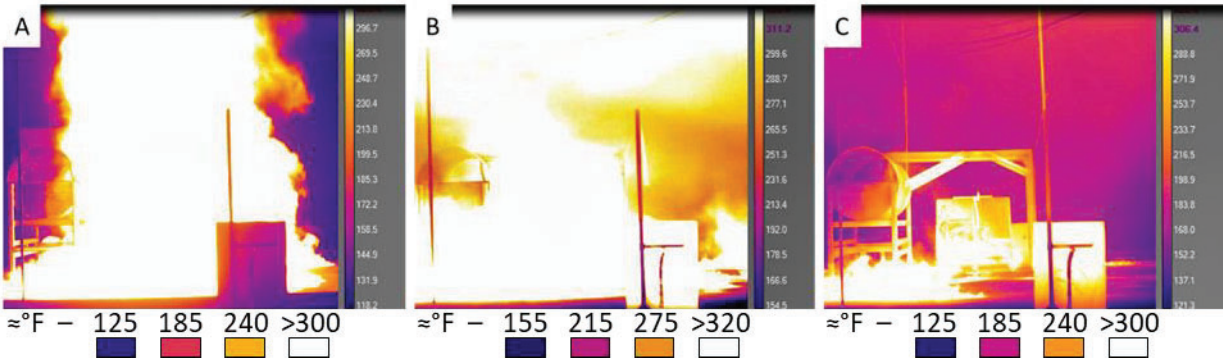

Figure 10. Infrared Images of a 30 gal Concrete Fuel Spill Fire at 15 s (A), 90 s (B), and 180 s (C) Time Points

The times recorded for self-extinction on concrete for various fuel sizes are summarized in Table 5. Test video was reviewed to determine the time when most flames had extinguished and only a few candle flames remained in the spill area. The end point range (99% self-extinguishment) for representative fires was ca. 4.5 to 6.5 min. The artificial small flames from fuel trapped under the spill hopper frame were not considered in this extinction time review. In all the unmitigated fires tests, the intensity of the fire was such that it could not be approached without protective gear more than three minutes after ignition, which is considered optimal response time for an aircraft rescue and firefighting (ARFF) team on a flight line. Accordingly, without a suppression system, other combustible materials may be damaged or ignited due to intense heat.

Table 5. Self-Extinction of Fuel Spill Fires on Concrete

Fuel Volume (gal)	99% Extinction Time (s)
15	298±52, n=3
22.5	265±22, n=3
30	325±4, n=3
42.5	345±9, n=3
55	384±23, n=3

4.1.1. Unmitigated Liquid Fuel Fires Heat Release Rate

There were no heat release rate (HRR) measurements conducted for the fuel spill fires in this study, however, estimates were made by using noted observations. These estimates were based on the initial fuel volume, approximations of the fuel spill sizes and intensities obtained from reviewing videos and photos, fuel properties (6) and calculations from a Nuclear Regulatory Commission (NRC) spreadsheet (7). The shape and size of the fuel spills was affected by the limits of the 30 x 30 ft. pan, the direction of the fuel spilled from the hopper, and the uneven surface of the floor. As a result, to simplify HRR estimation the fuel spill area was treated as a circular pool. Table 6 includes the fuel spill volume, estimated spill areas, estimated average fuel depth, estimated peak HRR, and the estimated time after the fuel spill commenced until the peak spill fire intensity (and presumed HRR) began to diminish based on video review. In general, the spill fires spread and reached peak flame heights (and thus presumed peak HRR) from 14 to 20 s after the fuel spill commenced. In all but the 15 gallon spill fires, ceiling height limited the ability to estimate flame height. A curve of the estimated (not measured) HRR during a 55 gal fuel spill fire on concrete is presented in Figure 11. For actual HRR determination, a large room calorimeter fuel spill fire test is recommended, however few test facilities are available for fuel spills of this size.

Elements discussed in the Fire Dynamics and Forensic Analysis of Liquid Fuel Fires (8) report were not factored into these estimates since the ignition and spill procedures in this study vary from the reported procedures and the estimated spill depths in this study (2.4 - 3.4 mm) were greater than the thinner depths (0.7 - 1 mm) evaluated in the report. If the report's thin fuel spill effects on heat release over time (8) were factored into the estimates, the HRR values in Table 6 would have been lower.

Table 6. Unmitigated Estimated Spill Fire Heat Release Rate

Fuel Spill Volume [gal (L)]	Estimated Spill Area [ft² (m²)]	Estimated Fuel Depth [in. (mm)]	Estimated Flame Height [ft. (m)]	Estimated Peak HRR (MW)	Estimated Time After Spill when Fire Intensity Diminished (s)
15 (56.8)	250 (23.2)	0.09 (2.4)	28 (8.5)	45	55
22.5 (85.2)	305 (28.3)	0.12 (3.0)	31 (9.4)*	55	54
30 (113.6)	415 (38.6)	0.11 (2.9)	31 (9.4)*	74	62
42.5 (160.9)	600 (55.7)	0.11 (2.9)	31 (9.4)*	107	73
55 (208.2)	650 (60.4)	0.13 (3.4)	31 (9.4)*	116	82

*limited by ceiling height

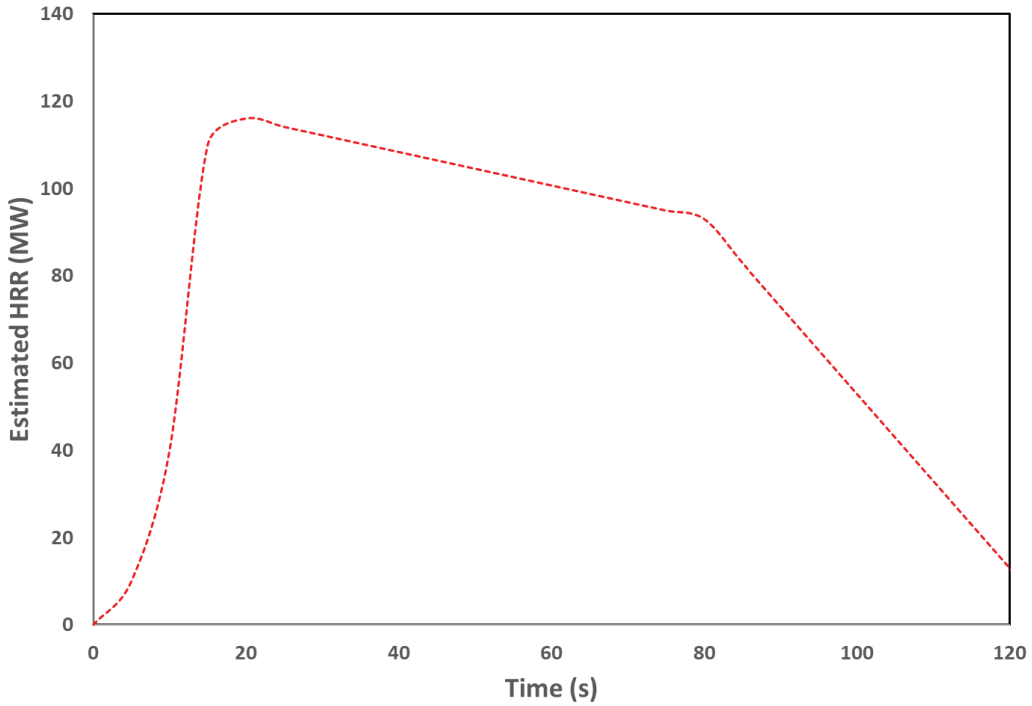

Figure 11. Estimated HRR from an Unmitigated 55 gal Fuel Spill Fire on Concrete

4.2. ILDFA Liquid Fuel Fires

Fuel spill fires on the ILDFA had different general shape and progression than those on bare concrete. The ILDFA drains and captures the fuel spill rapidly (by design), so there was comparatively little radial spread of fuel compared to bare concrete spills. Also, on the ILDFA, the fuel spill spreads predominantly from North to South with relatively little spread West and East (i.e., laterally), due to the flooring surface roughness and rapid drainage on the ILDFA. The combination results in an oval fluid flow distribution as demonstrated in Figure 12. In contrast, fuel spills on concrete spread unhindered and formed a more conventional circular spill pattern.

Figure 12. Oval Shape of fire on ILDFA floor
Key: Photos top to bottom; front view, right side view, and left side view

Images captured through IR imaging in Figure 13 compare the fuel spill fire on the two floors 15 s after the fuel was spilled from the hopper. In the larger volume fuel spills on the ILDFA, flame impingement on the wing is shown, however that contact is short lived, as the ILDFA flame heights drop rapidly. By comparison the concrete fuel spill fires entirely engulf the wing for much longer durations, and consistently reached the ceiling even at smaller fuel spill size (22.5 gal). A range of fuel spill volumes were evaluated and allowed to burn until the fire was out with the exception of a few candle size flames. Table 7 lists the times until 99% extinction.

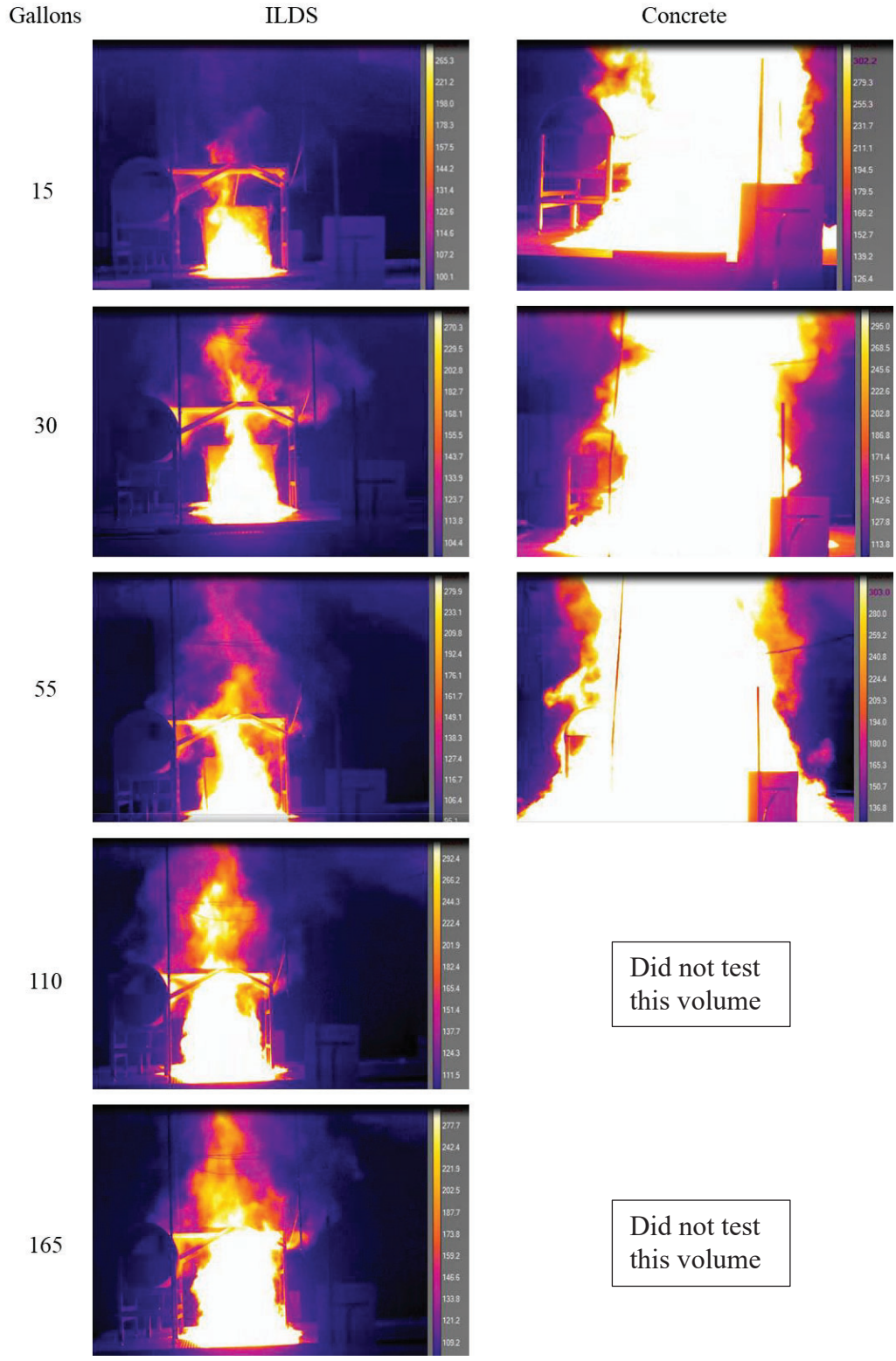

Figure 13. Comparison of Spill Fire Intensity at 15 s for ILDFA versus Concrete

Key: Fire intensity at 15s after hopper spill for 15 - 165 gal of synthetic JP-4

A range of fuel spill volumes was evaluated and allowed to burn until the fire was out with the exception of a few candle-size flames. Table 7 lists the times until 99% extinction.

Table 7. Self-Extinction of Fuel Spill Fires on the ILDFA with Flushing Water

Fuel Volume (gal)	99% Extinction Time (s)*
15	150 ± 7.5, n=3
30	168 ± 52.7, n=2
55	200 ± 7.6, n=3
110	295 ± 74.5, n=3
165	264 ± 42.2, n=3

4.2.1. IFDLA Liquid Fuel Fires Estimated Heat Release Rate

As with the concrete surface liquid fuel spill fire tests, an effort was made to estimate the peak HRR in the ILDFA fuel spill fires when the water flushing system was activated. Table 8 has the initial fuel volume and estimates of the fuel spill sizes and flame heights obtained from reviewing test videos. The fuel spills were affected by the floor surface, the quick draining into the ILDFA channels, and by the momentum from being poured from the hopper. The observed spill area on the ILDFA did not correlate to traditional pool fire expected flame heights because of the dynamic draining of fuel into the flooring. Therefore, to estimate peak HRR, spill area and fuel depth were not used. Flame heights over time and fuel properties (6) were used along with the NRC (7) to determine estimate peak HRR.

Table 8. ILDFA Estimated Spill Fire Heat Release Rate

Fuel Spill Volume [gal (L)]	Estimated Spill Area [ft^2 (m^2)]	Estimated Flame Height [ft. (m)]	Estimated Peak HRR (MW)	Estimated Time to Diminish Fire Intensity (s)
15 (56.8)	54 (5.0)	8 (2.4)	0.67	9
30 (113.6)	72 (6.7)	10 (3.0)	1.2	11
55 (208.2)	98 (9.1)	10 (3.0)	1.2	10
110 (416.4)	147 (13.7)	11 (3.4)	1.5	7
165 (624.5)	198 (18.4)	12 (3.7)	1.9	6

In general, the spill fires on the ILDFA spread, and then reached peak flame heights (and thus presumed peak HRR) approximately two seconds after the fuel spill commenced. Based on flame height observations, this peak HRR began to diminish in fewer than 10 s. A curve of an estimated HRR during 165 gal fuel spill fires on the ILDFA is presented in Figure 14. For accurate HRR results, a large room calorimeter fuel spill fire test is recommended.

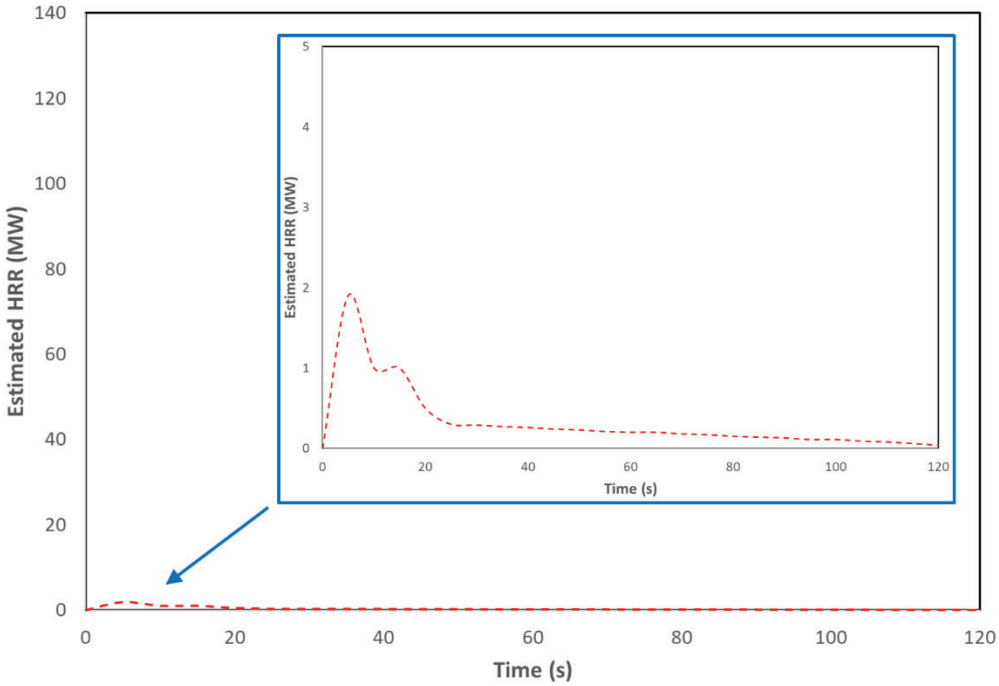

Figure 14. Estimated HRR from a 165 gal Fuel Spill Fire on ILDFA

Key: Inset in Figure shows an expanded view of the estimated HRR to see plot compared to full scale axis.

The ILDFA mitigated peak HRR estimates are much less than comparable spills on a concrete surface and the duration of the peak intensities are short as the spill volume rapidly reduces due to draining. Although not tested, it appeared the fires could have been readily extinguished or suppressed soon after the spill with a handheld, Class B fire extinguisher. The progress of the fire at three time intervals after the spill is demonstrated in Figure 15 for a 30 gal fuel spill. The primary signature in 90 s and 180 s images was the fuel hopper, likely heated while burning the fuel prior to tipping the hopper

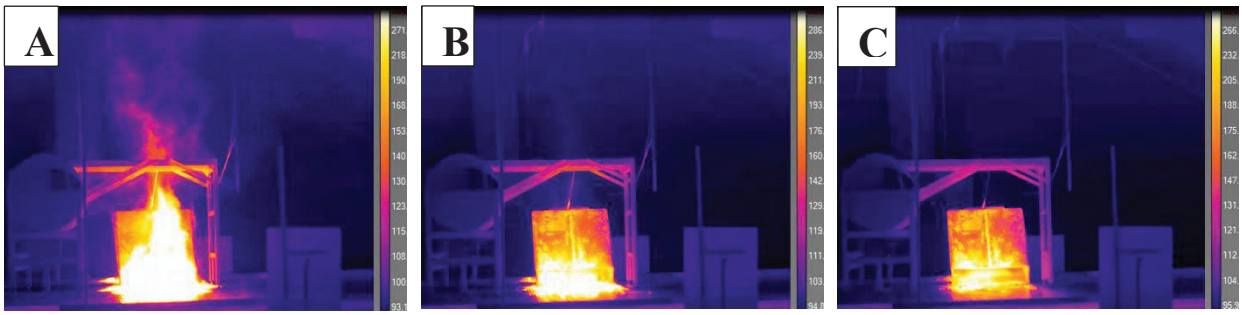

Figure 15. Infrared Images of a 30 gal ILDFA Fuel Spill Fire at 15 s (A), 90 s (B), and 180 s (C) Time Points

4.2.2. IFDLA Combustion Away from the Spill Location

During the ILDFA testing of fuel spills with and without water flushing activated, re-ignition of the fuel was observed at locations several feet away from the spill location and above the ILDFA channels. After the initial spill, the fire size decreased rapidly, at the origin but as the unburned fuel drained away in the subsurface channels, flames reemerged at the random distances several feet south and north from the spill origin and typically in the direction of the fuel draining toward the floor trench drain for a swift amount of time. The ignition may be attributed to oxygen deprivation in the channels near the spill origin; then when the vapors were released from the flooring channels and exposed to air, the temperature was sufficient to reignite. The secondary flames ranged in size from small candle flames up to two feet high and of modest intensity. These secondary flames were considered for determining total burn durations. Figure 16 shows secondary flames away from the original spill location during a 110 gal spill fire test.

Figure 16. Re-ignition of Fuel vapors on the ILDFA

The left snapshot shows smaller flames away from the spill origin as the initial spill fire subsides, the arrow in right image highlights the larger flames after re-ignition

While the fire threat is reduced using the ILDFA flooring, the threat is not eliminated. Fire sizes, durations, and potential damage were shown to decrease as compared to an unmitigated fuel spill, however small fires can still occur. In addition, there is the risk that fuel vapors released from the incident flooring channels can result in small flames at locations several feet away from the fuel spill. This poses an additional threat that should be considered in operational planning.

4.2.3. Comparison of ILDFA with and without Active Water Flushing

ILDFA tests were done with and without the water flushing system activated to compare the fire suppression difference in the case of a malfunctioning flushing system. The flowing water in the channels creates momentum to move fuel toward the main drain and may also provide cooling of the channels and fuel.

The total heat flux absorbed (in kJ/m^2) by each of the perimeter heat flux sensors for the duration of the fire was calculated for each test. The triplicate test results for each sensor and fuel spill size (from 15 to 165 gal) were averaged and are shown in Figure 17. To further consolidate the data and make comparisons, the data from each of the fuel spill sizes were averaged for each sensor and is presented in Table 9. To determine the statistical difference between IDLFA with water, IDLFA without water, this total heat from all trials was compared at each point using the analysis of variance (ANOVA) test. Within the data set, the East and West sensors are more representative of the radiative heat away from the flames as the fuel spills may have progressed

adjacent to the North and South sensors in some tests affecting these measurements. From Figure 17, the water flushing system resulted in slightly lower measured perimeter heat flux, however the uncertainties in Table 9 show that there is no statistical difference between the West and East sensors when the flushing manifold is on or off. Although, it is shown that there is a statistical increase in the heat measured with the surrounding are for the North and South sensors.

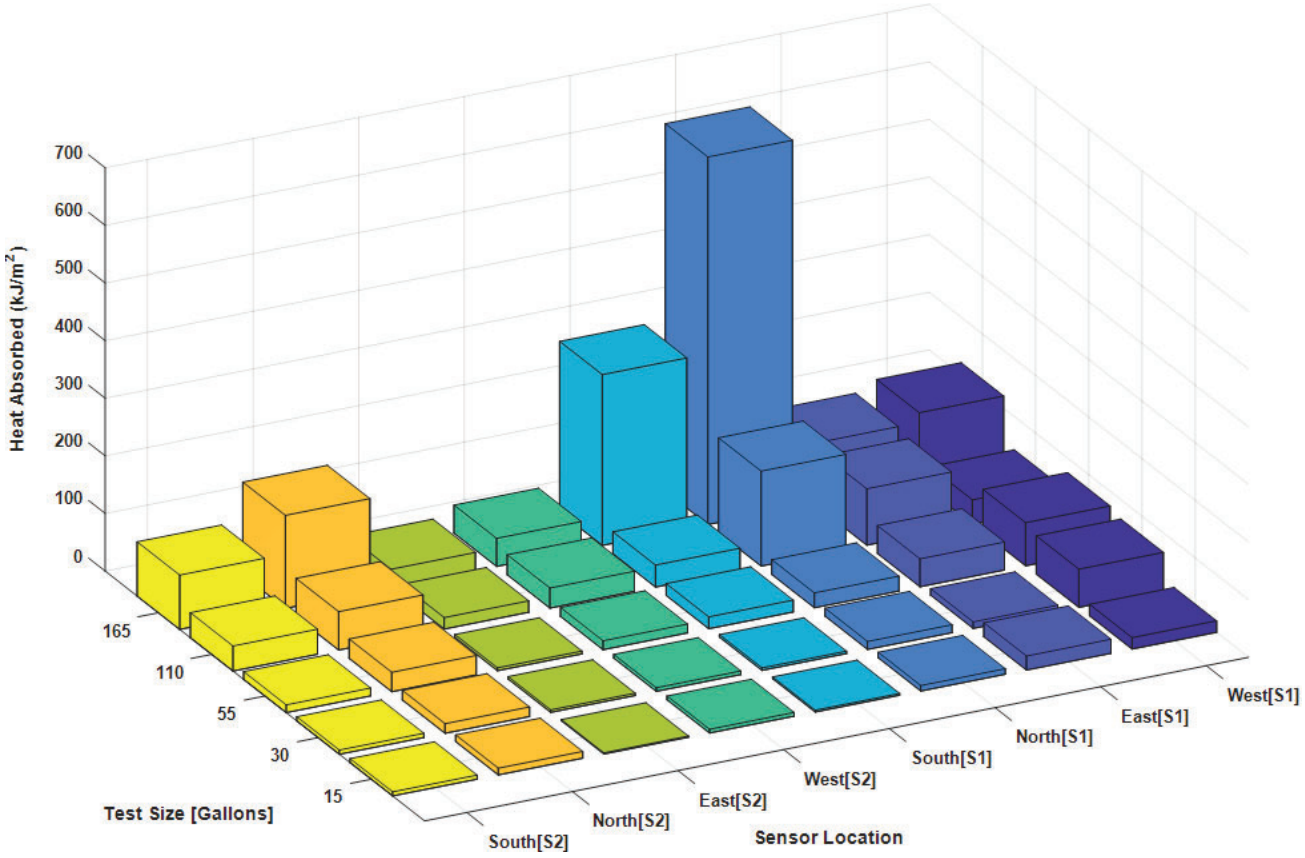

Figure 17. ILDFA Perimeter Energy Absorbed With [S1] and Without [S2] Flushing Apparatus Activated

Table 9. Mean ILDFA Perimeter Energy Absorbed in all Spill Sizes With and Without Flushing

	ILDFA with Water (kJ/m²)	*ILDFA without Water (kJ/m²)*	*Percent Difference*
West	22 ± 7 (*n*=15)	65 ± 47 (*n*=15)	66.15% (P=.02) (*n*=30)
East	13 ± 3 (*n*=15)	57 ± 39 (*n*=15)	77.19% (P=.02) (*n*=30)
North	58 ± 10 (*n*=15)	170 ± 56 (*n*=15)	65.88% (P=.19) (*n*=30)
South	33 ± 10 (*n*=15)	73 ± 46 (*n*=15)	54.79% (P=.26) (*n*=30)

In addition to heat flux, temperature data were reviewed to evaluate differences from having the ILDFA water flushing system activated or disabled (passive). Average peak temperature for the duration of each of the three 110 gal fuel spill fires at each of the 16 temperature sensors is shown in Figure 18 and Table 10 shows the average temperature of all 16 sensors for the duration of each size fuel spill fire with and without water flushing. To determine the statistical difference between IDLFA with water and IDLFA without water, the average temperature was compared using the ANOVA test. As with the heat flux measurements above, the uncertainties in Table 10 show that there is no statistical difference in the room temperature results with or without the water flushing system activated.

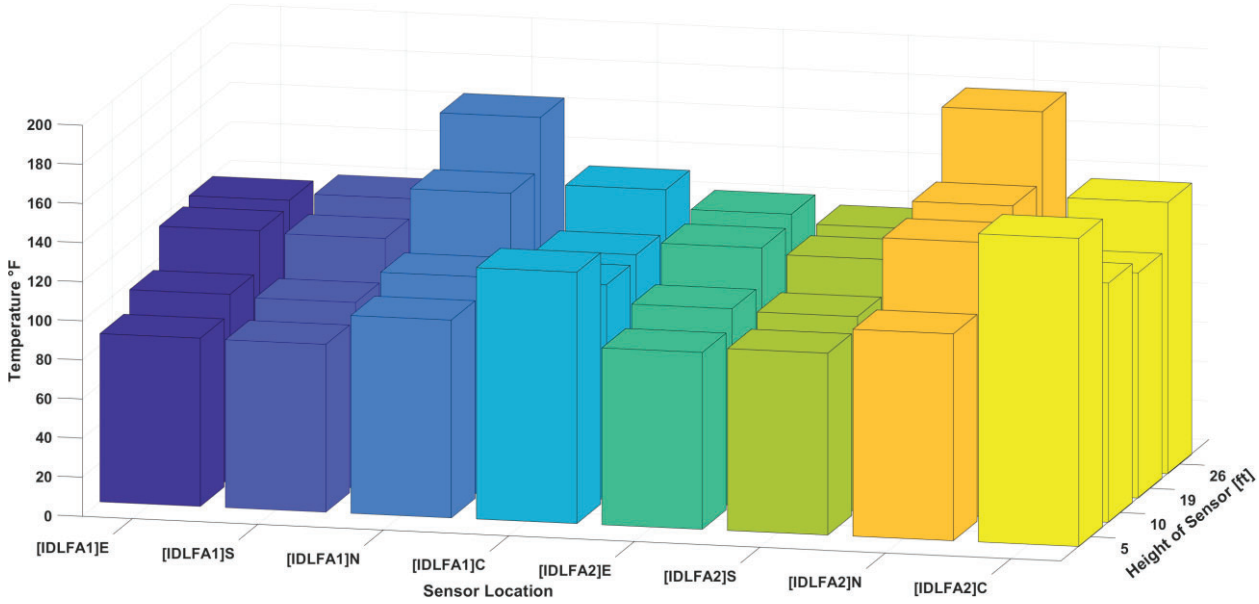

Figure 18. 110 gal ILFDA Mean Peak Temperatures With [IDLFA1] and Without [IDLFA2] Flushing

Table 10. ILFDA Mean Peak Temperatures With and Without Water Flushing

Fuel Volume (gal)	Active ILDFA (with flushing) (°F)	Passive ILDFA (without flushing) (°F)	Percent Change
15	88.74 ± 5.32 (*n*=16)	95.31 ± 5.93 (*n*=16)	6.66 (P=0.15) (*n*=32)
30	96.07 ± 13.89 (*n*=16)	94.29 ± 4.32 (*n*=16)	-1.46 (P=0.82) (*n*=32)
55	99.15 ± 13.29 (*n*=16)	106.94 ± 17.35 (*n*=16)	6.79 (P=0.50) (*n*=32)
110	102.85 ± 8.59 (*n*=16)	115.53 ± 19.53 (*n*=16)	9.32 (P=0.28) (*n*=32)
165	129.13 ± 34.82 (*n*=16)	108.51 ± 7.07 (*n*=16)	-20.57 (P=0.29) (*n*=32)

4.3. Temperature Profiles During Fire Testing

Analysis of the room temperature sensor profiles provides insight to thermal energy transfer and total heat release from the fires. At the same time, there are limitations to the 16 single point air temperature measurements in a large volume room. The temperature sensors may be measuring air temperatures or if in the flame, fire plume temperatures. Additional discussion of how air temperature measurements in this study compare to air temperatures measured in prior 165 gal JP-4 fuel spills can be found in Section 5.2.

The maximum measured temperatures at various heights above the floor were averaged from triplicate fire tests and plotted in Figure 19 for unmitigated concrete and ILDFA 55 gal fuel spill fires. These plots show air temperatures at each of the four 10 ft. high thermocouple sensors and reveal dramatic difference between the spill fires on concrete versus those on the ILDFA. The North and Center thermocouple positions were immersed in or adjacent to the fire plume in the concrete spill fires and were slightly further away from the fire plumes in the ILDFA fires due to those smaller-in-area spill sizes. The unmitigated spill fire thermocouple at the North location spiked at over 2,000 °F and the center spiked over 1,700 °F. Each of the four 10 ft. thermocouples measured temperatures exceeding 500 °F during unmitigated concrete spill fires, while the readings for the ILDFA were less than 100 °F, apart from one North sensor reading of 140 °F. Together the measured temperature analysis indicate that the ILDFA system significantly reduced the thermal energy risk and the fire intensity.

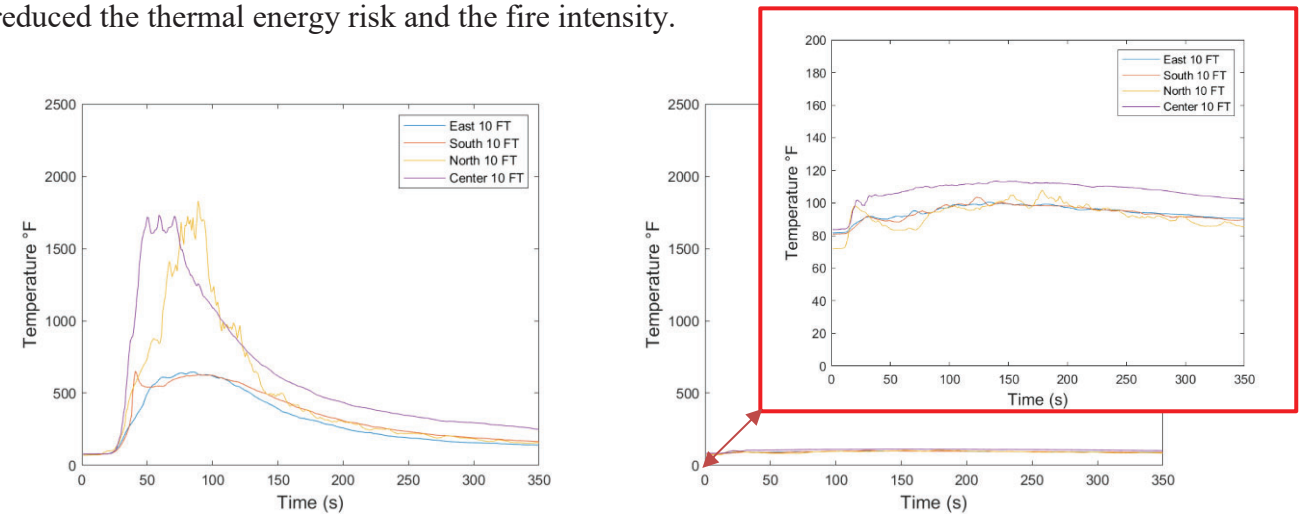

Figure 19. Mean Temperature Profiles of 55 gal Fuel Fires at 10 ft. – Unmitigated Versus Active ILDFA

Key: Concrete fire (left) and ILDFA fire (right). Data plot of the response for thermocouples 10 ft. above floor. Inset in right panel shows an expanded view of the ILDFA temperature profile in order to see plot compared to full scale axis.

From Figure 19, the peak temperature occurs at 77 ± 17 s and takes approximately 300 s to dissipate to less than 150 ºF. By comparison, fire testing with ILDFA recorded maximum temperature at the 10 ft. high center sensor that never exceeded 150 ºF. The ILDFA system rapidly removes the unburned fuel limiting spread and intensity of the fire. The peak temperature is significantly lower and the fire size begins to decline approximately 10 s after the fuel spills.

Figure 20 shows the average of the maximum measured air temperature for each of the 16 thermocouples during 55 gal concrete and ILFDA fuel spill fires. The maximum recorded temperatures were at the center thermocouple tree which was closest to the fuel spill and fire plume. For concrete fires, some thermocouple measurements exceeded 2,000 °F as the fuel spills were larger in surface area, flame height, and were directly below this thermocouple tree. The ILDFA limited the 55 gal fuel spill size so the ILDFA fires were lower in peak height and not directly below this thermocouple tree. Maximum temperature recorded in all three active flushing ILDFA tests were 175 °F and a maximum of 170 °F when the flushing system was inactive.

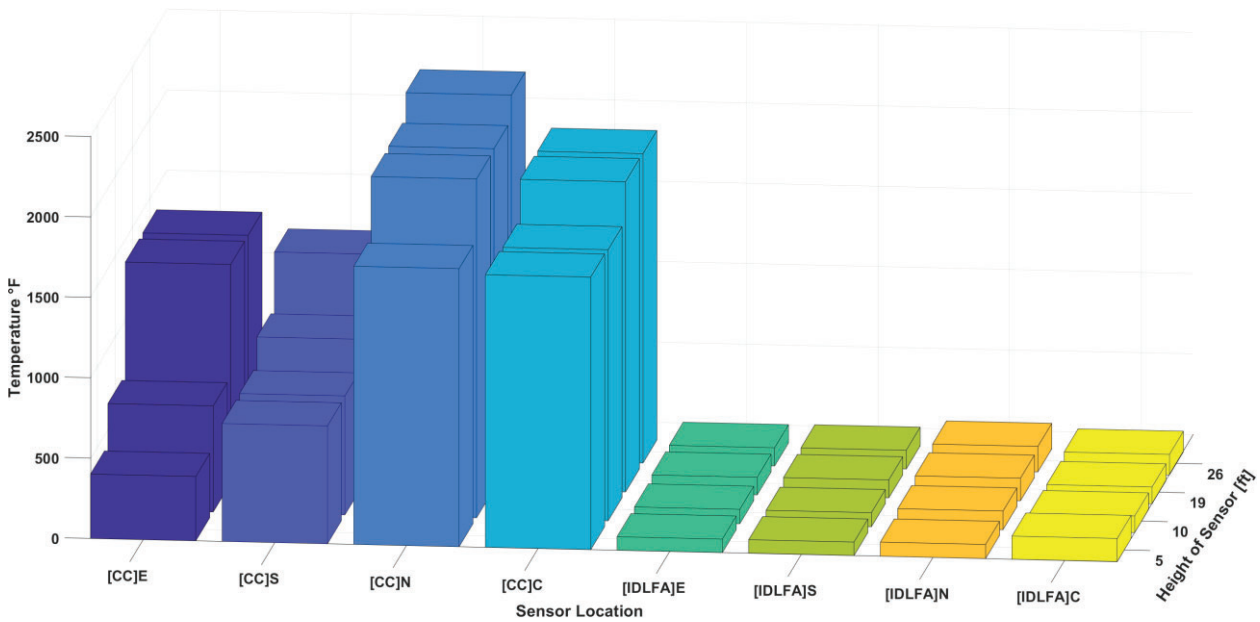

Figure 20. Mean Maximum Air Temperature for Concrete versus ILDFA 55 gal Fuel Spill Fires.

Key: sensor locations labeled E (East), S (South), N (North), and C (Center) on concrete (left side) versus fire tests with active flushing ILDFA (same sensor locations) (right side)

An additional illustration of the impact of the ILDFA is the average air temperature for the duration of combustion for each of three different fuel spill sizes from 15 to 55 gal. The measured mean room air temperature is summarized in Table 11 for concrete and ILDFA active and passive water flushing. These numbers were calculated using an average of all 16 thermocouples for all three tests at each fuel spill size and during the burn duration. The statistical difference between concrete and IDLFA with water, the average temperature was compared using the ANOVA test. In each case the average of all the measured temperatures in the ILDFA tests was below 120 °F and much greater in each of the concrete spill fires. The statistics confirm that the ILDFA, with or without water flushing, has a significant impact (>70% decrease) for reducing fire impact to the facility.

Table 11. Mean Room Temperature for Concrete and ILDFA Fuel Spill Fire Tests

Spill Size (gal)	Concrete (°F)	ILDFA (active) (°F)	ILDFA (passive) (°F)	Relative Reduction From Concrete to ILDFA (active) (%)
15	537±305 (*n*=48)	99±15 (*n*=48)	105 ± 15 (*n*=48)	72 ± 14 (*n*=96) (P=0.04)
30	995±497 (*n*=48)	102±19 (*n*=48)	107 ± 18 (*n*=48)	90 ± 11 (*n*=96) (P=.02)
55	1304±593 (*n*=48)	111±22 (*n*=48)	113 ± 21 (*n*=48)	91 ± 15 (*n*=96) (P=.02)

4.4. Heat Flux Profiles During Fire Testing

Heat flux sensors installed in the test facility to measure heat transmission to the area surrounding fuel spill fires and to the fuselage and wing surfaces of the mockup fighter jet are described in Section 3.1.4.2. Results from different groups of sensors are described below.

4.4.1. Perimeter Heat Flux

The data collected from the heat flux sensors are intended to record radiative heat from the fire, the sensors, however, the measurements are affected by factors including how close the spill fires spread to the sensors and by any obstructions between the spill fire and the sensors. The East and South sensors were not impacted by obstructions between the spill fire and the sensors, but the North and West sensors were partially obstructed by the hopper and mockup respectively. When flames directly impact a sensor the measured values increase disproportionately due to convective heat transfer as compared to mostly radiated heat transfer measured away from the flames. During all spills on concrete the fire spread close to the North sensors and during the larger spills the fire was close to the South and West sensor. The East perimeter heat flux sensor was more than eight feet from the flames during all tests and represents a mostly radiative component in all tests that was also not affected by obstructions. Accordingly, the East sensor may provide best synopsis of event without artifacts or collection anomalies.

The heat flux measurements by the East perimeter sensor are shown in Figure 21 for all concrete and active flushing ILDFA tests. Each plot is the averaged data from the three tests at that fuel

spill size. Since this sensor was adjacent to, but not in, the fuel spill, the intensity was similar to what would affect an aircraft or materials adjacent to the incident aircraft. The heat flux magnitude and duration of growth and decline of the concrete and ILDFA fuel spill fires described earlier in Sections 4.1.1and 4.2.1 is evident in these plots.

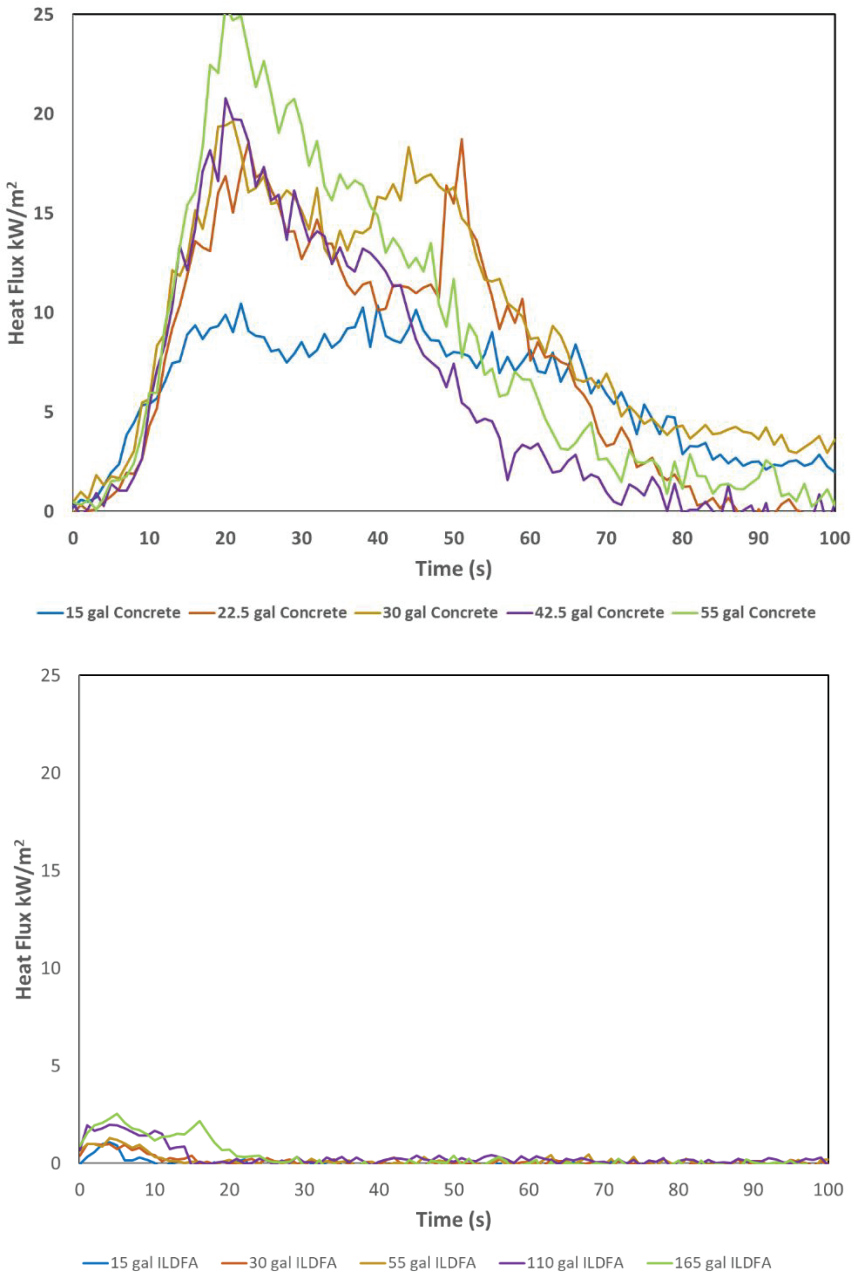

Figure 21. Perimeter Heat Flux at the East Sensor for Concrete (top) and Active ILDFA (Bottom) Fuel Spill Fires

The cumulative effect of heat flux at the perimeter sensors was calculated by integrating the measured heat flux over the time period of the fire, the result represents the total energy absorbed

at that location. The calculated results for each perimeter sensor are shown in Figure 22. Since the East sensor was furthest from the spill, the results are the lowest of the concrete spill fires. The result of flames approaching or engulfing the remaining three sensors can be seen in the larger total energy absorbed values as the concrete fuel spill size increased. The South sensor in particular was impacted by intense and prolonged fire vortexes (as discussed in Section 5.1) in several tests as the fuel spill spread to the sensor location. The impact of the ILDFA on heat absorption to material surfaces for much larger fuel spills than in the concrete fire tests is also evident in these plots. The 15 gal spill fires on concrete had greater heat flux impact at the perimeter sensor locations than the 165 gal spills on the ILDFA. By comparing equal fuel volumes, the ILDFA system at 55 gal results in a 91% reduction in total energy absorbed compared to the same size fuel spill on concrete.

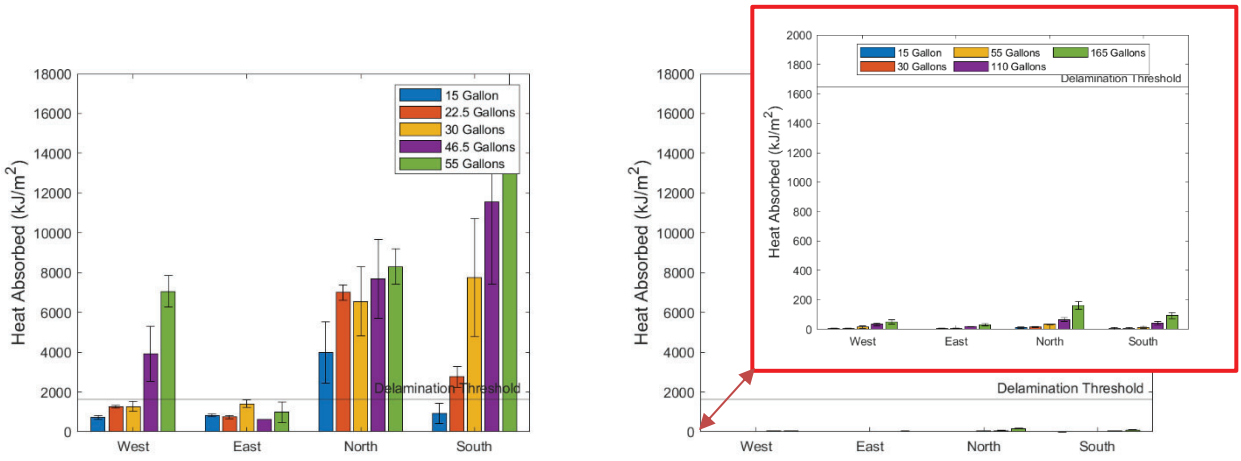

Figure 22. Mean Total Energy Absorbed at Perimeter Floor Sensors for Unmitigated Fuel Fires (Left) and Active ILDFA Fuel Fires (right). Inset Panel Shown to Illustrate Low Cumulative Heat Flux on the ILDFA.

Figure 22 also includes a delamination threshold line. The value indicates the total absorbed heat that will cause representative composite materials to lose structural strength and integrity. This value was exceeded at perimeter locations in several of the concrete tests as the fuel spill progressed toward those locations. Section 4.4.2 explains the calculation of this threshold and what composite materials were evaluated for this determination. This threshold was approached but not exceeded for concrete spill fires at the East sensor location. From Figure 22, this threshold was not approached or exceeded for the active ILDFA fuel spill fires. The energy absorbed for all floor sensors at the various fire sizes on the ILDFA system with and without water flushing are shown in Table 12. None of these values approached the composite material delamination threshold value.

Table 12. Mean Total Energy Absorbed at the Perimeter Heat Flux Sensors (kJ/m^2)

ILDFA Mode	Fuel Volume (gal)	W	E	N	S
Active	15	6 ± 2 (*n*=15)	2 ± 1 (*n*=15)	12 ± 5 (*n*=15)	7 ± 8 (*n*=15)
	30	6 ± 2 (*n*=15)	4 ± 3 (*n*=15)	17 ± 4 (*n*=15)	7 ± 5 (*n*=15)
	55	15 ± 9 (*n*=15)	5 ± 3 (*n*=15)	34 ± 1 (*n*=15)	14 ± 8 (*n*=15)
	110	35 ± 9 (*n*=15)	20 ± 2 (*n*=15)	67 ± 12 (*n*=15)	43 ± 11 (*n*=15)
	165	49 ± 15 (*n*=15)	32 ± 6 (*n*=15)	161 ± 27 (*n*=15)	94 ± 21 (*n*=15)
Passive	15	20 ± 29 (*n*=15)	24 ± 23 (*n*=15)	10 ± 7 (*n*=15)	3 ± 1 (*n*=15)
	30	66 ± 58 (*n*=15)	11 ± 8 (*n*=15)	14 ± 6 (*n*=15)	4 ± 2 (*n*=15)
	55	75 ± 25 (*n*=15)	49 ± 44 (*n*=15)	26 ± 5 (*n*=15)	21 ± 13 (*n*=15)
	110	42 ± 38 (*n*=15)	98 ± 74 (*n*=15)	165 ± 185 (*n*=15)	38 ± 25 (*n*=15)
	165	121 ± 83 (*n*=15)	104 ± 49 (*n*=15)	638 ± 75 (*n*=15)	296 ± 190 (*n*=15)

--Integrated using average fire duration time in Table 7

Additional discussion of how perimeter heat flux measurements in this study compare to a prior fuel spill fire study (3) can be found in Section 5.1.

4.4.2. Delamination of Composite Materials

In prior work for the Air Force Research Laboratory (4), materials were tested that represented three general classes of aircraft composites and concluded that the majority of mechanical strength of composite samples is lost when delamination occurs. Table 13 summarizes the heat flux levels and exposure durations that result in composite delamination (4) for three composite materials and was used as a point of reference herein.

Table 13. Delamination Predictions of Composites from Prior Study (4)

Composite Material (Delam. Temp., Thickness)	Est. Time to Delamination (s)		
	15 kW/m^2	25 kW/m^2	35 kW/m^2
IM7/977-3 (250 °C, 0.25 in)	272	142	90
IM7/RM3002 (250 °C, 0.13 in)	129	74	51
IM7/AFR-PE-4 (225 °C, 0.15 in)	129	72	47

Earlier documentation of aircraft composite material damage was also presented in work from the National Institute of Standards and Technology (NIST) (9), which concluded that skin of aircraft fuselages will fail after 45 s of spill fire exposure (10). Those data do not represent the decreased resistance to fire of modern composite material found in fighter aircraft, but 45 s was the baseline response time used in determining threshold distances.

The data in Table 13 was converted to total absorbed energy required for delamination based on constant heat flux magnitudes of 15, 25, and 35 kW/m^2 and exposure durations and are shown in

Table 14. Due to heat transfer properties of composite materials, they can absorb more energy before delamination at lower magnitudes because a portion of the energy has time to conduct and radiate away from the material surface. It is also evident from this data that the ability to conduct heat away from the surface in the thicker materials results in the ability to absorb more heat before delamination. All fuel spill fires on concrete resulted in heat intensity on the mock-up aircraft surface that far exceeded the heat needed to cause damage to aircraft skin as described in Sections 4.4.3 and 4.4.4.

Table 14. Calculated Absorbed Energy for Composite Delamination (4)

Composite Material (Delam. Temp., Thickness)	Integrated Heat Flux for Delamination (kJ/m^2)		
	15 kW/m^2	25 kW/m^2	35 kW/m^2
IM7/977-3 (250 C, 0.25 in.)	4,080	3,550	3,150
IM7/RM3002 (250 C, 0.13 in.)	1,935	1,850	1,785
IM7/AFR-PE-4 (225 C, 0.15 in.)	1,935	1,800	1,645

4.4.3. Fuselage Heat Flux

Four heat flux sensors were mounted on the fuselage mockup surface to measure the fuel spill fire impact on aircraft surfaces. The four sensor locations were: two (F1 and F2) at the center of the mock fuselage, and two (F3 and F4) closer to the south end of the mock fuselage as shown in Figure 23 and described in Section 3.1.4.2. F1 and F3 are located at the bottom of the fuselage, whereas F2 and F4 are placed 45° toward the fuel spill side of the fuselage. As a result, F2 and F4 sensors registered higher heat flux than F1 and F3 in all tests since the fuel spills were on that side of the fuselage, did not spread directly under the fuselage in the smaller fuel spills, and in the larger spills burned for a shorter time under the fuselage than on the side.

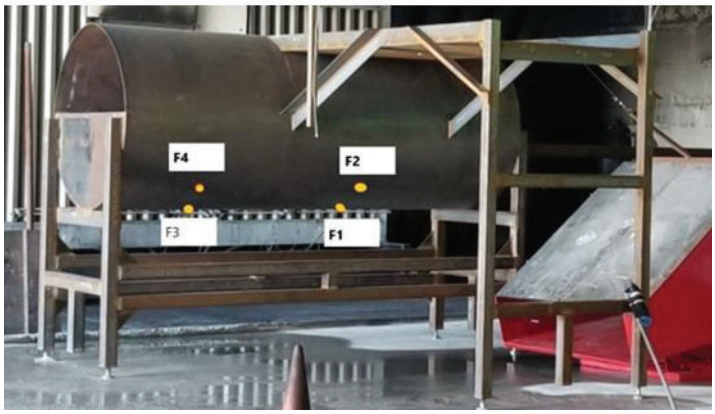

Figure 23. Heat Flux Sensor Locations on the Mock-Up Fuselage

From Figure 13 it is observed that as the concrete fuel spill sizes increase, the flames get closer to and engulf the fuselage. The average fuselage heat flux from each of the triplicate tests at each fuel spill volume on concrete and on the active flushing ILDFA are plotted in Figure 25. The F2 and F4 sensors were either on the edge of the fire plume or inside the edge of the plume in all spill tests. This relative location is obvious in the >50 kW/m^2 heat flux recorded at these sensors in all tests as shown in Figure 24. In larger spills as these sensors were in more direct contact with the flames for longer periods, higher heat flux is recorded. For spills smaller than 30 gal on

concrete, the F1 and F3 sensors had little to no direct flame exposure. As the concrete spill sizes increase, the flames spread more under the fuselage and resulted in increased heat flux to the bottom sensors. For spills 30 gal and larger, these sensors were directly exposed to flames during a portion of the burn and this exposure time was longer as the larger spills spread further under the fuselage. Heat flux exposure exceeded 50 kW/m^2 in the two largest spill scenarios on concrete.

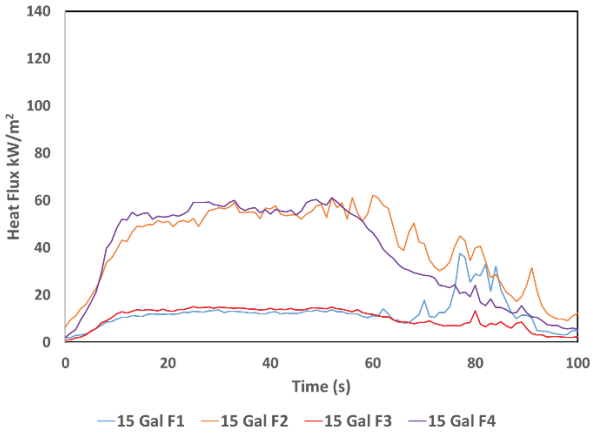

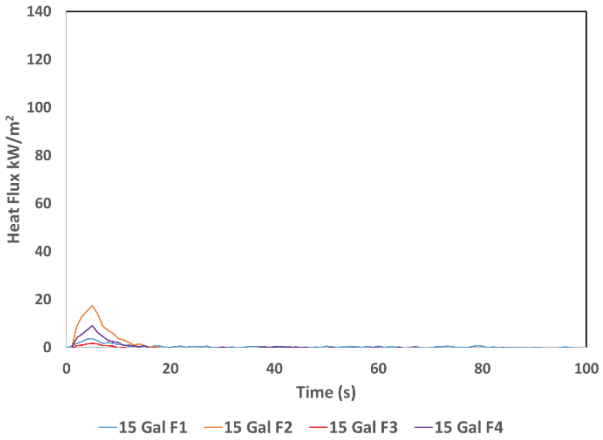

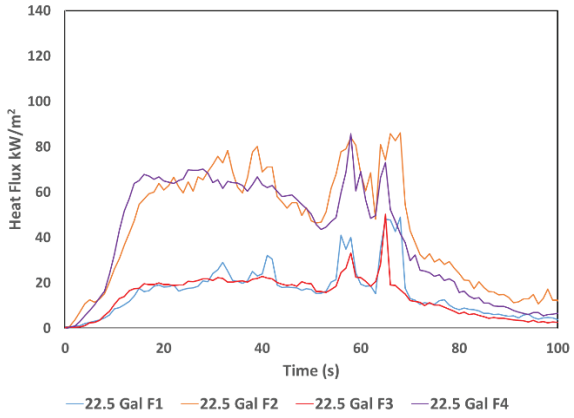

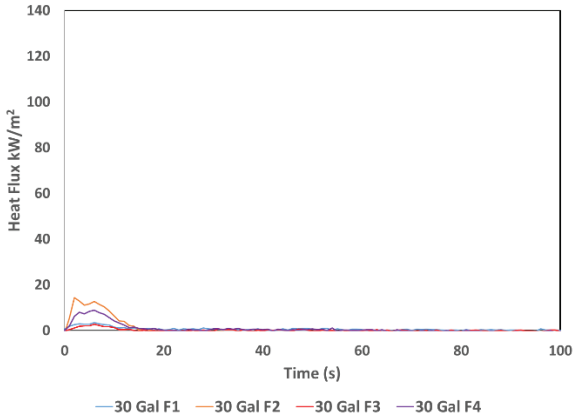

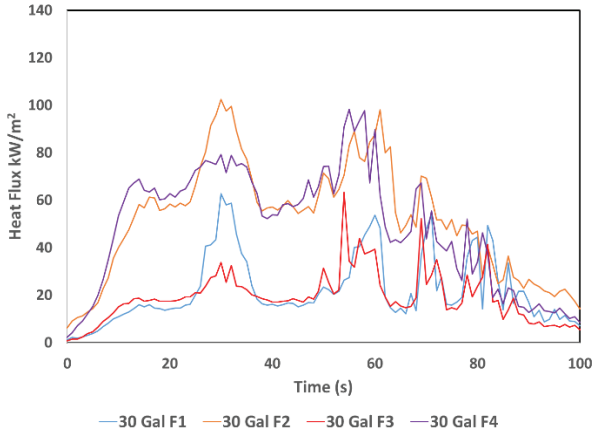

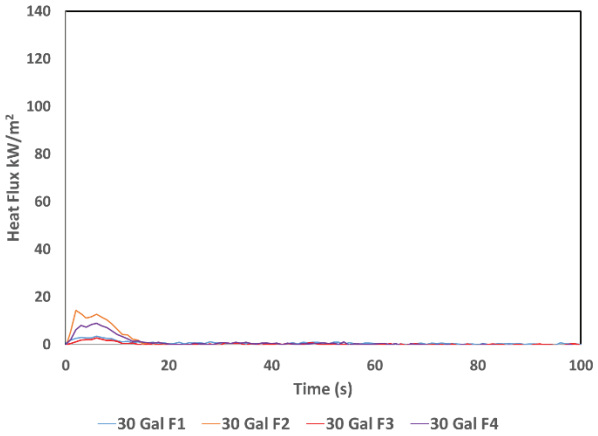

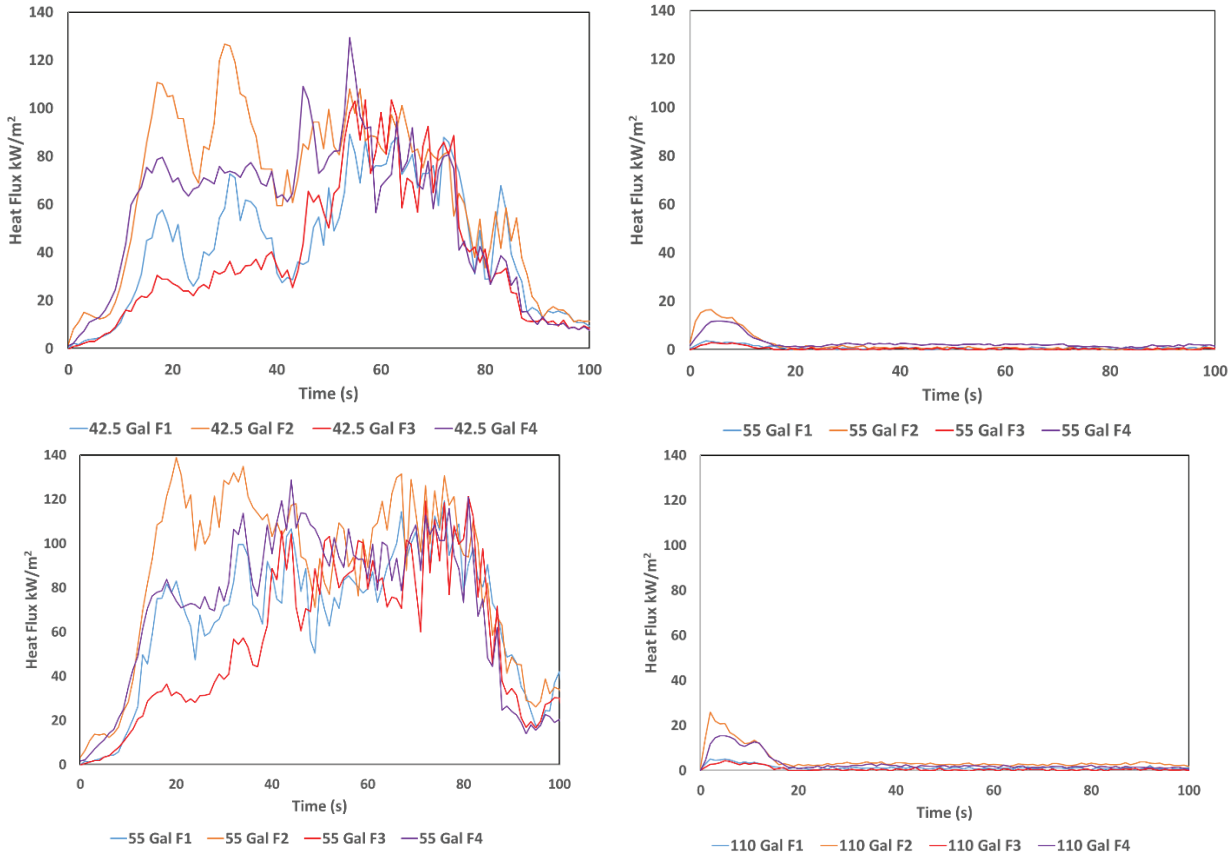

Figure 24. Fuselage Heat Flux for Each Spill Size on Concrete (left) and Active ILDFA (right)

The ILDFA reduced heat flux at the fuselage sensors in magnitude and duration for all tests. Like the concrete spill fire results, sensors F2 and F4 were exposed to higher heat flux than sensors F1 and F3, but unlike the concrete tests, the heat flux magnitude never exceeded 40 kW/m^2 for the side sensors or 10 kW/m^2 for the bottom fuselage sensors. These ILDFA heat flux magnitudes are not insignificant, but when combined with the short duration of exposure should result in minimal damage for most aircraft materials and equipment unless other flammable materials in the vicinity are ignited to further fuel fire.

As described in Section 4.4.2, the total energy absorbed by the aircraft material surface is directly related to structural damage. Plots of this total absorbed energy are shown in Figure 25 and the subsequent data can be found in Table 15 for unmitigated concrete spill fires and for the ILDFA with active flushing spill fires. In each unmitigated test on concrete, the F2 and F4 sensors exceeded the designated composite delamination threshold and in most tests the F1 and F3 sensors did as well. By comparison the threshold value was never reached at any sensor for tests using the ILDFA.

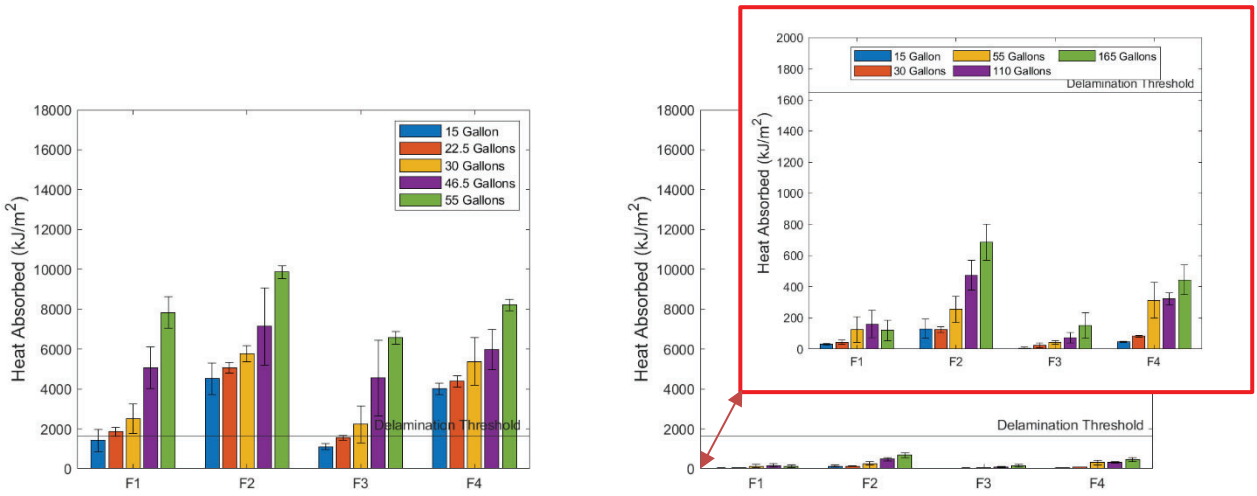

Figure 25. Mean Total Energy Absorbed at Fuselage Sensors for Unmitigated Fuel Fires (Left) and Active ILDFA Fuel Fires (right). Inset Panel Shown to Emphasize Low Levels on ILDFA.

Table 15. Mean Total Energy Absorbed at Fuselage Sensors for Unmitigated Fuel Fires and Active ILDFA Fuel Fires (kJ/m^2)

Test	Fuel Volume (gal)	Sensor Position: Center (F1)	Center 45 (F2)	South (F3)	South 45 (F4)
Concrete	15	1422 ± 555 (n=15)	4514 ± 782 (n=15)	1105 ± 161 (n=15)	4005 ± 282 (n=15)
	22.5	1851 ± 211 (n=15)	5072 ± 266 (n=15)	1558 ± 118 (n=15)	4376 ± 289 (n=15)
	30	2521 ± 742 (n=15)	5769 ± 418 (n=15)	2231 ± 923 (n=15)	5383 ± 1188 (n=15)
	45.5	5055 ± 1037 (n=15)	7136 ± 1941 (n=15)	4544 ± 1906 (n=15)	5961 ± 1005 (n=15)
	55	7827 ± 787 (n=15)	9862 ± 311 (n=15)	6568 ± 328 (n=15)	8217 ± 287 (n=15)
IDLFA Active	15	31 ± 5 (n=15)	131 ± 63 (n=15)	7 ± 5 (n=15)	48 ± 4 (n=15)
	30	45 ± 12 (n=15)	124 ± 19 (n=15)	24 ± 15 (n=15)	82 ± 5 (n=15)
	55	124 ± 82 (n=15)	254 ± 85 (n=15)	44 ± 12 (n=15)	314 ± 115 (n=15)
	110	160 ± 88 (n=15)	474 ± 96 (n=15)	73 ± 33 (n=15)	322 ± 39 (n=15)
	165	120 ± 66 (n=15)	687 ± 116 (n=15)	152 ± 81 (n=15)	443 ± 95 (n=15)

--Integrated using average fire duration time in Table 7
--Triplicate tests done for all conditions

The total absorbed energy at each sensor for each test are reported in Table 16. Table 17 shows statistical comparisons between the center (F1 and F2) and south (F3 and F4) sensors, bottom (F1 and F3) and 45° side (F2 and F4) sensors, and with and without the water flushing system

activated. The data comparisons revealed that the water flushing system resulted in lower total heat flux to the mockup sensor locations, however, with active flushing or passive drainage there were a significant decreases in heat flux compared to concrete fuel spill fires.

Table 16. Mean Total Energy Absorbed at Fuselage Sensors for Fuel Spill Fires With (Active) and Without (Passive) Active ILDFA Water Flushing (kJ/m^2)

ILDFA Mode	Fuel Volume (gal)	Sensor Position			
		Center (F1)	Center 45 (F2)	South (F3)	South 45 (F4)
Active	15	31 ± 5 (*n*=15)	131 ± 63 (*n*=15)	7 ± 5 (*n*=15)	48 ± 4 (*n*=15)
	30	45 ± 12 (*n*=15)	124 ± 19 (*n*=15)	24 ± 15 (*n*=15)	82 ± 5 (*n*=15)
	55	124 ± 82 (*n*=15)	254 ± 85 (*n*=15)	44 ± 12 (*n*=15)	314 ± 115 (*n*=15)
	110	160 ± 88 (*n*=15)	474 ± 96 (*n*=15)	73 ± 33 (*n*=15)	322 ± 39 (*n*=15)
	165	120 ± 66 (*n*=15)	687 ± 116 (*n*=15)	152 ± 81 (*n*=15)	443 ± 95 (*n*=15)
Passive	15	123 ± 63 (*n*=15)	362 ± 136 (*n*=15)	85 ± 88 (*n*=15)	168 ± 37 (*n*=15)
	30	170 ± 155 (*n*=15)	316 ± 151 (*n*=15)	108 ± 80 (*n*=15)	236 ± 163 (*n*=15)
	55	227 ± 119 (*n*=15)	836 ± 189 (*n*=15)	218 ± 78 (*n*=15)	373 ± 144 (*n*=15)
	110	298 ± 96 (*n*=15)	906 ± 210 (*n*=15)	239 ± 31 (*n*=15)	390 ± 55 (*n*=15)
	165	556 ± 310 (*n*=15)	1012 ± 69 (*n*=15)	232 ± 163 (*n*=15)	460 ± 82 (*n*=15)

--Integrated using average fire duration time in Table 7
--Triplicate tests done for all conditions

Table 17 Relative Differences Among Fuselage Heat-Flux Sensors

Active Flushing		Passive Flushing		Total difference		
South vs Center	Bottom vs 45◦	South vs Center	Bottom vs 45◦	South vs Center	Bottom vs 45◦	Water vs no Water
71% P=.03	75% P=.014	60% P=.006	45% P=.002	63% P=.005	58% P=.003	50% P=.007

4.4.4. Wing Heat Flux

Heat flux sensors were placed at two locations on the underside of the wing (as described in Section 3.1.4.2) to measure the impact of the fuel spill fires on the under-wing surface. The fuel volume affected the area coverage of the spill in each concrete floor test, but as the fuel spread out over the floor, the different fuel volumes tested had minimal effect on the resulting fuel depth (see Table 6) which was similar in each spill and only increased slightly from smallest to largest spill. Since the wing was in the middle of the spill in each test and the depth of the fuel is directly related to burn duration, the wing was exposed to a similar and slightly increasing total heat impact in each of the concrete spill fire tests. The average heat flux from each of the triplicate

tests at each fuel spill volume on concrete and on the active flushing ILDFA are shown in Figure 27 The peak heat flux and durations are similar in all of the concrete tests. The slight increase in burn duration with volume is also perceptible in the concrete spill fire plots. The heat flux to the wing sensors was much less in magnitude and duration for the ILDFA tests. Some of the magnitudes measured on the wing were not insignificant as flames impinged on the surface. The short duration of this flame exposure should result in minimal damage for most aircraft materials and equipment unless other flammable materials in the vicinity were ignited. It can be seen in the Figure 26 ILDFA plots that the larger amounts of fuel spilled does result in increased exposure to the wing area.

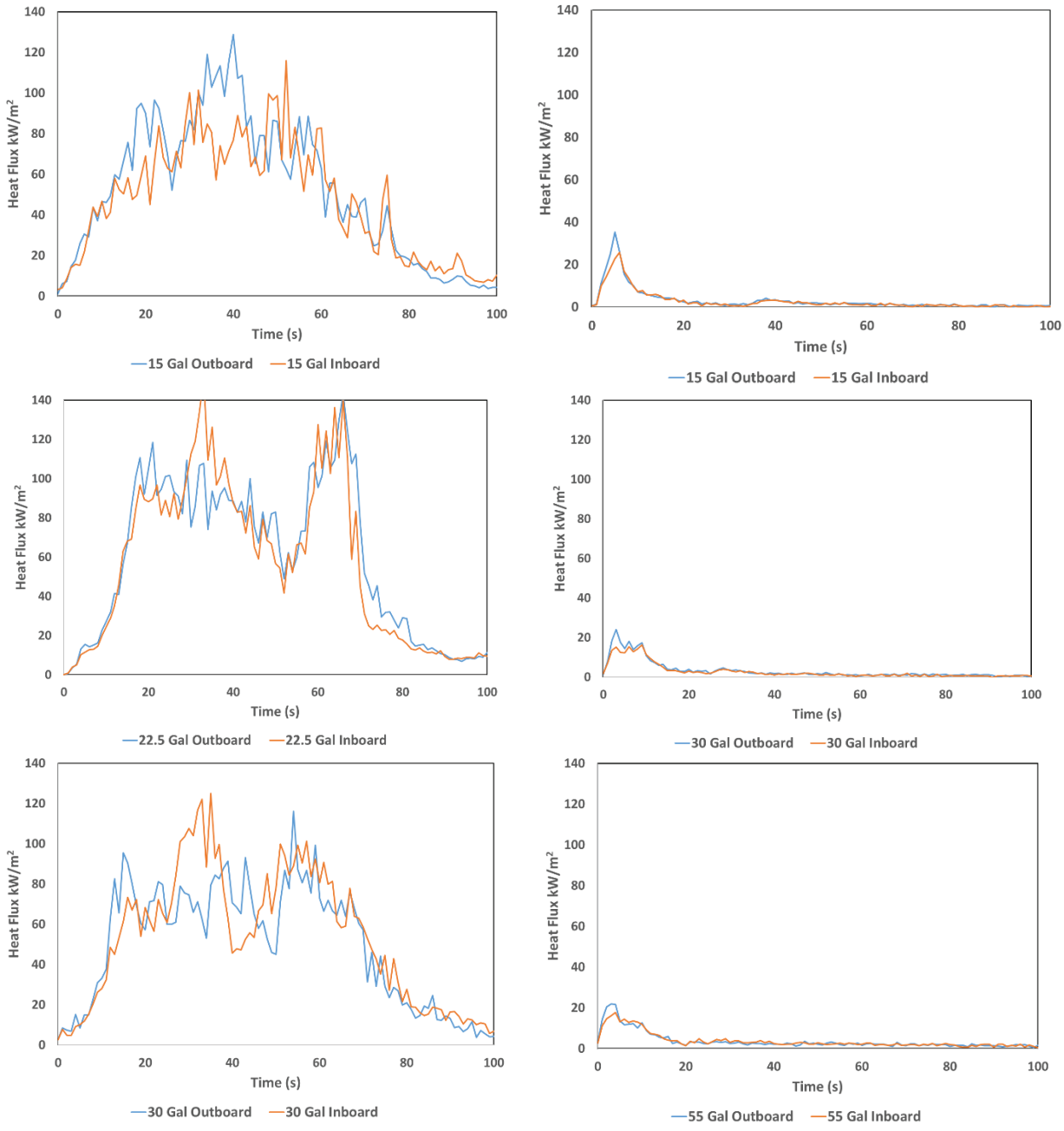

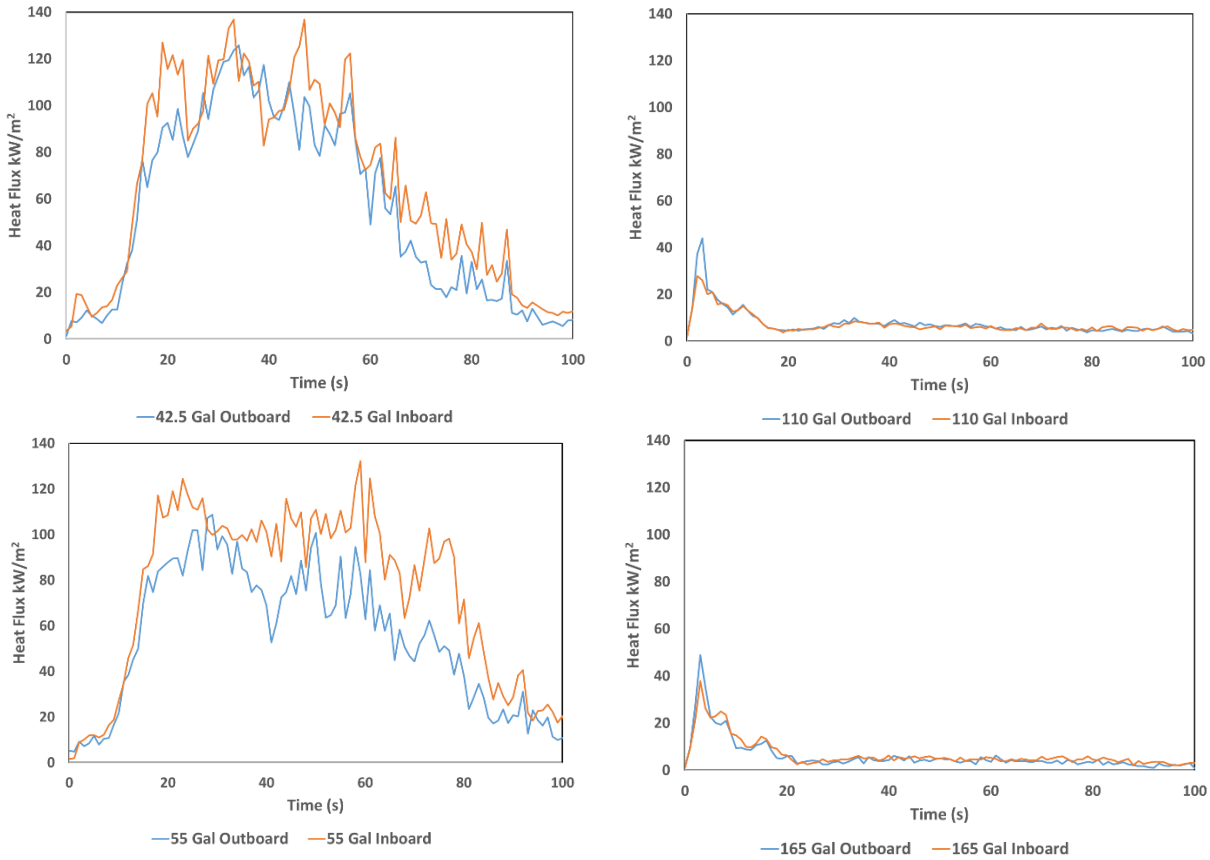

Figure 26. Wing Heat Flux for Each Spill Size on Concrete (left) and Active ILDFA (right)

When the heat flux values are integrated over the time of combustion, the total absorbed energy on the wing is significantly lower for fuel spill fires on the ILDFA than on concrete. When the similar 15, 30 and 55 gal trials on concrete and ILDFA are compared with each other, on average the ILDFA results in a decrease in total energy absorbed by 64.60%. When the total absorbed energy from the larger 110 and 165 gal spills on the ILDFA are compared to the 55 gal spill on concrete there is an average 66±20% reduction drop observed. The total energy absorbed at the two wing sensor locations is shown in Figure 27. Each concrete spill fire would have resulted in delamination of composite materials on the wing surface. With the ILDFA in place, the energy absorbed by the wing was significant, but less than what is required for composite delamination according to values in Table 14 above. A statistical test was performed to determine if there is a difference between the inboard and outboard sensor locations on the wing for both the concrete trials and ILDFA trials. It is found that in both cases that there is no statistical difference in the measured values.

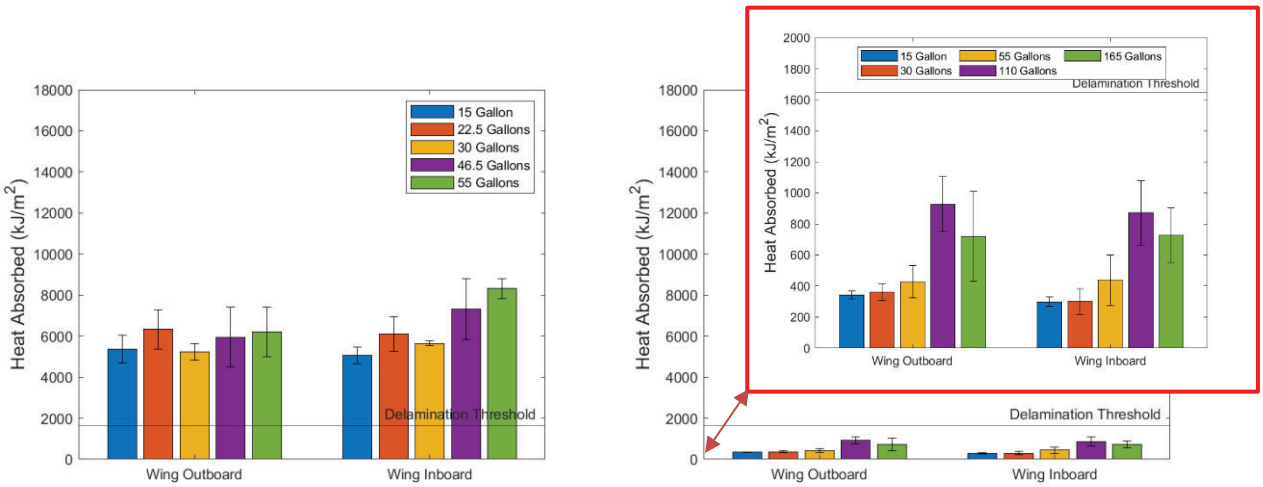

Figure 27. Total Energy Absorbed on the Wing for Concrete and ILDFA Fuel Spills

Table 18 has data for comparing energy absorbed in fuel spill fire tests with and without the ILDFA water system activated. In general the total heat absorbed was higher when the flushing water was not activated however there was some overlap in the data uncertainty.

Table 18. Wing Sensor Energy Absorbed for Fuel Spill Fires With (Active) and Without (Passive) ILDFA Water Flushing in Operation

Test Surface	Fuel Volume (Gal)	Sensor Position: Wing Outboard (kJ/m^2)	Sensor Position: Wing Inboard (kJ/m^2)
IFLDA (Active Flushing)	15	342 ± 25 (*n*=15)	299 ± 34 (*n*=15)
	30	361 ± 53 (*n*=15)	300 ± 82 (*n*=15)
	55	427 ± 105 (*n*=15)	438 ± 163 (*n*=15)
	110	925 ± 178 (*n*=15)	871 ± 207 (*n*=15)
	165	720 ± 290 (*n*=15)	726 ± 176 (*n*=15)
ILDFA (Passive Flushing)	15	485 ± 227 (*n*=15)	605 ± 182 (*n*=15)
	30	99 ± 45 (*n*=15)	267 ± 211 (*n*=15)
	55	874 ± 488 (*n*=15)	1012 ± 344 (*n*=15)
	110	1395 ± 327 (*n*=15)	1172 ± 416 (*n*=15)
	165	1096 ± 48 (*n*=15)	1161 ± 180 (*n*=15)
Concrete	15	5367 ± 664 (n=15)	5066 ± 393 (n=15)
	22.5	6330 ± 965 (n=15)	6106 ± 834 (n=15)
	30	5227 ± 399 (n=15)	5649 ± 110 (n=15)
	45.5	5953 ± 1474 (n=15)	7313 ± 1474 (n=15)
	55	6214 ± 1203 (n=15)	8320 ± 491 (n=15)

4.4.5. Center Heat Flux

Heat flux was measured at a point 10 ft. above the floor on the thermocouple tree in the center of the 30 x 30 ft. test area. This sensor was mounted, adjacent to the center tree 10 ft. thermocouple as described in section 3.1.4. The location of this thermocouple tree resulted in it being immersed in or adjacent to the fire plume in all concrete spill fires. For ILDFA fires it was slightly further away from the fire plumes due to smaller-in-area spill sizes. Figure 28 shows the results of the heat flux measured in the concrete spill fires and in the ILDFA spill fires with the water flushing system activated. The data presented in Figure 28 is an average of the sensor data collected in the three tests at each fuel spill size. The maximum ILFDA measured heat flux at this location was 5.4 kW/m^2 and occurred within 20 s after the fuel spill. Spills on concrete generated much more heat flux at this location, mostly in the 15 to 40 kW/m^2 range with peaks above 70 kW/m^2.

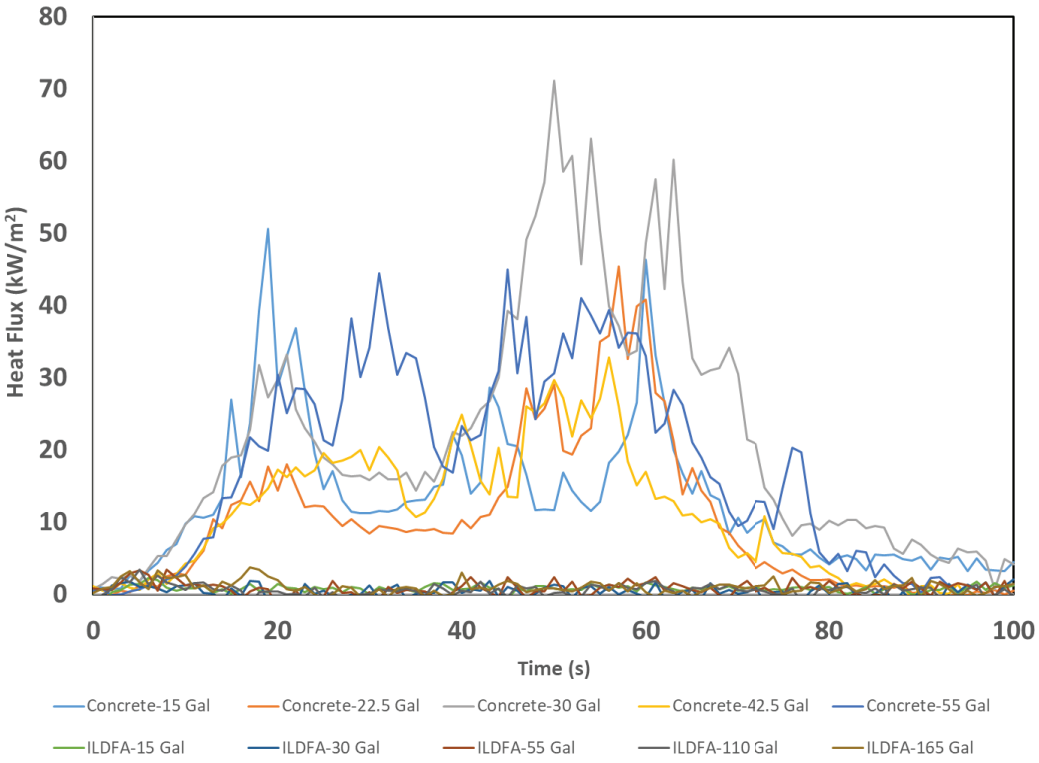

Figure 28. Mean Heat Flux at the Center, 10 ft. High, Heat Flux Sensor

The heat flux values at the sensor location were integrated over time to determine the total absorbed energy. Table 19 presents this data for fires on concrete and fires on the ILDFA with and without the water flushing system activated. These results are averages and standard errors of the data from three tests at each fuel spill size. When these results are compared to the three composite materials' properties discussed in Section 4.4.2, the absorbed heat required for composite material delamination was not reached or approached in any of the ILDFA tests. For concrete spill fire tests, the average absorbed heat approached but was lower than the lowest delamination value in Table 14 of 1,645 kJ/m^2, however, in two individual tests, the absorbed heat at this location did exceed 1,645 kJ/m^2. There was little difference in the results from the ILDFA with and without the water flushing system activated.

Table 19. Mean Energy Absorbed at the Center, 10 ft. High, Heat Flux Sensor

Fuel Volume (gal)	Concrete (kJ/m^2)	ILDFA with Water Flushing (kJ/m^2)	ILDFA without Water Flushing (kJ/m^2)
15	1,400 ± 136 (*n*=3)	3 ± 1 (*n*=3)	43 ± 31 (*n*=3)
22.5	772 ± 171 (*n*=3)	n/a*	n/a*
30	1,362 ± 469 (*n*=3)	125 ± 76 (*n*=3)	137 ± 105 (*n*=3)
42.5	970 ± 398 (*n*=3)	n/a*	n/a*
55	1,402 ± 659 (*n*=3)	111 ± 20 (*n*=3)	331 ± 286 (*n*=3)
110	n/a*	46 ± 34 (*n*=3)	166 ± 91 (*n*=3)
165	n/a*	155 ± 104 (*n*=3)	192 ± 16 (*n*=3)

* Test not conducted at this fuel spill volume.

4.4.6. Adjacent Aircraft Fuselage Heat Flux

After the initial seven tests were completed, a heat flux sensor was installed at a location 4 ft. above the floor, on the fuel spill side of the mockup fuselage, 33 ft. from the fuselage and approximately 29 ft. from the center of the fuel spill, and in line with the mockup wing. This sensor was installed to measure the heat flux at a location close to where an adjacent aircraft fuselage would be in a maintenance hangar relative to the incident aircraft. The sensor was present for all ILDFA tests and for eight fuel spill fires on concrete (three each of the 22.5 and 42.5 gal, and two of the three 55 gal tests.

At this distance from the fuel spill incident, minimal heat flux was present. In each of the ILDFA tests the heat flux measured could not be distinguished from the sensor noise and was less than 3 kW/m^2 at the adjacent fuselage location. For the eight tests on concrete, the heat flux exceeded the sensor noise level for approximately 20 s in each test but never exceed 10 kW/m^2 during these 20 s for any of the eight fuel spill fires.

5. DISCUSSION

5.1. Fuel Spill Perimeter Heat Flux - Comparison to Prior Study

Heat flux at specific points adjacent to a JP-8 spill fire were previously reported (3) for unsuppressed and water sprinkler suppression fire testing in aircraft hangars. Table 20 shows the measured results of unsuppressed fire tests including the maximum average perimeter heat flux (average of the three lowest measurements) from 25 and 30 gal JP-8 spill fires on concrete. The lowest three measurements were used for an average because in some cases the fire spread close to a sensor resulting in measuring radiation within the flames instead of radiation adjacent to the flames. Perimeter hear flux data from 30 gal spills in this study are compared to the prior study. The data provide a good indication of the impact to aircraft and equipment adjacent to the fuel spill area. In the prior study, the sensors were placed around a 28 x 30 ft. concrete pad, and in this study a 30 x 30 ft. pad. The JP-8 fuel used in the prior study had a lower flash point and was ignited after the fuel spilled resulting in different burn durations, slower ramp up of the fire intensity, and slightly lower peak intensity. Different methods were used to spread the fuel in each study which also led to different spill shapes. The depth of the spill was not measured in this study but can be estimated.

Table 20. Summary of Previous Unsuppressed JP-8 Spill Fire Tests (3)

Fuel Volume (gal)	Max Heat Flux (kW/m^2)	Fuel Spread (ft^2)	Max Fire Area (ft^2)	Max Height (ft.)	Avg Spread Rate (in./s)
25	12	370	350	33	2.8 +/- 1.0
25	5	335	300	23	1.2 +/- 0.3
30	10	360	400	33	1.6 +/- 0.4

The three 30 gal synthetic JP-4 fuel spills on concrete averaged 14 s preburns in the hopper before the fuel was spilled onto the floor. The smoke layer in the ceiling dropped to within five feet of the floor approximately 60 s after the spill and obscured the flames from visible spectrum video cameras. From the infrared video, the flames remained higher than 10 ft. for approximately 70 s. A fire vortex formed by the South perimeter heat flux sensor (the high intensity area on the right side of Figure 29) approximately 45 s after the spill in all three tests and remained for approximately 70 s then rapidly diminished. The vortex was apparent in all tests larger than 30 gal and resulted in high measured heat flux at the South sensor, which is indicative of greater heat flux in flames than the heat flux adjacent to flames. The fuel spills spread lengthwise from the hopper to the South side of the 30 x 30 ft. spill area and adjacent to the North sensor. The width of the spills ranged from approximately 8 to 20 ft. wide resulting in total coverage of approximately 415 ft^2. Based on this coverage, the average fuel depth was ~0.11 in. Figure 30 shows the extent of the fuel spill recorded using the IR camera located outside the South door of the test facility.

Figure 29. Fire Vortex Adjacent to the South Perimeter Heat Flux Sensor

Figure 30. IR Image when the 30 Gal Fuel Spill Reached Maximum Coverage (Test 4).

Spill diameters on the ILDFA appeared to be much smaller than on concrete (Table 21). The shape and size of the spills in prior study (3) and present study hindered direct comparisons. In the present study the fuel and fire focused at two of the perimeter heat flux sensors (North and South, Table 1) resulting in high measurements at both locations (Table 20). In the prior study, data from sensors close to the fuel spill were excluded from the analysis so the same exclusion made in current analysis. The West sensor was closer to the spill than the East sensor, however the flame radiation was partially blocked by the mockup's fuselage. The East sensor provides the best unobstructed comparison to the prior study (3). The differences in ignition methods, fuel source, and rate of fire spread due to fuel flash points will definitely affect the absolute values, the testbed designs, however, were matched well and legitimate conclusions obtained.

Table 21. Results of 30 gal Synthetic JP-4 Spill Fires on Concrete

Fuel Volume (gal)	Flooring	Max Perimeter Heat Flux (kW/m^2)				Spill Area (ft^2)	Max Flame Height (ft^2)
		West	East	North	South		
30	Concrete	31	21	204	150	415	31
30	Concrete	31	23	199	222	415	31
30	Concrete	30	19	166	210	415	31
30	ILDFA	1.6	1.4	4.2	1.3	70	10
30	ILDFA	1.5	1.5	3.3	2	70	10
30	ILDFA	1.2	1.2	2.5	1.7	70	10
165	ILDFA	4.1	3.1	6.8	5.7	200	12
165	ILDFA	4.2	2.8	6.9	6.3	200	12
165	ILDFA	3.2	2.8	7.5	6.6	200	12

The maximum average perimeter heat flux in the prior study ranged from 5 to 12 kW/m^2 (Table 20). By comparison, the heat flux sensor for indirect measurements in current study (East) were higher, 19 - 23 kW/m^2 for the three, 30 gal synthetic JP-4 fuel spills. The measurements tally the heat flux impact adjacent to a fuel spill fire event from a slow spreading, high flash point fuel spill fire or from a fast spreading, low flash point fuel spill fire. The scenario mimics potential effect on another aircraft in the maintenance hangar. The ILDFA mitigation of the heat flux was significant. For the same 30 gal fuel spill the heat flux was negligible at the perimeter locations and even the 165 gal fuel spill flux with the low flash point fuel averaged less than the prior 25 to 30 gal JP-8 results. The 165 gal spill fire covered approximately 200 ft^2 (Table 20). The spill and fire area were limited by the 30 ft. length of the floor channels, accordingly the abrupt end introduced an artifact, the spread may have grown on a floor with longer channels.

5.2. Air Temperatures - Comparison to Prior Study

Air temperature data collected from the ILDFA evaluations were compared to the prior report describing Halon fire protection systems for hardened aircraft shelters (HAS) (2). The HAS report described three Halon 1211 system designs (designated A, B, and C) against a series of fire scenarios that each included a 165 gal JP-4 fuel spill. A summary of the results of the prior HAS tests is in Table 22 including the pre-burn time (time from ignition until the suppression system discharged), maximum temperatures recorded, and the number of thermocouples that measured temperatures above 400 °F. Additional details of the prior test instrumentation and results is in Appendix A.

Table 22. Summary of ESL-TR-86-13 Fire Test Results (2)

Test	Preburn Time (s)	Total Burn Time (s)	Max Temp (°F)	Temperature Readings > 400 °F
A-1	2	4	270	0 of 4
A-2	17	>30	1,900	4 of 4
B-1	3	~20	670	8 of 13
B-2	5	>30	1,084	8 of 13
C-1	1	Not reported	Ambient	0 of 13
C-2	3	Not reported	160	0 of 13

Key: All fires are for 165 gal of JP-4, with exception of B-2 and C-2 which included a 3-D internal aircraft preburn followed by 165 gal of spilled JP-4.
Results of prior testing (2) show a clear correlation between pre-burn time and maximum temperature. Figures in Appendix A identify the three instrumentation setups for the prior test format.

Temperature data collected during the current study will not directly correlate with temperatures recorded in prior fire suppression tests in the same facility (2) due to too many differences in the test variables from the original fire scenario: fuel spill procedures, pre-burn times, fire duration, thermocouple locations, and the Halon mitigation process itself. The results, however, were analyzed qualitatively and compared to the best extent possible.

5.2.1. Unmitigated Spill Fires

The present study compared unmitigated fuel spill fires and ILDFA-mitigated fires. The prior HAS study (2) evaluated Halon-mitigated fires, however test A-2 during the prior tests included a 165 gal spill fire allowed to burn for 17 s before the Halon system was activated. That HAS test, although three times the fuel spill volume, is most similar to the unmitigated fires from 55 gal spills on concrete in current test series. The results are compared and interpreted below.

The 17 s test A-2 unmitigated fuel spill fire, which was 3 times as large in volume as the 55 gal spill, resulted in high internal facility temperatures, and “noticeable cracking” in the concrete structure. Test A-2 used four thermocouples: one five feet above the floor at the aircraft mockup nose, one each on the left and right side of the nose mockup at 12 and 19 ft. above the floor, and one near the back door 12 ft. above the floor as shown in Figure A- 3. All four thermocouples exceeded 400 °F. The peak temperatures recorded in the first 30s of the test were 1,900 °F on two of the thermocouples, 1,400 °F, and 700 °F (it was not clear from the temperature results graph in the report which thermocouple locations corresponded to which data plot).

In the present study, thermocouples were installed at heights of 5, 10, and 19 ft. above the floor in the four thermocouple trees described in Section 3.1.4.3 (12 total thermocouples). In the three 55 gal unmitigated tests, average peak temperatures at 19 ft. ranged from 870 - 2,170°F, at 10 ft. ranged from 580 - 2,340 °F, and at five foot ranged from 390 - 2,110 °F. When the time frame is limited to the first 30 s of these tests, the average peak temperatures ranged from 290 - 1,550 °F and 10 of the 12 thermocouples’ average peak temperature exceeded 400 °F. Measurements from the first 180 s of the final 55 gal spill fire are shown in Figure 31. The prior HAS data were reported for the first 30 s and test peak temperatures (700 - 1,900 °F) are higher for that 30 s time

frame, and all four thermocouples exceeded 400 °F. The larger fuel spill quantity (165 gal vs. 55 gal) is the most likely reason for the higher peak temperature in prior test. Overall, the unmitigated air temperature results from both projects compare well when the respective fuel spill quantity differences are considered and both produced room temperatures that can cause extensive damage.

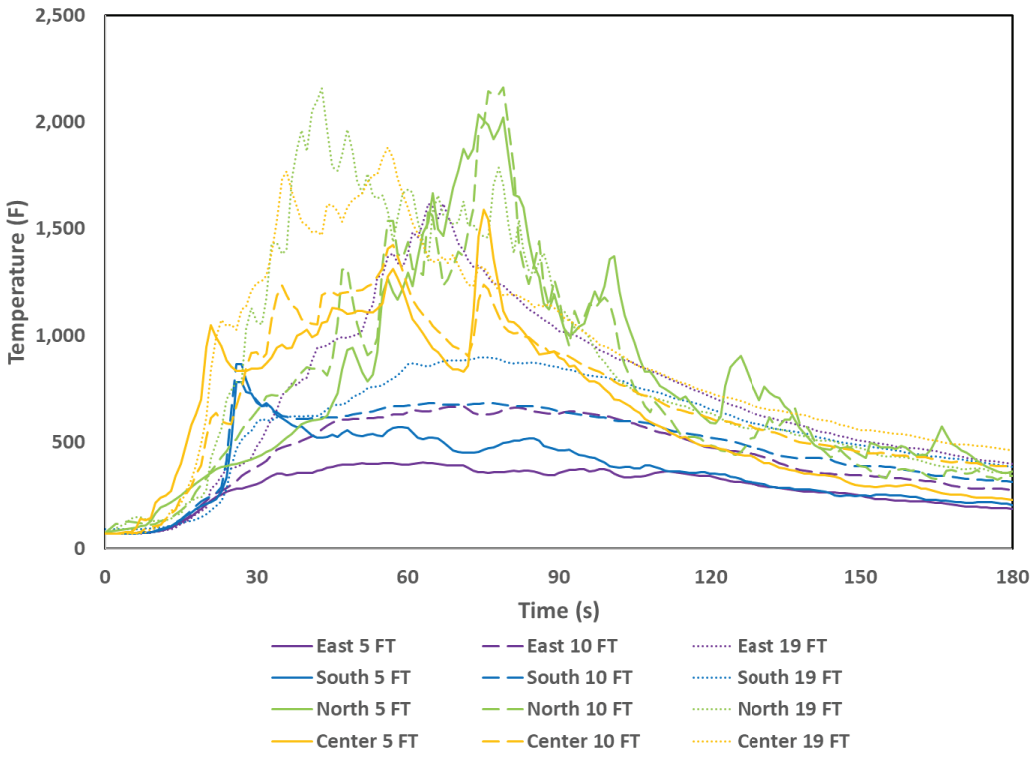

Figure 31. Air Temperatures from Unmitigated Fire (55 gal JP-4 on Concrete)

5.2.2. Mitigated Spill Fires

This study and the prior HAS study (2) evaluated two methods to mitigate fuel spill fire damages in an aircraft hangar, the Halon 1211 system and the ILDFA. In both project, 165 gal of fuel was spilled and the tests with these fuel spill sizes are compared here. In the ILDFA tests, twelve thermocouples were installed at heights of 5, 10, 17 ft. on the four thermocouple trees described in Section 3.1.4.3. Four additional thermocouples were installed on the thermocouple trees (three at 24 ft. and one at 21 ft.). The HAS test details are provided in Appendix A. In the prior Design A tests, four thermocouples were installed as shown in the Figure A- 3. In the Design B and C tests, a total of 13 thermocouples were installed at heights of 5, 12, 19, and 26 ft. above the floor in the four thermocouple trees on as shown in Figure A- 4 and Figure A- 5.

In five of the six prior Halon system tests (2), the pre-burn times were less than five seconds before suppression system was activated (Table 22). In the configuration for Design B, there were mechanical problems and the suppression system did not discharge correctly, not considered here for comparison. In those two Design B tests, the faulty Halon system took longer to suppress the fires, maximum temperatures of 670 °F and 1,084 °F were recorded and 8 of the 13 thermocouples recorded temperatures above 400 °F. Accordingly, neither are considered here for comparison to

ILDFA suppression. In the remaining three Design A and C tests, flame detectors activated the system between 1-3 seconds after ignition resulting in maximum temperatures recorded of 270 °F, 160 °F, and ambient. In each of these tests, no thermocouple recorded a temperature above 400 °F.

The ILDFA testing included six tests each using 165 gal fuel, three with, and three without the channel water flushing system activated. Peak temperatures at each thermocouple height were averaged for the three tests conducted. In the tests with the water flushing system activated, the peak average temperature at the 24 ft. height was the greatest at 195 °F with one test's peak temperature of 209 °F at that height (Figure 32). In the tests with the water flushing system deactivated, the peak average temperature at the 24 ft. height was the highest at 195 °F with one test's peak temperature of 305 °F at the height of 10 ft. (Figure 33). The resulting air temperature from the ILDFA system with or without the water flushing system activated were similar to results from the prior (2) Design A system activating in two seconds and was somewhat higher than the Design C system when activating in one to three seconds.

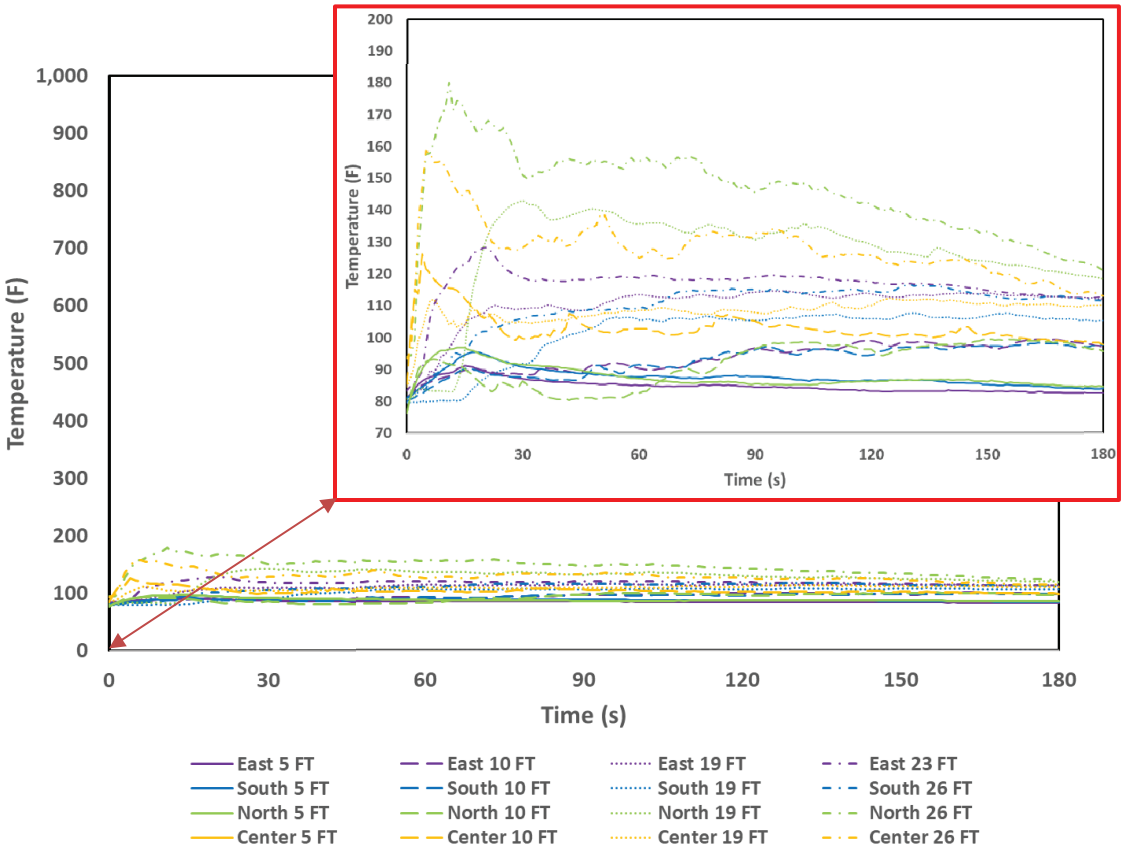

Figure 32. Air Temperatures from ILDFA-Mitigated Fire (Water Flushing Active, 165 gal JP-4)

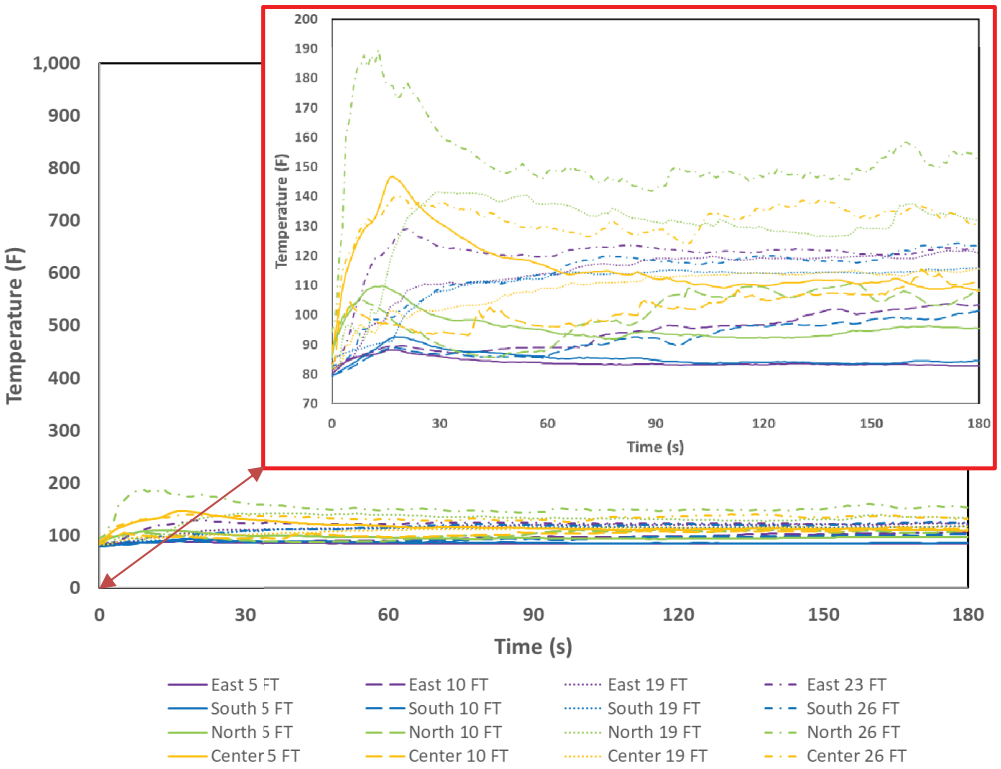

Figure 33. Air Temperatures from ILDFA-Mitigated Fire (Water Flushing Inactivated, 165 gal JP-4)

In summary, unmitigated 55 gal fuel spill fires resulted in room air temperature measurements ranging from 290 - 1,550 °F. The prior tests of Halon system with 165 gal fuel fires, showed that when activated within three seconds (as flame detector could accomplish) all measured air temperatures were below 270 °F. During six ILDFA-mitigated 165 gal fuel spill fires, the peak temperature measured was 305 °F. Both Halon and ILDFA effectively reduced air temperatures from these large fuel spill fires.

6. CONCLUSIONS

In all unmitigated fires from fuel spills on bare concrete, the fire spread rapidly, resulting in thermal buildup and thick smoke forming at the ceiling that would translate to significant damage. Fire size on bare concrete consistently spread beyond the spill location, reaching the edges of pan when 30 gal or greater was spilled. In the scenarios and testbed, the wing and fuselage mockup was partially or completely engulfed in flames, exposing it to heat flux levels that will cause composite material delamination and degrade strength of the components.

The ILDFA system, by comparison, reduced the fuel spill area, flame heights, smoke and fire intensity duration when compared to baseline concrete spill fire tests. The reduction eliminates or limits thermal damage to a smaller and more confined area of aircraft or structure. A direct volume to volume comparison of thermal damage for spills over 55 gal was not possible due to the intensity and inherent danger of fire testing of such an unconfined fuel spill fire, however, spills up to 165 gal on the ILDFA resulted in lower temperature and heat flux measurements than the 15 gal unmitigated fuel spills on concrete. There was also a visually apparent reduction of smoke within the building, which will protect personnel and aid first-responders

Based on composite material delamination and strength loss documented in a prior study, total heat absorbed at each sensor location was evaluated to find whether any exceeded the damage threshold (1,645 kJ/m^2) (4). The damage threshold was surpassed for each concrete fuel spill fire at the inboard and outboard wing sensors located directly above the spill fire location of the test bed. Similarly, the damage threshold was surpassed at three of the heat flux sensor locations on the mockup for all unmitigated fuel spill fires, and surpassed for the 30 gal and larger fires at the fourth mockup sensor location. At the perimeter heat flux sensor locations, the damage threshold was surpassed for all unmitigated fuel spill fires at the North and South locations except for the 15 gal spill at the South location. For the East and West locations, the threshold was only surpassed at the West location for spills of 42.5 and 55 gal. The damage threshold at the center of the test pan (10 ft. high), was exceeded in 30 and 55 gal unmitigated fuel spill fires. This damage threshold was never surpassed at the adjacent aircraft fuselage sensor location for concrete or ILDFA tests and was not surpassed at any heat flux sensor locations for ILDFA spills up to 165 gal with or without active water flushing.

The analysis of the ILDFA mitigated fuel spill fires showed HRR was significantly reduced in magnitude and duration compared to the fires on bare concrete. For HRR estimation purposes the determined fuel spill area was treated as a circular pool. In general the spill fires on concrete reached peak flame heights (and thus presumed peak HRR) 14 to 20 s after the fuel spill commenced. These fires roughly maintained this peak intensity for 54 to 82 s before the flames began to diminish. Peak HRR for these unmitigated fuel spill sizes from 15 to 55 gal were estimated at 45 - 116 MW. The mitigated spill fires on the ILDFA spread and reached peak flame heights (and thus presumed peak HRR) approximately two seconds after the fuel spill commenced. Based on flame height observations, the peak HRR began to diminish in less than 10 s, much less than unmitigated tests. Peak HRR for the ILDFA fuel spill sizes from 15 to 165 gal were estimated from 0.67 to 1.9 MW, also much less that unmitigated tests.

While the fire threat is reduced using the ILDFA flooring, the threat is not eliminated. Small fires still occur with spill fires on the ILDFA. In addition, there is the risk that fuel vapors released

from the incident flooring channels can result in small flames at locations several feet away from the fuel spill location. This poses an additional threat that should be considered in operational planning.

A comparison of air temperatures in this study and in the prior study, *Fire Protection System for Hardened Aircraft Shelters* (2), suggest that both a Halon 1211 installed facility fire suppression system and the ILDFA proved to markedly reduce air temperatures from these large fuel spill fires.

7. RECOMMENDATIONS

Based on the results of this work, the ILDFA may be incorporated in operations and coupled with other protection schemes that decrease potential to affect personnel safety, aircraft damage, and environmental impact. Future goals are to evaluate combinations of installed floor drain systems along with ancillary water suppression systems to increase protection of aircraft assets and fire suppression efficiency. A complementary water suppression strategy might include water mist, wet-pipe sprinklers, or water deluge systems.

Further analysis of the system may be warranted. The continuation should include quantitative HRR determinations for better resolution of actual fire suppression. In order to obtain the data, a large room calorimeter fuel spill fire test is needed and recommended.

8. REFERENCES

1. *Aircraft Maintenance Hangars.* April 2017. UFC 4-211-01.

2. Zallen, D.M., et al. *Fire Protection System for Hardened Aircraft Shelters.* October 1987. ESL-TR-86-13.

3. Hill, S. A., Scheffey, J. A., Walker, F., Williams, F. W. *Tests of Alternative Fire Protection Methods for USAF Hangars.* February 1999. NRL/MR/6180-99-8337.

4. Bocchieri, R., et al. *Firefighting and Emergency Response Study of Advanced Composites.* May 2013. AFRL-RX-TY-TR-2011-0046.

5. Giubbini, Kyle. *Testing Report on Spill Areas of Elevated Discharges from Military Aircraft.* s.l. : Safespill Systems, 2019.

6. Hurley, M.J. Heat Release Rates chapter. *SFPE Handbook of Fire Protection Engineering, Fifth Edition.* 2016.

7. Fire Dynamics Tools (FDTs) – Quantitative Fire Hazard Analysis Methods for the U.S. Nuclear Regulatory Commission Fire Protection Inspection Program. June 2013. Vols. Supplement 1, Volumes 1 & 2. NUREG-1805.

8. Mealy, Christopher L., Benfer, Matthew E., Gottuk, Daniel T. Fire Dynamics and Forensic Analysis of Liquid Fuel Fires. s.l. : U.S. Department of Justice, May 2012.

9. Joseph E. Gott, Darren L. Lowe, Kathy A. Notarianni, William Davis. *Analysis of High Bay Hangar Facilities for Fire Detector Sensitivity and Placement.* s.l. : Building and Fire Research Laboratory, National Institute of Standards and Technology, February 1997. NIST Technical Note 1423.

10. *Loss Prevention Data.* Norwood, MA : Factory Mutual Engineering Corporation, Inc., March 1991. Loss Prevention Data Sheet 7-93N.

11. David O. Hubble, Tom E. Diller. A Hybrid Method for Measuring Heat Flux. *ASME Journal of Heat Transfer.* Mar 2010. Vol. 132.

12. Vega, T., Lattimer, B. and Diller, T. E. Fire Thermal Boundary Condition Measurement Using a Hybrid Heat Flux Gage. *Fire Safety Journal.* 2013. Vols. 61, pp. 127-137.

Appendix A: ESL-TR-86-13 (2) SUMMARY AND INSTRUMENTATION LOCATIONS

Summarized below are results from the report "Fire Protection System for Hardened Aircraft Shelters" (2). The subject work included air temperature and suppression time measurements during Halon suppression system tests in an aircraft hangar with a 165 gal fuel spill fire scenario. Some scenarios also included a three dimensional (3-D) fire. Three different Halon systems (Designs A-, B-, and C-) and different activation times of those systems were tested. The tests resulted in some short duration burns of the spilled fuel and some longer duration burns. The three different instrumentation setups (A-, B-, C-) for the prior tests conducted are also illustrated in Figure A- 3, Figure A- 4, and Figure A- 5

Design A used three dual IR flame detectors and Halon 1211 fed through a 20 ft. header and nozzle section. Design B used UV/IR flame detectors and a modified manifold system (Halon 1211, fed into individual headers and nozzle assemblies). Design C used eight UV/IR flame detectors. A summary of the prior tests is below.

Test A-1: The 165 gal JP-4 spill fire flowing from the tail to the nose was extinguished by the Halon system in four seconds. Figure A-1 is a frame from a video of this test just before the fire was extinguished and the discharged Halon can be seen on the West and East sides of the fire as it exits the header and nozzles and interacts with the flames. The maximum temperature recorded in the room was 270 °F at five feet above the floor.

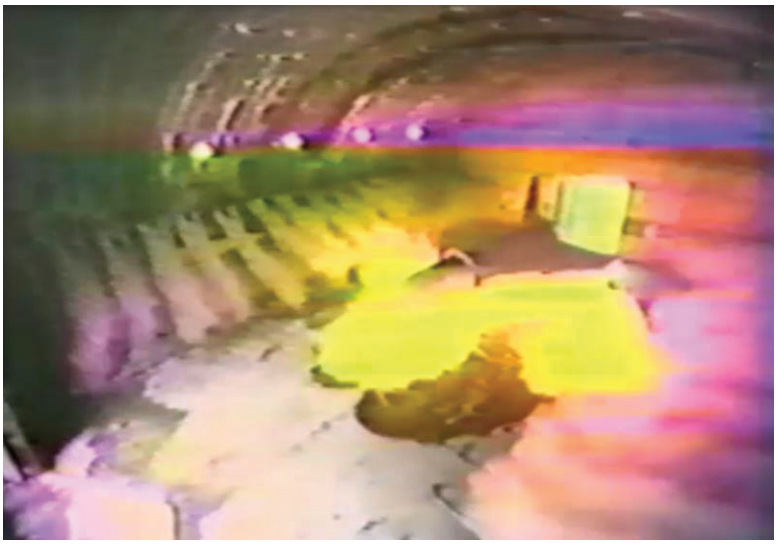

Figure A-1. Halon System Activation to Extinguish the 165 gal JP-4 Spill Fire

Test A-2: The 165 gal JP-4 spill fire was allowed to burn for 17 s, then the Halon suppression system was activated. Figure A-2 shows the fire three seconds after ignition from an internal camera and 11 s after ignition from an external camera. The maximum temperature recorded was 1,900 °F on two of the four thermocouples. The fire was not extinguished by the Halon system and AFFF was subsequently used for suppression.

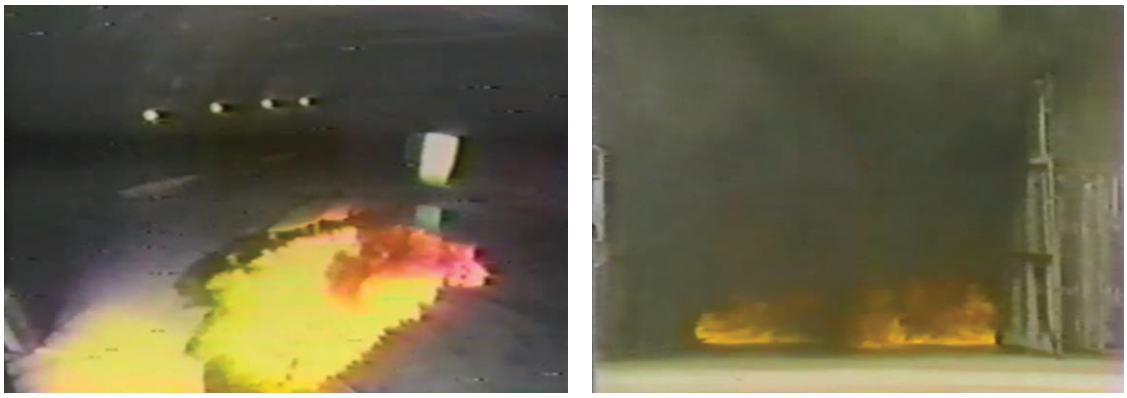

Figure A-2. JP-4 Spill Fire Three Seconds (left) and 11 s (right) After Ignition

Test B-1: The 165 gal JP-4 spill fire was extinguished by the Halon system, however two of the four cylinders did not discharge agent on time. The maximum temperature recorded was 670 °F at the mockup tail location, five feet above the fuel spill and 24 s after ignition. Eight of the thirteen thermocouples exceeded 400 °F at the mockup wing (5 ft.), nose (26 ft.), wall (12, 19, 26 ft.), and tail (5, 12, 19 ft.) locations.

Test B-2: The 20 gal 3-D internal aircraft fire was allowed to burn for 20 s before the 165 gal JP-4 spill fire burned for an additional five seconds before Halon system activation. The maximum temperature recorded was 1,084 °F (8) at the wall 26 ft. above the floor, 16 s after ignition. Eight of the thirteen thermocouples exceeded 400 °F at the mockup nose (26 ft.), tail (5, 12, 19 ft.), and wall (5, 12, 19, 26 ft.) locations.

Test C-1: The 165 gal JP-4 spill fire flowing from the tail to the nose was detected and the Halon system activated one second after ignition. No temperatures were recorded above ambient.

Test C-2: The 3-D internal aircraft fire was allowed to burn for 10 s then the 165 gal JP-4 spill fire burned for an additional three seconds before fire detection and suppression system activation. The maximum temperature recorded was 160 °F at five feet above the floor.

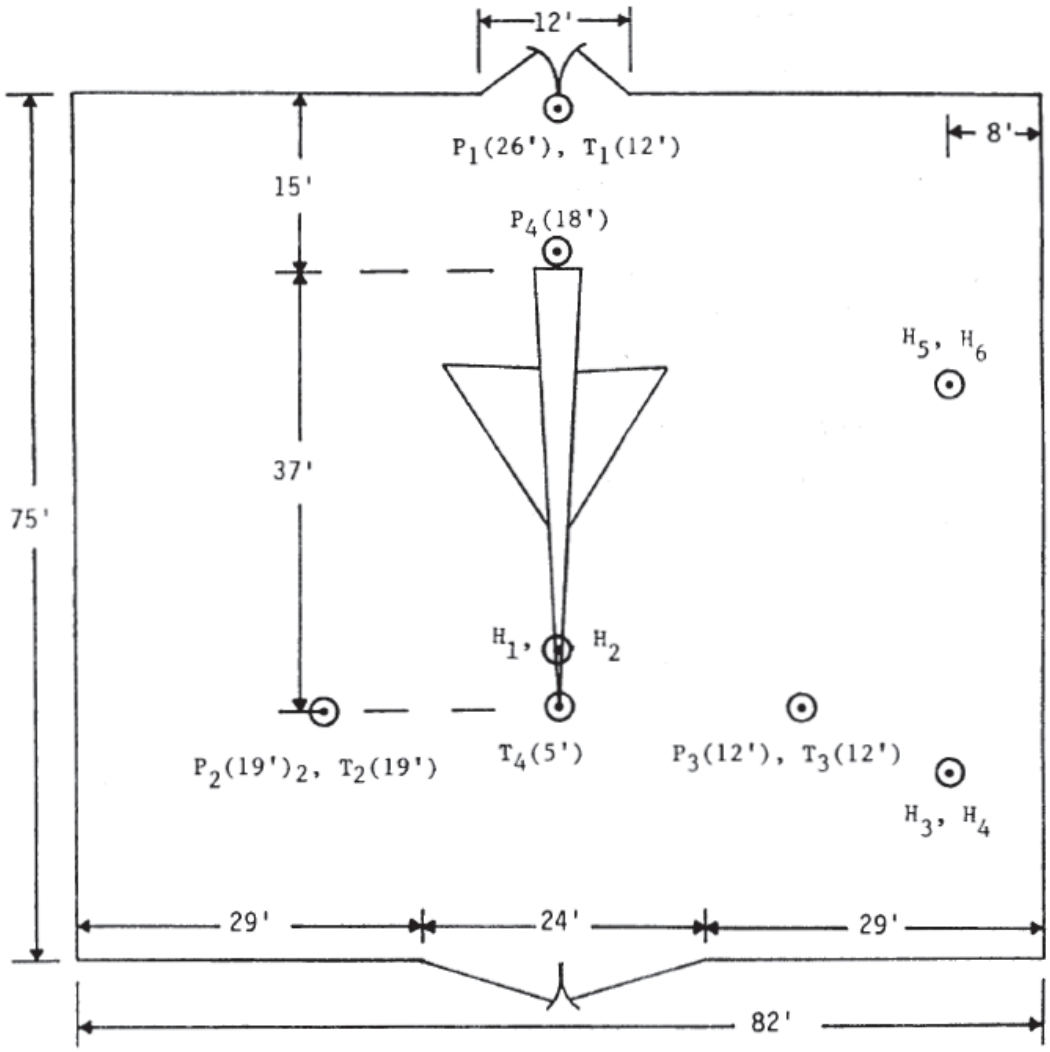

Notes: (1) T = thermocouple, P = pressure gage, and
H = Perco halon gas concentration probe inlet.

(2) Numbers in parentheses are elevations above floor.

Figure A- 3. Test A-1 and A-2 Instrumentation Setup from ESL-TR-86-13 (2)

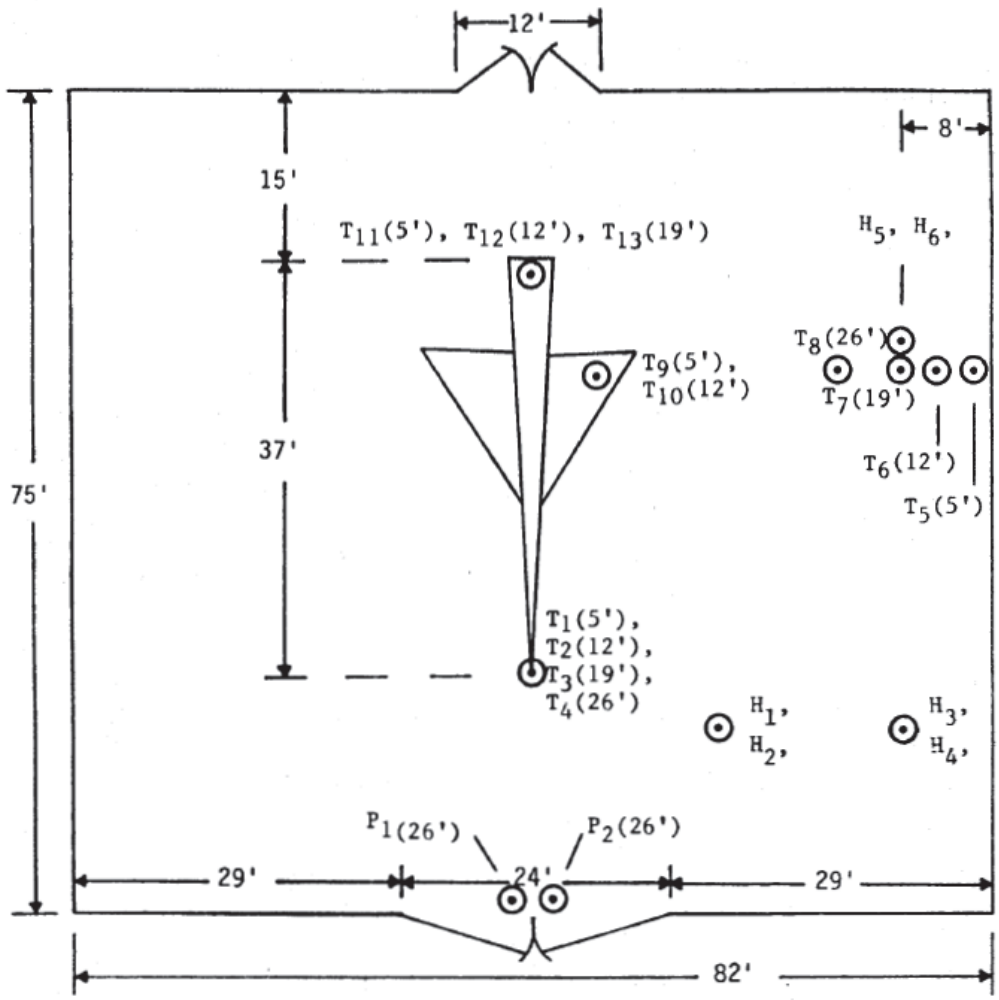

Notes: (1) T = thermocouple, P = pressure gage, and
H = Perco halon gas concentration probe inlet.

(2) Numbers in parentheses are elevations above floor.

Figure A- 4. Test B-1 and B-2 Instrumentation Setup from ESL-TR-86-13 (2)

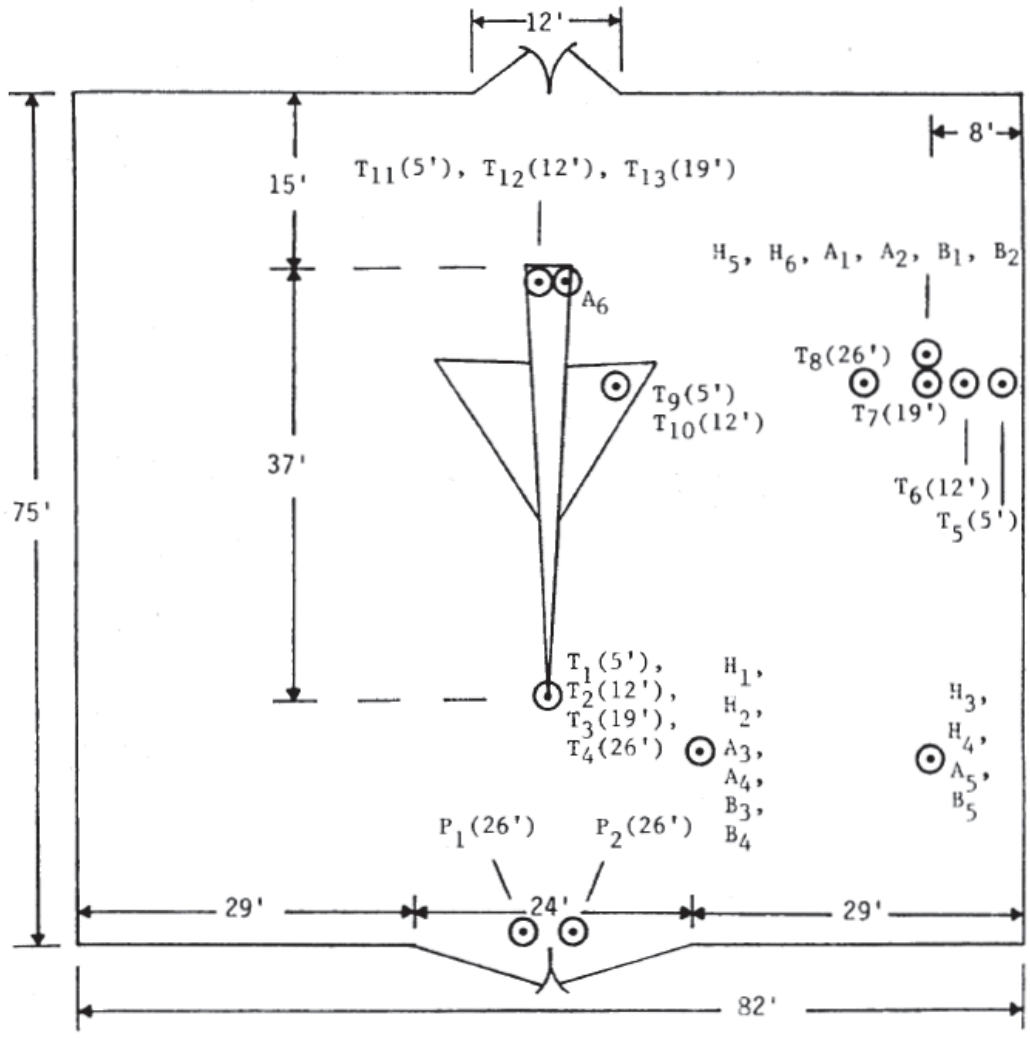

Notes: (1) T = thermocouple, P = pressure gage, and H = Perco halon gas concentration probe inlet.

(2) Numbers in parentheses are elevations above floor.

Figure A- 5. Test C-1 and C-2 Instrumentation Setup from ESL-TR-86-13 (2)

Appendix B: ILDFA SURVEY SUMMARY TAKEAWAYS:

The following survey information was taken from users of the ILDFA installed at Edwards AFB. Maintenance and operations personnel were asked questions related to how easy the installation was, any struggles with maintenance, and difficulty in performing standard operations on the platform. Survey questions were designed to understand the level of difficulty to perform standard tasks on the ILDFA system. Written responses were assigned a category of positive, neutral, or negative while ease-of-use questions had a five point scale ranging from very easy to very difficult.

The following comments and notes summarize responses to the questions. Individual responses to questions are shown in the Figures below.

Comments and Notes:

- Six total respondents and 13 total questions.
- None of the respondents said that day-to-day spill cleanup, maintenance, or visibility was made more difficult by the floor.
- Two of the respondents said that the floor made the movement of equipment with wheels/casters difficult. One respondent specifically stated that T38 aircraft jacks were difficult to move on the surface. All six said that equipment transportation was not difficult around the ramped edges of the floor.
- Four of the respondents said that the floor made locating foreign objects dropped (FOD) easier, one said it made locating FOD more difficult.
- Three of the respondents said that kneeling on the floor was uncomfortable, two of the six said that it was comfortable. Four respondents said that the floor was less slippery than the traditional concrete. One said that it was more slippery. One respondent noted that the rough surface of the floor could make falls more dangerous.
- Three of the respondents said that they noticed damage to the floor when equipment was dropped on it.
- None of the respondents thought that the grounding points were inconvenient, but one noted that the grounding points are located where equipment is usually stored during maintenance on small aircraft.
- None of the respondents noticed any restrictions to the facility caused by the floor.

Table B- 1. Response Category Summary

	Positive	*Neutral*	*Negative*
Respondent 1:	7	2	1
Respondent 2:	6	3	1
Respondent 3:	10	2	1
Respondent 4:	11	0	0
Respondent 5:	7	5	0
Respondent 6:	5	3	2
Total:	46	15	5

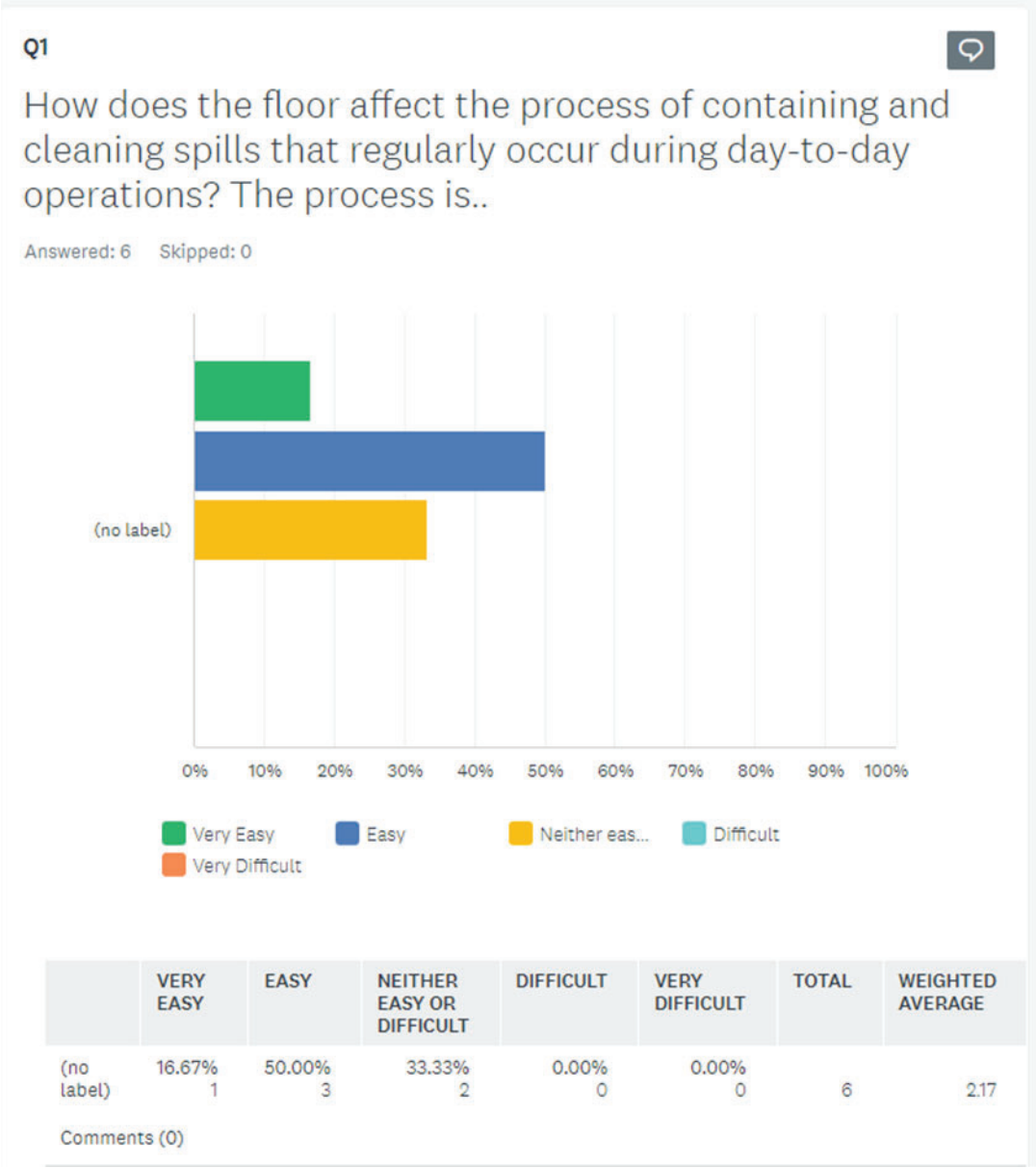

Figure B- 1. Survey of Maintenance and Operations Personnel. Question 1

Q2

How does the floor affect day-to-day maintenance in the facility? Day-to-day maintenance is..

Answered: 6 Skipped: 0

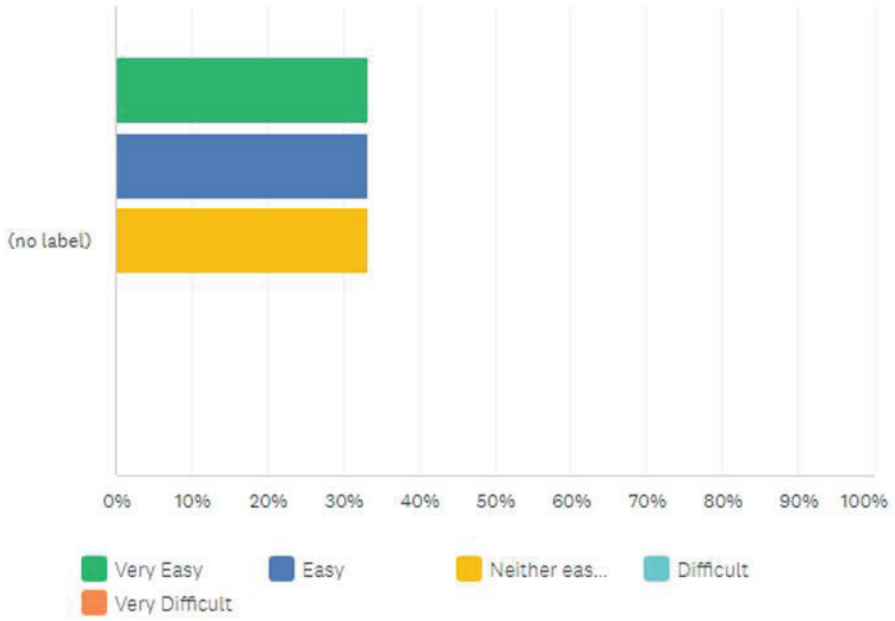

	VERY EASY	EASY	NEITHER EASY OR DIFFICULT	DIFFICULT	VERY DIFFICULT	TOTAL	WEIGHTED AVERAGE
(no label)	33.33% 2	33.33% 2	33.33% 2	0.00% 0	0.00% 0	6	2.00

Comments (0)

Figure B- 2. Survey of Maintenance and Operations Personnel. Question 2

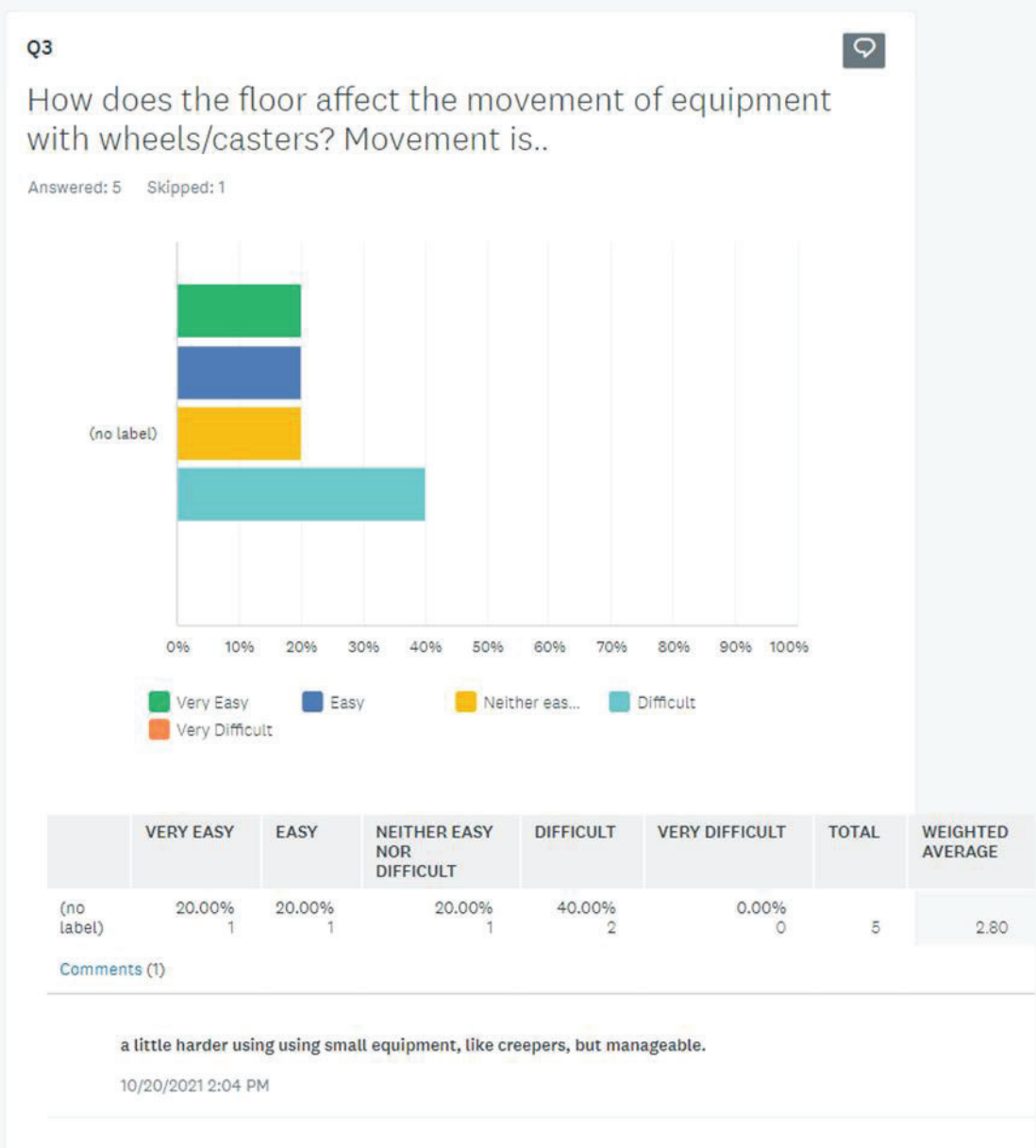

	VERY EASY	EASY	NEITHER EASY NOR DIFFICULT	DIFFICULT	VERY DIFFICULT	TOTAL	WEIGHTED AVERAGE
(no label)	20.00% 1	20.00% 1	20.00% 1	40.00% 2	0.00% 0	5	2.80

Comments (1)

a little harder using using small equipment, like creepers, but manageable.

10/20/2021 2:04 PM

Figure B- 3. Survey of Maintenance and Operations Personnel. Question 3

Q4

How does the floor impact visibility during the day with the hangar doors shut? Visibility is..

Answered: 6 Skipped: 0

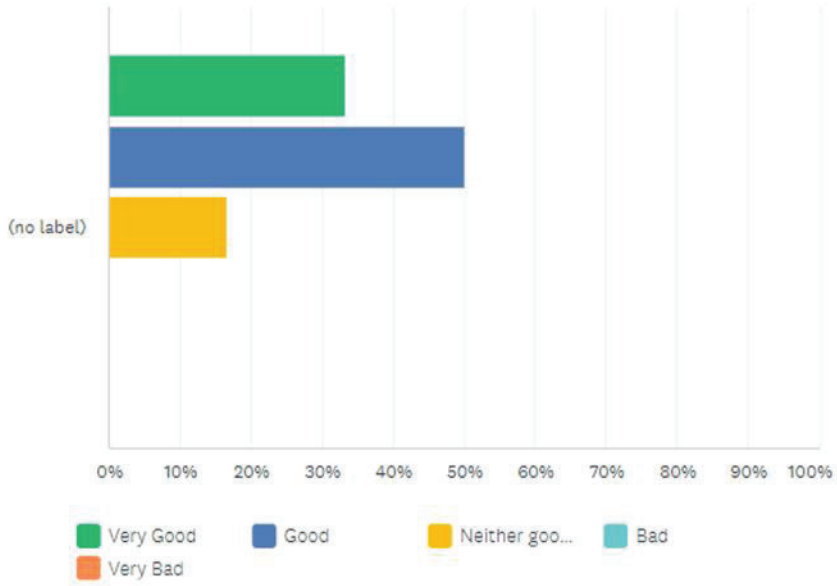

	VERY GOOD	GOOD	NEITHER GOOD NOR BAD	BAD	VERY BAD	TOTAL	WEIGHTED AVERAGE
(no label)	33.33% 2	50.00% 3	16.67% 1	0.00% 0	0.00% 0	6	1.83

Comments (0)

Figure B- 4. Survey of Maintenance and Operations Personnel. Question 4

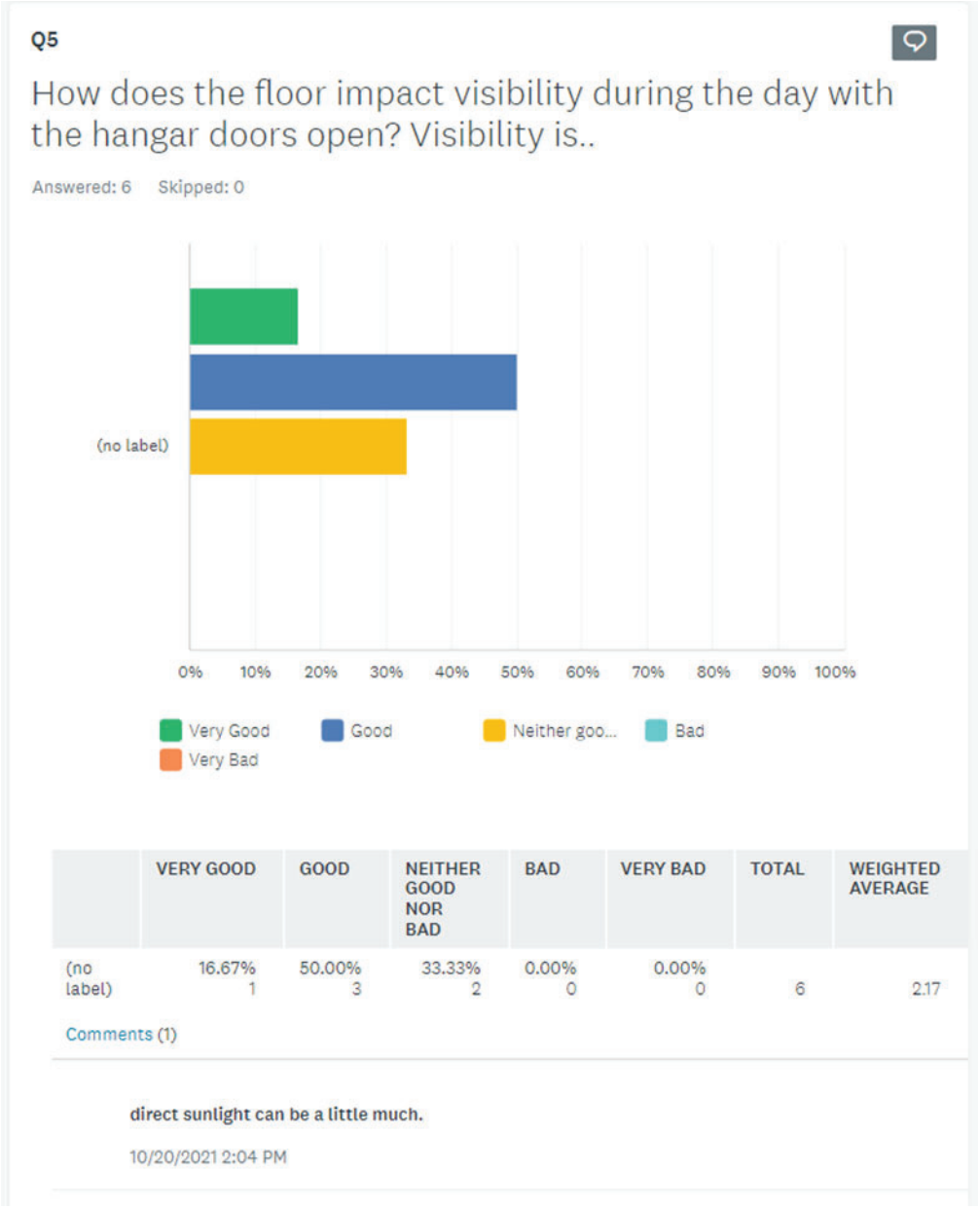

	VERY GOOD	GOOD	NEITHER GOOD NOR BAD	BAD	VERY BAD	TOTAL	WEIGHTED AVERAGE
(no label)	16.67% 1	50.00% 3	33.33% 2	0.00% 0	0.00% 0	6	2.17

Comments (1)

direct sunlight can be a little much.

10/20/2021 2:04 PM

Figure B- 5. Survey of Maintenance and Operations Personnel. Question 5

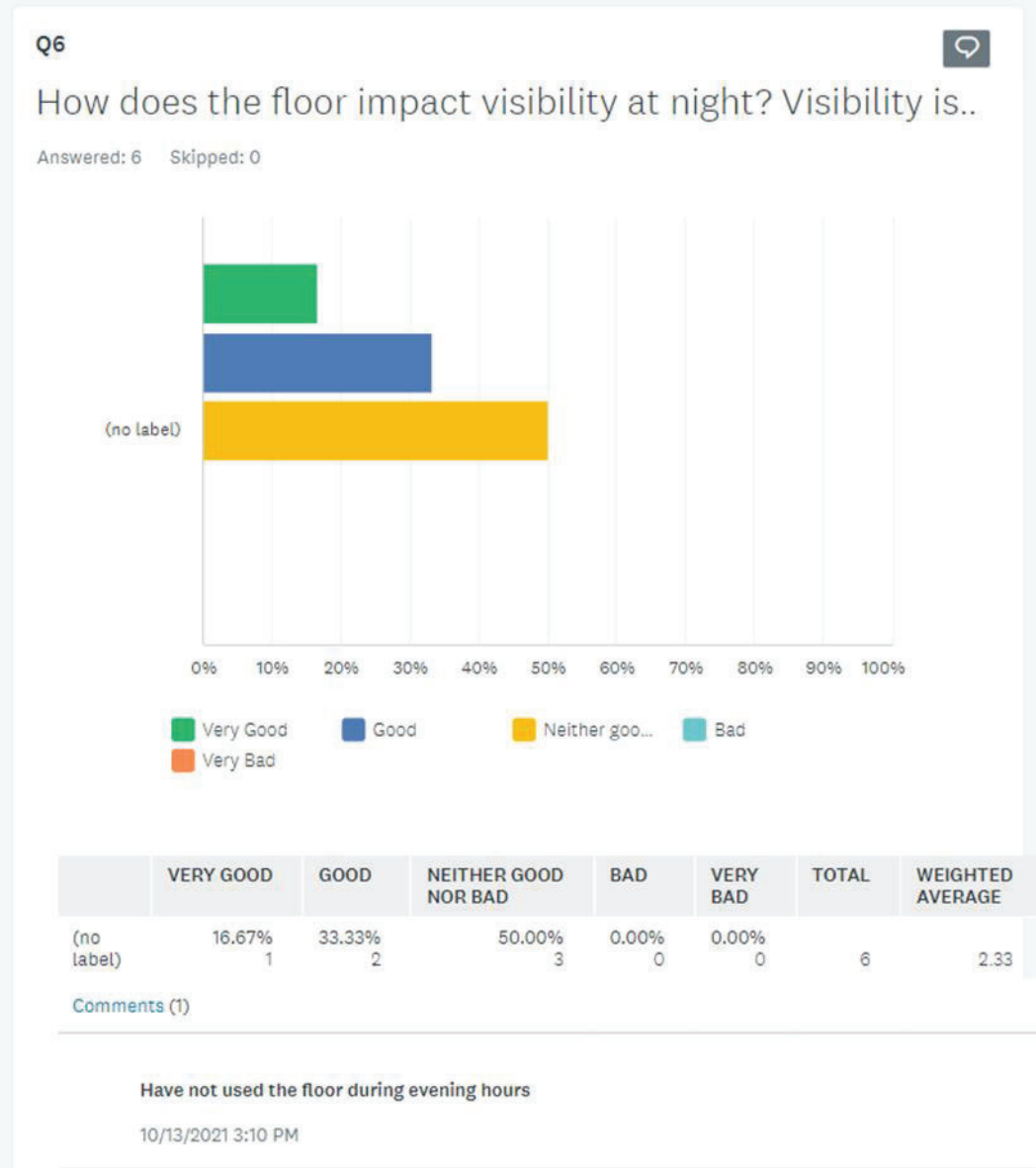

	VERY GOOD	GOOD	NEITHER GOOD NOR BAD	BAD	VERY BAD	TOTAL	WEIGHTED AVERAGE
(no label)	16.67% 1	33.33% 2	50.00% 3	0.00% 0	0.00% 0	6	2.33

Comments (1)

Have not used the floor during evening hours

10/13/2021 3:10 PM

Figure B- 6. Survey of Maintenance and Operations Personnel. Question 6

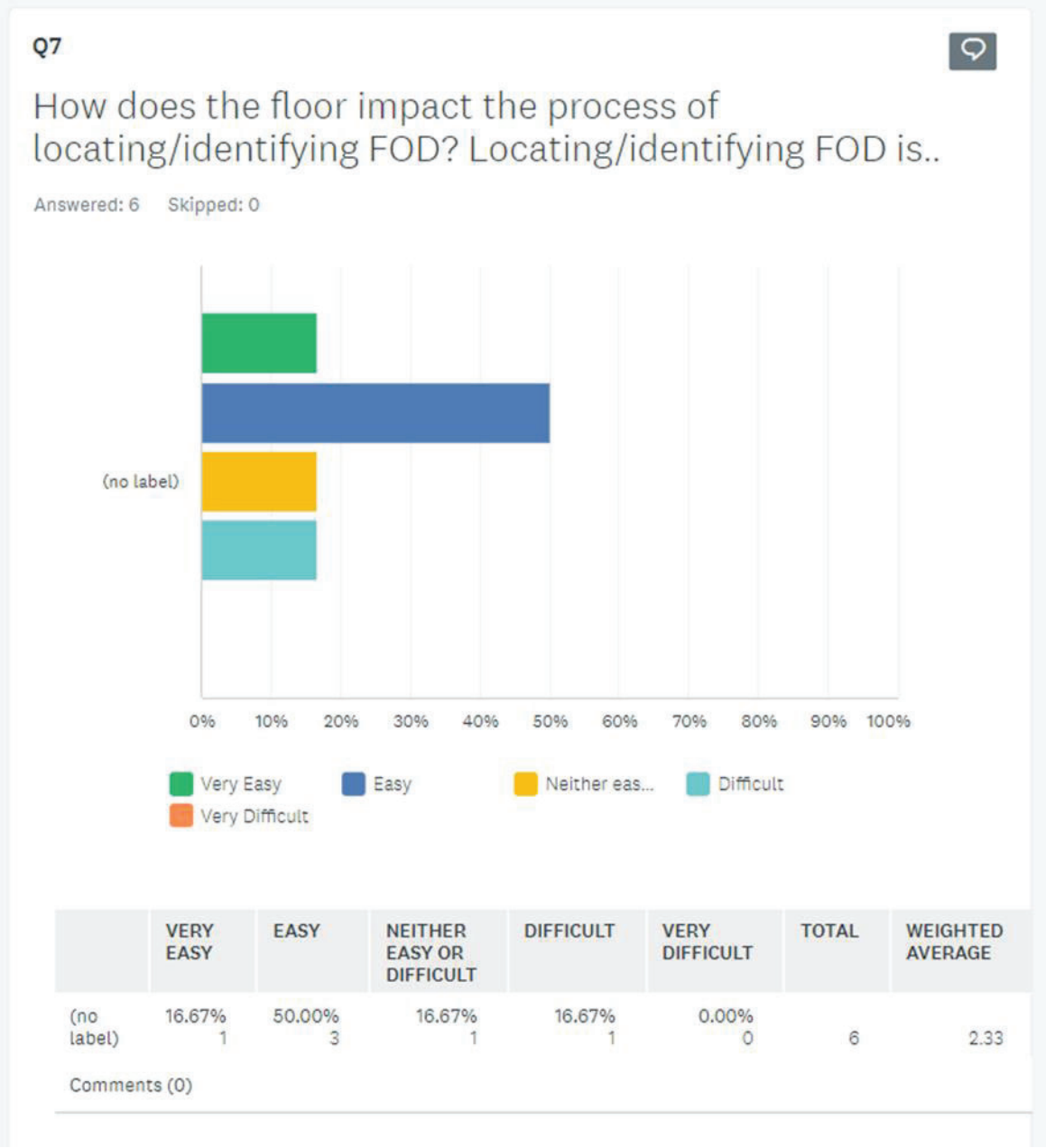

	VERY EASY	EASY	NEITHER EASY OR DIFFICULT	DIFFICULT	VERY DIFFICULT	TOTAL	WEIGHTED AVERAGE
(no label)	16.67% 1	50.00% 3	16.67% 1	16.67% 1	0.00% 0	6	2.33

Comments (0)

Figure B- 7. Survey of Maintenance and Operations Personnel. Question 7

	VERY COMFORTABLE	COMFORTABLE	NEITHER COMFORTABLE NOR UNCOMFORTABLE	UNCOMFORTABLE	VERY UNCOMFORTABLE	TOTAL	WEIGHTED AVERAGE
(no label)	16.67% 1	16.67% 1	16.67% 1	33.33% 2	16.67% 1	6	3.17

Comments (3)

just have to be more carful when kneeling.

10/20/2021 2:04 PM

Kneeling is a little less comfortable

10/20/2021 12:19 PM

No different then kneeling on the floor or the concrete

10/13/2021 3:10 PM

Figure B- 8. Survey of Maintenance and Operations Personnel. Question 8

Q9

Have you noticed any damage to the floor from dropped equipment?

Answered: 6 Skipped: 0

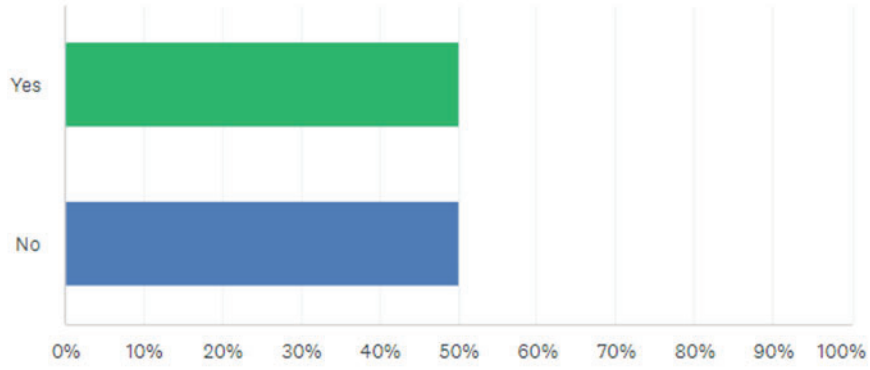

ANSWER CHOICES	RESPONSES	
Yes	50.00%	3
No	50.00%	3
TOTAL		6

Comments (1)

dropped (3)three foot braker bar on floor made small dent

10/13/2021 3:10 PM

Figure B- 9. Survey of Maintenance and Operations Personnel. Question 9

Q10

How do the ramps around the edges of the floor affect equipment transportation? Transportation is..

Answered: 6 Skipped: 0

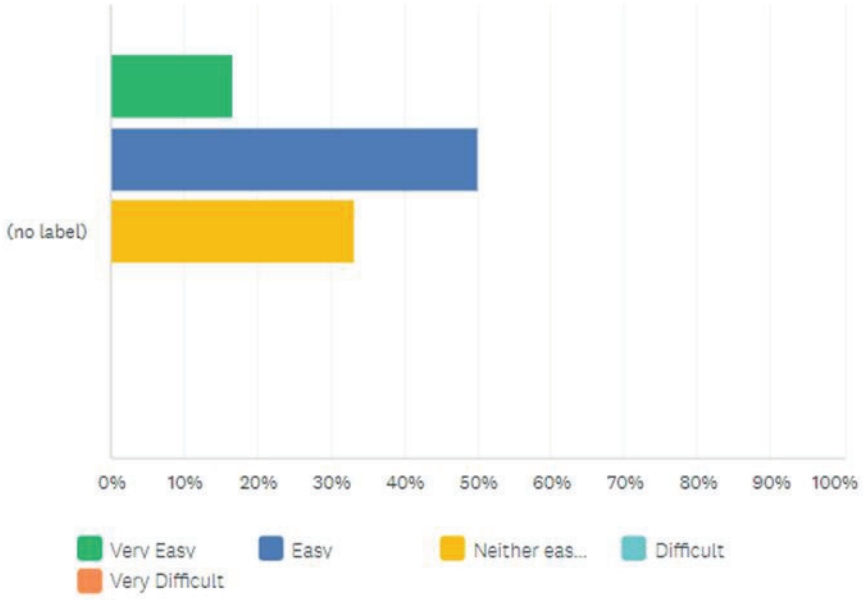

	VERY EASY	EASY	NEITHER EASY OR DIFFICULT	DIFFICULT	VERY DIFFICULT	TOTAL	WEIGHTED AVERAGE
(no label)	16.67% 1	50.00% 3	33.33% 2	0.00% 0	0.00% 0	6	2.17

Comments (1)

the longer edges work best

10/20/2021 2:04 PM

Figure B- 10. Survey of Maintenance and Operations Personnel. Question 10

	VERY CONVENIENT	CONVENIENT	NEUTRAL	INCONVENIENT	VERY INCONVENIENT	TOTAL	WEIGHTED AVERAGE
(no label)	16.67% 1	50.00% 3	33.33% 2	0.00% 0	0.00% 0	6	2.17

Comments (1)

Could be placed different for our smaller aircraft the points are where we would noprmally put our age equipment

10/13/2021 3:10 PM

Figure B- 11. Survey of Maintenance and Operations Personnel. Question 11

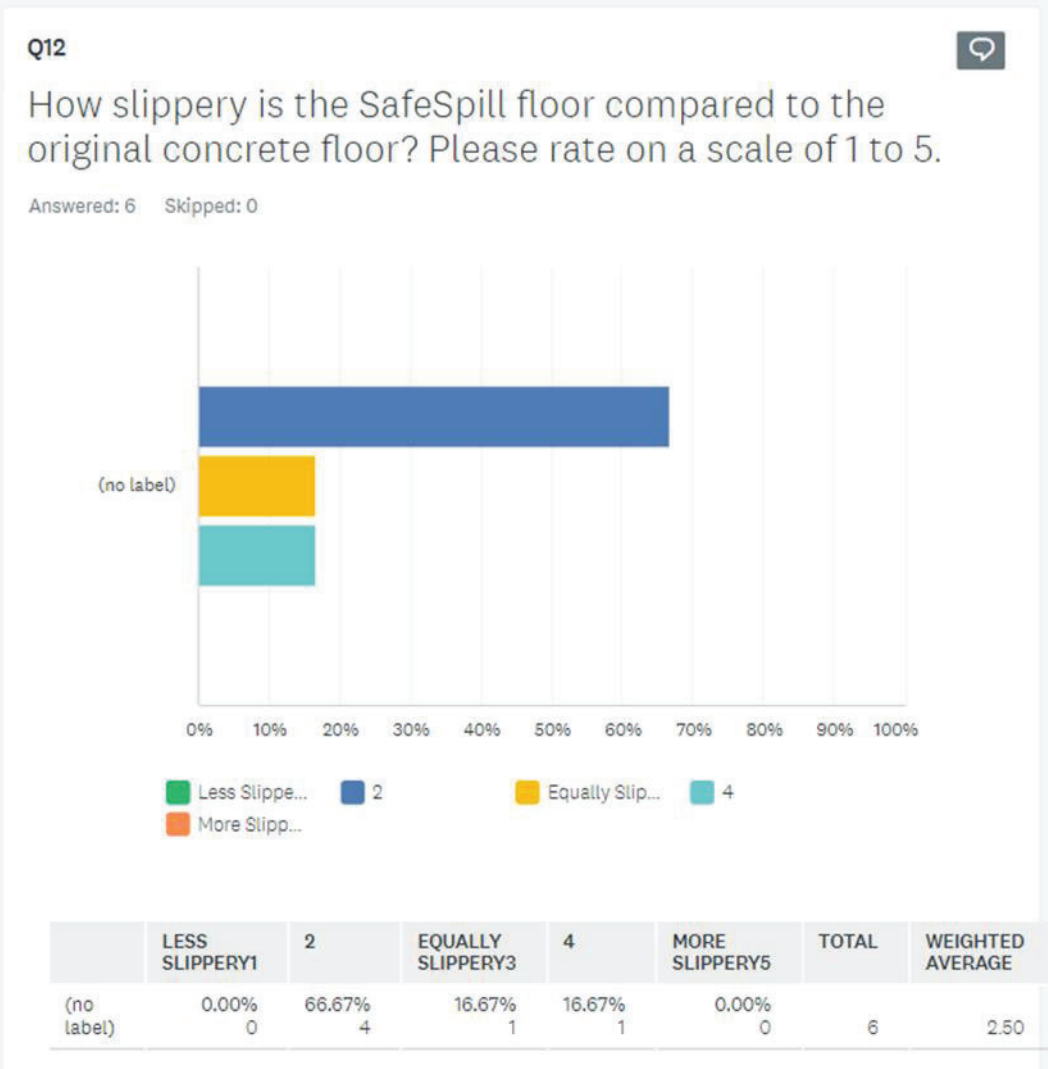

	LESS SLIPPERY1	2	EQUALLY SLIPPERY3	4	MORE SLIPPERY5	TOTAL	WEIGHTED AVERAGE
(no label)	0.00% 0	66.67% 4	16.67% 1	16.67% 1	0.00% 0	6	2.50

Figure B- 12. Survey of Maintenance and Operations Personnel. Question 12

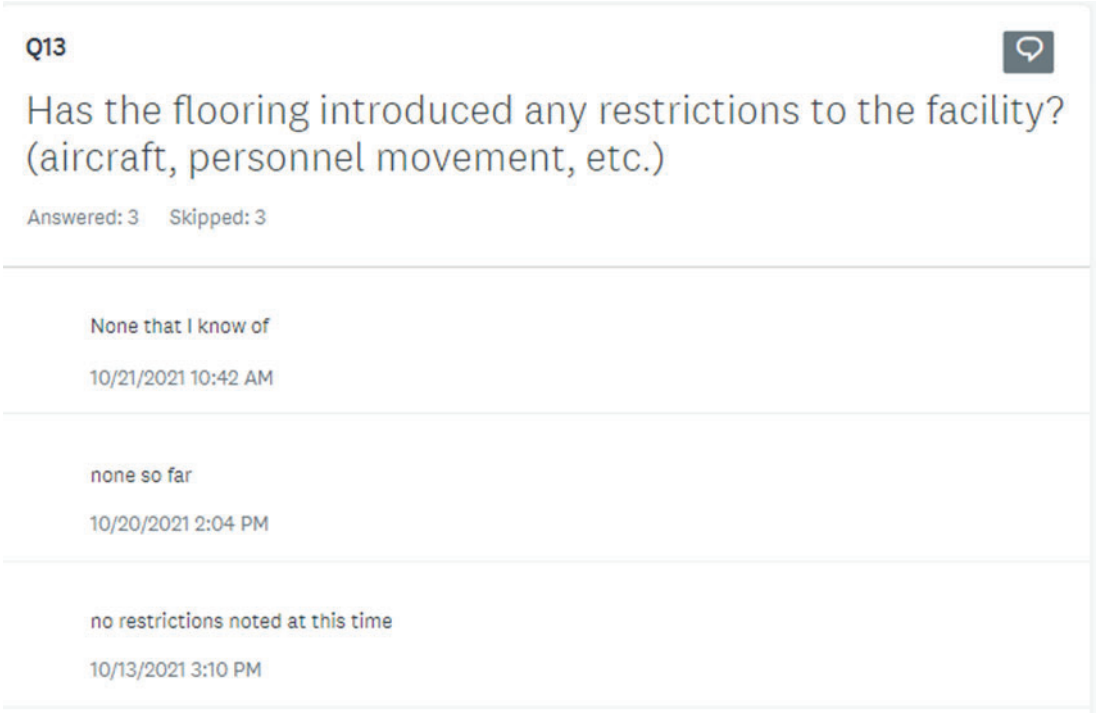

Figure B- 13. Survey of Maintenance and Operations Personnel. Question 13

Appendix C: LIST OF SYMBOLS, ABBREVIATIONS, AND ACRONYMS

AFB.: Air Force Base.
AFCEC: Air Force Civil Engineering Center.
AFCEC/CXAE: Airbase Technologies Branch.
AFFF: Aqueous Film-Forming Foams.
ANG: Air National Guard.
ANOVA: Analysis of Variance.
ARFF: Aircraft Rescue and Fire Fighting.
C or Center: Central Thermocouple.
COTS: Commercial Off-The-Shelf.
DoD: Department of Defence.
E or East: East Heat Flux. ; East Thermocouple.
F1: Fuselage Point 1.
F2: Fuselage Point 2.
F3: Fuselage Point 3.
F4: Fuselage Point 4.
FOD: foreign objects dropped.
HAS: hardened aircraft shelters.
HD: High-Definition.
Hi-Ex: High Expansion.
HRR: Heat Release Rate.
ILDFA: Ignitable Liquid Drainage Floor Assembly.
IR: Infrared.
N or North: North Heat Flux. ; North Thermocouple.
NIST: National Institute of Standards and Technology.
NRC: Nuclear Regulatory.
PFAS: Poly- and Perfluoroalkyl Substances.
PFOA: Perfluorooctanoic Acid.
PFOS: Perfluorooctane Sulfonate.
S or South: South Heat Flux. ; South Thermocouple.
TC: Thermocouples.
UFC: Unified Facilities Criteria.
USAF: United States Air Force.
VAC: Volts of Alternating Current.
W or West: West Heat Flux.